UNIVERSITY OF CALGARY

A Cross-Layer Design for Wireless Location

by

Mohamed Youssef

A THESIS SUBMITTED TO THE FACULTY OF GRADUATE

STUDIES IN PARTIAL FULFILMENT OF THE REQUIREMENTS

FOR THE INTERDISCIPLINARY DEGREE OF DOCTOR OF PHILOSOPHY

DEPARTMENT OF GEOMATICS ENGINEERING

and

DEPARTMENT OF ELECTRICAL AND COMPUTER ENGINEERING

CALGARY, ALBERTA

DECEMBER 2008

UNIVERSITY OF CALGARY

FACULTY OF GRADUATE STUDIES

The undersigned certify that they have read, and recommend to the Faculty of Graduate Studies for acceptance, a thesis entitled "A Cross-Layer Design for Wireless Location" submitted by Mohamed Youssef in partial fulfilment of the requirements of the degree of Doctoral of Philosophy.

Supervisor, Dr. Naser El-Sheimy, Department of Geomatics Engineering

---

Co-Supervisor, Dr. Michel Fattouche, Department of Electrical and Computer Engineering

---

Dr. Kyle O'Keefe, Department of Geomatics Engineering

Dr. Fadhel Ghannouchi, Department of Electrical and Computer Engineering Department

---

Dr. Simon Park, Department of Mechanical and Manufacturing Engineering

---

Dr. Mohamed Ibnkahla, Department of Electrical and Computer Engineering, Queens University

NOV 25 - 2008

Date

Abstract

The thesis introduces robust cross-layer (Physical Layer, Selection Layer, Positioning Layer, and Network Layer) solutions for existing wireless location problems for both infrastructure and distributed systems. The proposed physical layer solution provides a novel Multi-Resolution Estimation (MRE) technique based on an orthogonal search to enhance the sensitivity of the Maximum Likelihood Estimator (MLE) and to estimate the propagation delay between a transmitter and a receiver without bias by resolving the Direct Path (DP) ray from the Multipath (MP) rays. Above the physical layer, a novel Skew-Normal Outlier Detection (SNOD) technique is introduced at the selection layer to offer further robustness against multipath rays. The SNOD technique is based on the $\mathcal{S}$kew-$\mathcal{N}$ormal ($\mathcal{SN}$) distribution which is a new class of distributions that have not been considered before either in wireless communication nor in wireless location. On top, several novel robust estimation techniques based on Iterative Reweighted Least Squares (IRLS), and $L_1 - norm$ are introduced at the positioning layer to provide a robust position estimate for a radio device with unknown location. These robust estimation techniques have also been introduced at the network layer to put forward a reliable solution for the unavailability of Reference Stations (RSs) in distributed systems.

Acknowledgements

This work would not have been possible without the support of my family and mentors. Specifically, I would like to thank my supervisor, Dr. Naser El-Sheimy, who has given me all the support and guidance I needed as a doctoral student. He also made sure I had resources when I needed them. I would also like to thank the excellent teacher, my co-supervisor Dr. Michel Fattouche. I have been always amazed by both his industry and academic expertise. It is fair to say that I could not have done this without their help.

Special thank has to be addressed to Dr. Aboelmagd Noureldin. I am very grateful to have had his trust on my skills and capabilities.

I would like to acknowledge NSERC, GEOIDE, and the University of Calgary for the financial support they gave during my PhD studies.

This thesis was also made possible by collaboration and consultation with many colleagues. I would like to thank Mostafa Soliman, Taher Hassan, and my students at the Embedded Wireless Systems course for the great discussions we had together.

I owe a huge gratitude to my family and extended family. Their support, encouragement, patient, and understanding made everything possible.

Dedication

To the most influential person in History: Prophet of Islam, Mohamed, peace be upon him, whose life is a role model of success in all aspects.

Table of Contents

List of Tables

List of Figures and Illustrations

List of Symbols, Abbreviations and Nomenclature

Symbol	Definition
P_E	Positioning error
R_E	Ranging error
n_b	Number of biased circles
n_i	Number of intersecting circles
σ_{los}^2	Variance of the Line-Of-Sight Signal
σ_{nlos}^2	Variance of the non-Line-Of-Sight Signal
2D-CTM	Two-Dimensional Coordinate Transformation Model
AGPS	Assisted Global Positioning System
AOA	Angel-Of-Arrival
AWG	Additive White Gaussian
AWGN	Additive White Gaussian Noise
cdf	Cumulative density function
CL	Collaborative Localization
CLC	Cluster Local Coordinates
CRLB	Cramer-Rao Lower Bound
DGPS	Differential Global Positioning System
DS	Device Station
FIM	Fisher Information Matrix
FNA	Free Network Adjustment
GDOP	Geometrical Dilution Of Precision
GLS	General Least Square
GNSS	Global Navigation Satellite System
GPS	Global Positioning System
HS-GPS	High Sensitivity Global Positioning System
IRLS	Iterative Reweighted Least Square
KTSFM	Karasawa Three State Fade Model
LORAN	Long Range Navigation
LOS	Line-Of-Sight
LS	Least Square
MF	Matched Filter
ML	Maximum Likelihood
MLE	Maximum Likelihood Estimation
MMS	Multimedia Messaging Service
MSE	Mean Square Error
NLOS	Non-Line-Of-Sight
P_D	Probability of Detection
pdf	Probability density function
P_{D_p}	Probability of partial Detection
P_{D_t}	Probability of total Detection
PFA	Probability of False Alarm
RS	Reference Station

RSS	Received Signal Strength
RSSI	Received Signal Strength Indicator
RTD	Round Trip Delay
SMS	Short Message Service
SNOD	Skew-Normal Outlier Detection
SNR	Signal-to-Noise Ratio
TDOA	Time-Difference-Of-Arrival
TOA	Time-Of-Arrival
U. S.	United States
UTSFM	Urban Three State Fade Model
WLAN	Wireless Local Area Network
WSN	Wireless Sensor Network
$H.O.T$	Higher Order Term
$\mathcal{N}(\mu, \sigma^2)$	Gaussian Distribution with mean μ and variance σ^2
$\mathcal{SN}$	Skew-Normal Distribution
$\mathcal{SN}(\mu, \sigma^2, \lambda)$	Skew-Normal Distribution with mean μ, variance σ^2, and skewness λ
λ	Skewness Parameter
μ	Mean Value
σ	Standard Deviation

Chapter One: **INTRODUCTION**

Wireless technologies have dramatically changed people's life style. Wireless networks allow people on the move to communicate using a range of services such as voice, Short Message Service (SMS), Multimedia Messaging Service (MMS), and email. With such technological advances, people start to have more expectations regarding future wireless networks. Reliable and affordable communications among people and devices regardless of physical limitations is already a prime objective. Another challenging objective is the need for a reliable wireless location solution.

Wireless location, also commonly termed *radiolocation*, has recently received increased attention from both industry and academia. Wireless location refers to the method of obtaining the position information of a radio device using wireless networks. The position information is usually given in terms of geographic coordinates [1][2]. In this chapter, I will briefly review the history of wireless location and its applications. Challenges and motivations are also discussed. Finally, an overview of the thesis, its contributions, and its outcomes are presented.

1.1 History Perspective of Localization

Determining location is an old question that reappeared in many different contexts throughout history. Figure 1 illustrates the time frame of several localization methods discussed in this subsection. Localization first appeared in the context of navigation when travelling through land or sea where the stars have been used as Reference Stations (RSs). In the 1940s, the hyperbolic navigation system known as LORAN (LOng RAnge Navigation) was developed in the United States (U.S.), hence, the start of the wireless location era. In LORAN, the RSs are located on the earth surface and the accuracy of the system ranges between a few hundred meters to a few kilometres. The potential of localization changed in the 1960s when a need to track satellites in space came up. This was followed in the late 1980s by a roll-out of the US developing the Global Positioning System (GPS) where satellites are used as RSs. The late 1990s witnessed the emergence of network-based wireless location systems that are capable of locating mobile users. Finally, in the 2000s a new localization application has emerged in the form of distributed networks, especially in localizing sensor nodes for many applications using Wireless Sensor Networks (WSNs). In distributed systems, there is no infrastructure; and therefore, there are no predetermined RSs to rely on!

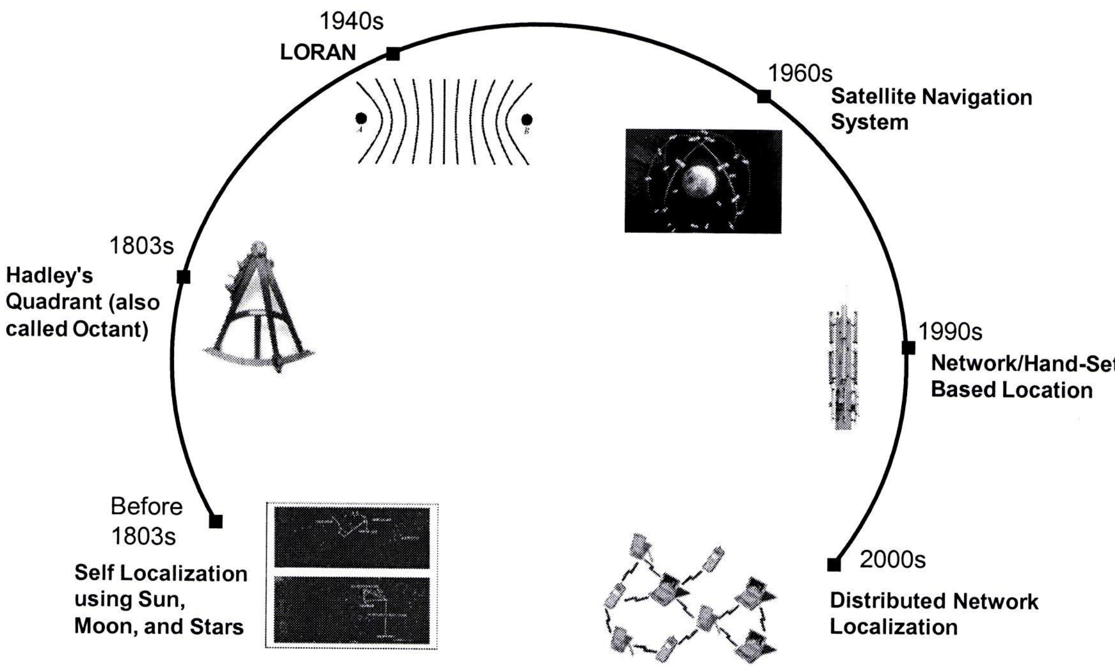

Figure 1 Shows the history of localization methods

1.2 Applications based on Location Awareness

Wireless location provides a multitude of new applications and services. Among the new services and applications are: 1) Outdoor person/asset tracking, 2) Enhanced-911, 3) Location sensitive billing, 4) Fraud protection, 5) Fleet management, 6) Intelligent transportation systems, 7) Cellular system design and management, and 8) Mobile yellow pages. In addition, many new applications for distributed systems are waiting for a practical and reliable localization solution. In this thesis, I select WSNs as a model for distributed systems. Unfortunately, to date, there is no single practical nor reliable localization solution for WSN. If localization exists, many new applications, are enabled. For example: 1) indoor (i.e. people, assets and merchandise) tracking, 2) animal tracking, and 3) disaster monitoring. In addition, new research directions based on location awareness such as location-aware routing [3] and network security are currently being investigated for WSNs [4].

Wireless location technologies can be divided into two main categories: infrastructure and distributed systems. Infrastructure systems can be further divided into: hand-set based, and network-based. This section provides a brief review the basic ranging measurements techniques followed by a concise review of the theory of operation behind several wireless location systems.

1.3 Ranging Measurement Techniques

Received Signal Strength (RSS), Time-Of-Arrival (TOA), Time-Difference-Of Arrival (TDOA), Round Trip Delay (RTD), and Angle-Of-Arrival (AOA) are the basic approaches for estimating ranges between the device to be localized and a set of RSs. In this subsection, I review the definition of each of the ranging measurement techniques:

1. RSS: measures the power of the signal at a receiver using a Received Signal Strength Indicator (RSSI) algorithm, and estimates the range

between transmitter and receiver according to some channel propagation loss model, assuming that the power of the transmitted signal is known.

2. TOA: measures the time of arrival of the transmitted signal at the receiver with respect to a local clock. In order for the TOA to be useful, all local clocks should be synchronized and the time of transmission should be known.

3. TDOA: measures the time of arrival of the transmitted signal at a receiver with respect to the time of arrival of the transmitted signal at another receiver, in order to remove the need to know the time of transmission of the transmitted signal.

4. RTD: measures the forward link propagation delay (from transmitter 1 to receiver 2) and the backward link propagation delay (from transmitter 2 to receiver 1). In this case, clock synchronization and time of transmission are not required.

5. AOA: measures the angle of arrival, of the transmitted signal at the receiver. In this case, only two RSs are required to estimate the 2D position of the device.

1.4 Wireless Location for Infrastructure Systems

Infrastructure wireless location technologies fall into two main categories:

1.4.1 Hand-Set Based Wireless Location

In hand-set based wireless location systems, the radio device to be localized (i.e. the GPS receiver or the Cellular phone) determines its location from signals received from some RSs (i.e. from some GPS Satellites or from some Base Stations). TOA and AOA are the two main ranging measurement techniques used in hand-set based location systems. For example, in GPS-based estimations, the GPS receiver receives and estimates the signal parameters from at least four satellites out of the current network of 24 GPS satellites. The parameter measured by the GPS receiver for each satellite is the propagation delay between a number of RSs (i.e. a number of satellites) and itself [1].

Also a hybrid technique uses both the GPS technology and the cellular infrastructure and is known as Assisted-GPS (A-GPS). In this case, the cellular network is used to aid the GPS receiver that is embedded in the cellular telephone to improve accuracy and acquisition time.

1.4.2 Network-Based Wireless Location

Network-based location technology relies on a network of RSs, which attempts to determine the position of the radio device by measuring its signal parameters when received at the RSs. In this technology, the estimated parameters are relayed to a central site for further processing to provide an estimate of the location of the device. TDOA is the ranging measurement technique most commonly used for Network based wireless location [1][5].

1.5 Wireless Location for Distributed Systems

Current infrastructure localization techniques are typically inadequate for many of the WSN applications due to stringent hardware requirements on the radio device (i.e. on the sensor node) such as: low-cost, small size, and low battery consumption. In addition, current systems have inherent accuracy limitations that inhibit them in some WSN applications [4].

WSNs are one form of distributed wireless networks. Hence, there are no predetermined Reference Stations (RSs) available to rely on, neither in wireless communication nor in wireless location. Therefore, sensor nodes must cooperate to define their reference sensor nodes, build their own local coordinate system within each cluster, and then merge these local coordinates to a unique coordinate system for the WSN. This type of wireless localization has been called Collaborative Localization (CL). Figure 2 illustrates different stages for CL.

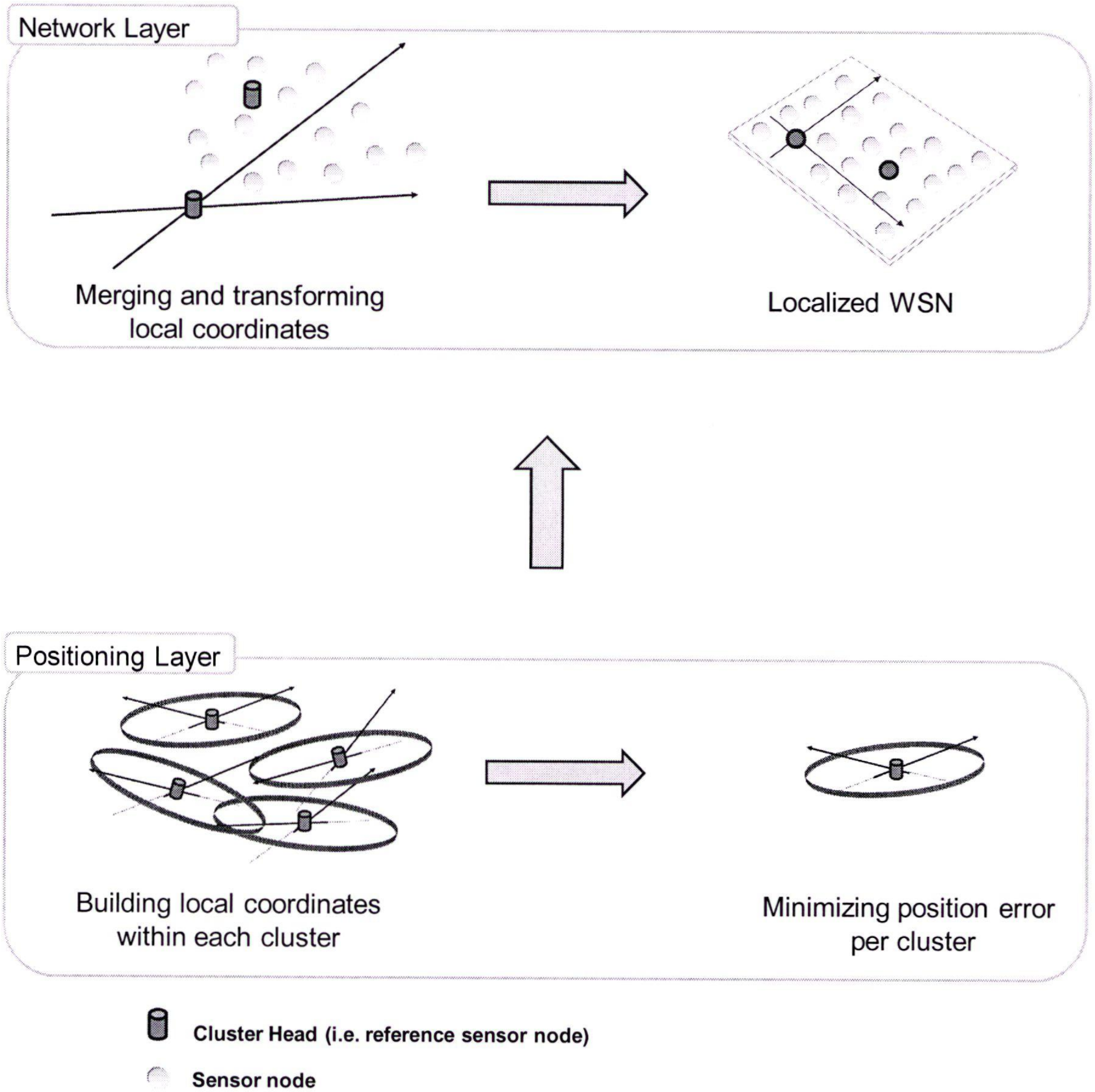

Figure 2 The Collaborative Localization (CL) process.

1.6 Challenges and Motivation

A Cross-layer approach has never been investigated before for wireless location. The cross-layer approach allows researchers to use different tools, to collaborate across layers, and to concatenate diverse methods to optimize their solutions toward the objective of improving wireless location performance. A simplified layer stack for wireless location is proposed in this thesis and is shown in Figure 3. The responsibility of the physical layer is to estimate ranges (i.e. Euclidean distances between transmitters and receivers) using any of the many available ranging measurement techniques which will be discussed later in this chapter. The fusion of these ranging estimates is used to estimate, fix, the position of a device with unknown location. This fusion process takes place at the positioning layer after a set of ranging estimates is selected at the selection layer.

Due to the unavailability of RSs in distributed systems, local coordinates have to be built to fix positions of radio devices. The network layer for infrastructure networks (e.g. Global Positioning System (GPS), Network based systems, and Hand-set based systems) is predesigned before network operation (i.e. the RSs have known coordinates and have synchronized clock). While in distributed systems, there is neither infrastructure nor RSs with known location to rely on. Hence, devices have to cooperate at the network layer in order to merge local coordinates, which have been built at the positioning layer within the many network clusters. Different wireless location applications can fit within the application layer. Hence, the wireless location layer stack provides a comprehensive representation for most problems related to wireless location.

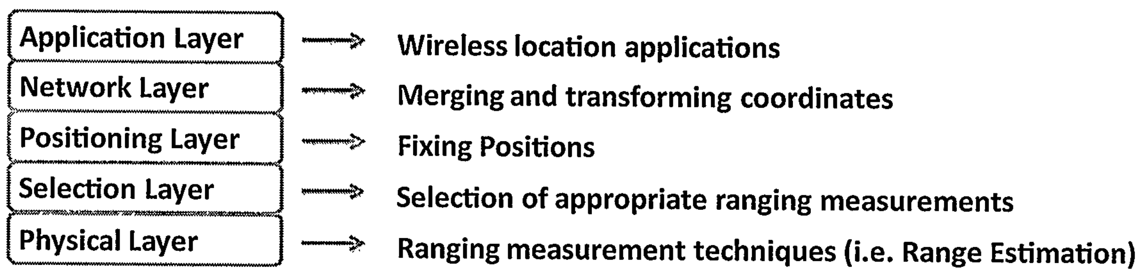

Figure 3 Simplified layered structure for wireless location

This thesis proposes to use a cross-layer approach as shown in Figure 3 to investigate three major problems in wireless location. These problems are 1) weak received signal (i.e. low received SNR), 2) multipath reception (i.e. correlated and non-correlated), and 3) the unavailability of RSs in distributed systems (e.g. Wireless Sensor Networks (WSNs)). The following represents the motivation behind the thesis in the context of the first four layers:

1. At the Physical Layer: Several ranging measurement techniques are based on estimating the propagation delay between a transmitter and a receiver. The receiver commonly uses a correlator followed by a peak detector to estimate such delays, assuming that the correlation peak is unbiased. Such

an assumption is not generally true. A Non-Line-Of-Sight (NLOS) channel, where Multipath (MP) rays which follow the Direct Path (DP) ray, can cause a bias to the estimated time delays out of the peak detector and consequently to the position estimate. To separate closely spaced MP rays from the DP ray, super-resolution estimation algorithms have to be used. A number of super-resolution algorithms have been introduced in the literature. I can classify them based on their theory of operation into: 1) Least Square (LS) methods, which introduce significant additional errors due to noise enhancement that arises from the ill-conditioning of the matrices that are involved in the LS operation. 2) Sub-space methods, which rely on the unrealistic assumption that the received rays, i.e. the DP and the closely spaced MP rays, are uncorrelated. Therefore, a new method has to be developed to consider closely spaced MP rays (i.e. correlated MP rays). This is the motivation behind chapter two of this thesis.

2. <u>At the Selection Layer</u>: Large ranging errors implicit over a MP channel and with low received SNR can cause large positioning error. Several Cramer-Rao Lower Bound (CRLB) studies recommend the detection and rejection of RS observations, which are encountering such large delay errors rather than estimating and removing their respective biases. Several techniques have been developed to detect signals with large ranging errors.

Generally, they model the problem of detecting MP signals as a binary hypothesis detection problem. If the distribution under the MP hypothesis is known, then the detection problem can be solved using conventional hypothesis testing [23]. However, the distribution of ranging measurements under the MP hypothesis is usually unknown. After natively, Geometrical Dilution of Precision (GDOP) and Receive Signal Strength (RSS) can be used to help in selecting appropriate RSs, however optimality is not guaranteed in this case. Therefore, a practical detection technique, which does not assume the knowledge of the distribution of the large ranging errors, should be developed. This is the motivation behind chapter three.

3. At the Positioning Layer: Current techniques that are used to fix the position of a radio device generally assume that the channel is an Additive White Gaussian Noise (AWGN) channel with no large ranging errors. Such assumption is not realistic and require a new positioning method that is robust against large ranging errors. This is the first motivation behind chapter four of this thesis. The second motivation behind chapter four of this thesis is as follows. In distributed systems, the unavailability of RSs encourages researchers to think about building local coordinates within the distributed networks. A method found in [62] is used to build local coordinates for WSNs. This is the only work of its kind as far as building

local coordinates within a WSN is concerned. The algorithm has the following drawbacks: 1) the method requires that each sensor node build its local coordinate system. Hence, the number of local coordinate systems grows linearly with the size of the WSN. 2) The algorithm does not consider the effect of measurement imperfections such as noise and large ranging errors. 3) The algorithm does not consider the effect of GDOP on the location accuracy.

4. At the Network Layer: Infrastructure systems have a unique coordinate system which belongs to the coordinate system of the RSs. On the other hand, distributed systems do not have a unique coordinate system. Therefore, merging local coordinates, is mandatory in distributed systems in order to have a unique set of global coordinates for the entire network. A method found in [62], referred to as the directional method, is used to merge local coordinates built by sensor nodes. The drawbacks of this method are 1) the local coordinates are merged without attention to positioning errors implicit to any WSN, which can lead to substantial positioning error within the entire WSN due to the propagation of ranging errors. 2) The directional method requires more than twice the number of computations compared to a technique proposed in this thesis: Two-Dimensional Coordinate Transformation Models (2D-CTMs). 3) The directional method does not consider the scaling factor between the

various local coordinates systems as a merging parameter to be estimated. This is the motivation behind chapter five of this thesis.

1.7 Overview of Contributions

This thesis attempts to address fundamental problems in current wireless location systems. Novel methods are proposed in this thesis which can advance the wireless location industry, both for infrastructure wireless location networks (i.e. GPS and Network Based Location), and for distributed systems. The contributions of the thesis in the context of the first four layers: physical layer, selection layer, positioning layer, and network layer are as follows:

***Contribution* 1 – At the Physical Layer:** 1.1) A novel Multi-Resolution Estimation (MRE) technique based on an orthogonal search is introduced to enhance the sensitivity of the wireless location receiver. 1.2) In addition, the proposed technique attempts to resolve the problem of closely spaced rays (i.e. correlated MP rays) and to estimate their time delays without bias. These contributions are contained in chapter two of the thesis.

***Contribution* 2 – At the Selection Layer:** 2.1) A novel Skew-Normal Outlier Detection (SNOD) technique has been introduced to offer further robustness against MP rays in particular, and large ranging errors in general. The SNOD technique is based on the $\mathcal{S}$kew-$\mathcal{N}$ormal ($\mathcal{SN}$) distribution which is a new class of distributions that have not been considered before either in wireless communication nor in wireless location. 2.2) In addition, the SNOD technique is the only detection technique that considers multiple time delay estimates from a single RS. These contributions are contained in chapter three of the thesis.

***Contribution* 3 – At the Positioning Layer:** 3.1) Robust positioning error minimization techniques based on IRLS (e.g. Huber, and $L_1 - L_2$), $L_1 - norm$, and combined estimators are introduced. 3.2) I propose the subspace method to be used within the Free Network Adjustment (FNA) technique to resolve the singularity found within the normal matrix. FNA is a common technique used in Geomatics Engineering to minimize positioning error. 3.3) I propose augmented FNA techniques, which are robust against large ranging errors. 3.4) A novel CL technique is introduced to overcome the unavailability of RSs in WSNs. The proposed CL technique is self-configurable, scalable, and independent of any positioning system. The introduced CL technique uses the RSS and the GDOP found at the selection layer as factors for building Cluster Local Coordinates (CLCs). These contributions are contained in chapter four of the thesis.

***Contribution* 4 – At the Network Layer:** 4.1) I introduce 2D-CTMs which are commonly used in Surveying Engineering to merge CLCs in distributed systems. 4.2) I also introduce augmented 2D-CTMs, which are robust against large ranging errors. 4.3) The scale factor is considered as a merging parameter to be estimated due to different ranging errors that are found between the clusters in the distributed network. 4.4) A complete 2D-CTM based on $L_1 - norm$ estimation, is introduced. These contributions are contained in chapter five of the thesis.

Figure 4 shows the thesis contributions in the context of the first four layers: the physical layer, the selection layer, the positioning layer, and the network layer.

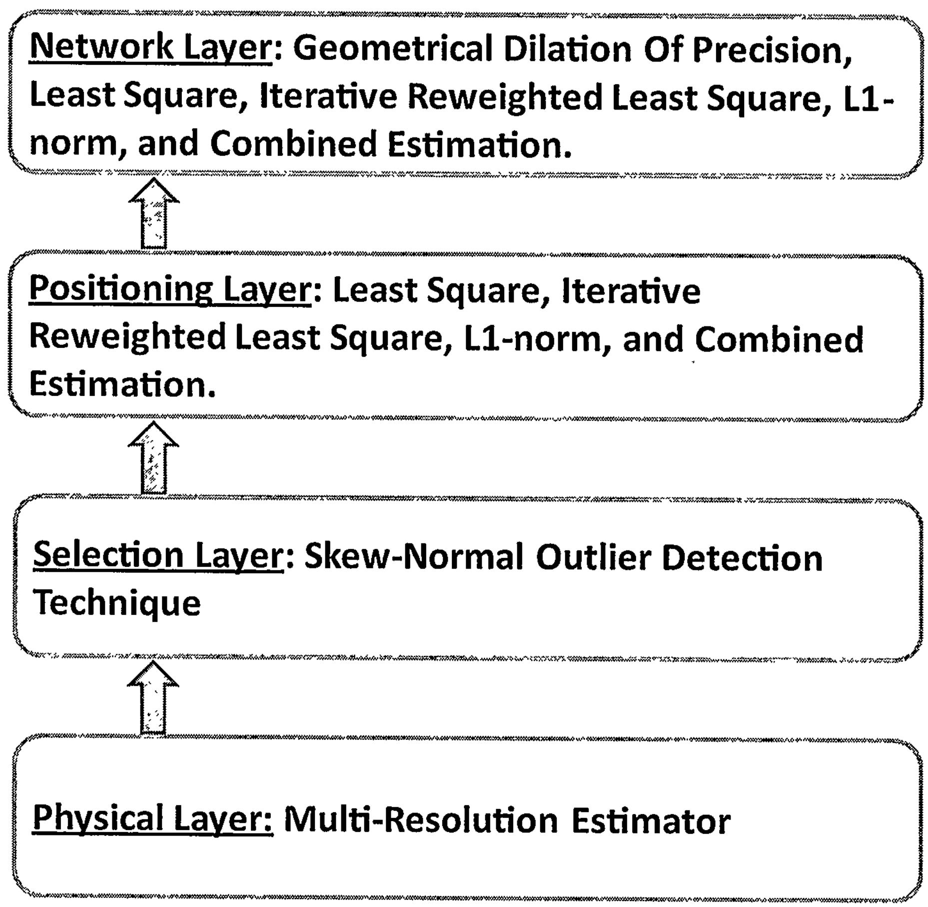

Figure 4 Contribution of the thesis with respect to the layers in wireless location.

1.8 Outline of the Dissertation

This thesis consists of six chapters. The first chapter is an overview of wireless location applications and systems. Challenges and motivation behind the research work in the thesis are also addressed in the first chapter as well as thesis contributions and outcomes. Chapter two introduces a novel MRE technique in the physical layer, while chapter three proposes the SNOD technique in the selection layer. In chapter four, robust positioning error minimization techniques are introduced at the positioning layer, as well as a unique solution to resolve the wireless location problem associated with the unavailability of RSs in distributed systems (i.e. WSNs). Chapter five introduces robust merging coordinate techniques to be used at the network layer to merge CLCs of the distributed systems. Finally, chapter six concludes the thesis and addresses future potential work.

Chapter Two: **PHYSICAL LAYER**
A NOVEL MULTI-RESOLUTION PROPAGATION DELAY ESTIMATION TECHNIQUE USING ORTHOGONAL SEARCH

This chapter deals with the problem of estimating the range between a transmitter and a receiver using measurements obtained over the wireless channel. In this chapter, I propose a Multi-Resolution Estimation (MRE) technique based on an orthogonal search to enhance the sensitivity of the Maximum Likelihood Estimator (MLE) and to estimate the propagation delay between a transmitter and a receiver without bias by resolving the Direct Path (DP) ray from the Multipath (MP) rays.

2.1 Introduction

The most widely employed ranging measurement technique is based on estimating the propagation delay (or its differences) as measured via DP from the transmitter to the receiver. A maximum Likelihood Estimator (MLE) uses a correlator followed by a peak detector to estimate such delays. This estimation technique is asymptotically unbiased only when the separation between the DP and the MP rays is asymptotically larger than the Rayleigh resolution of the system as shown in Figure 5. In many cases, the DP ray is followed closely by a number of MP rays that arrive at the receiver within a short time delay. If this delay is smaller than the duration of the Rayleigh resolution of the system, as shown in Figure 6, then the two rays can significantly overlap thereby causing a bias in the time delay estimated by the peak detector.

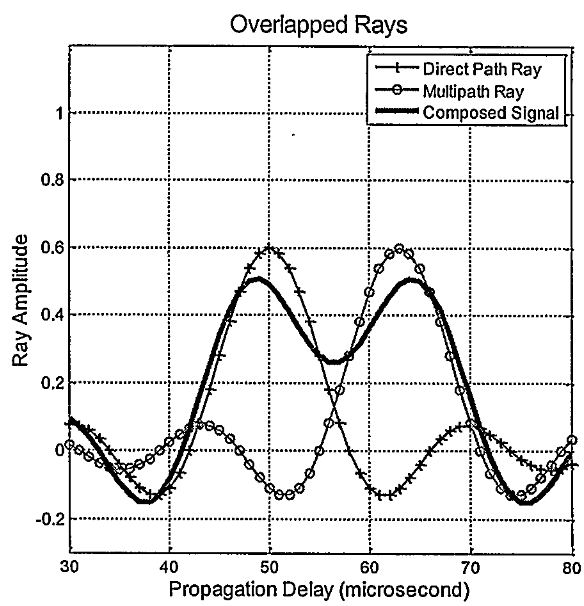

Figure 5 The DP ray leads the MP ray by a time delay larger than the Rayleigh resolution of the system.

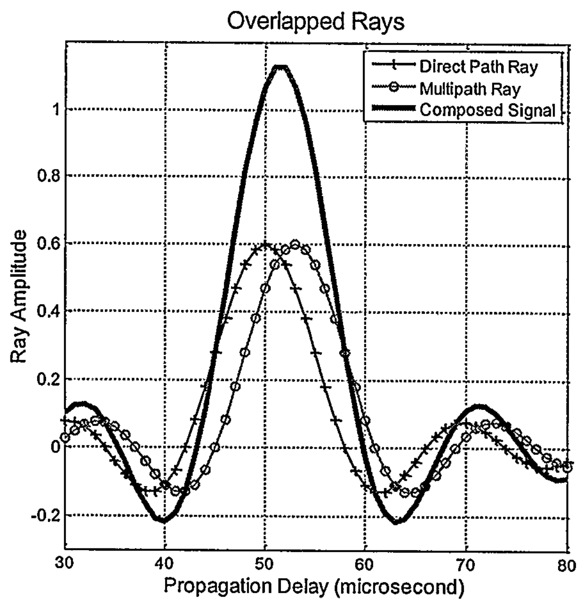

Figure 6 The DP ray leads the MP ray by a time delay less than the Rayleigh resolution.

To separate rays that are spaced closer than the Rayleigh resolution, several super-resolution estimation algorithms have been proposed. Based on their theory of operation, I can classify them into: 1) Least Squares (LS) methods and 2) Sub-space methods. LS methods can introduce significant additional errors when the rays are spaced closer than the Rayleigh resolution due to the noise enhancement that arises from the ill-conditioned nature of the matrices that are involved in the LS operation [1]. In order to overcome the noise enhancement problem related to LS methods, sub-space approaches have been introduced. In sub-space methods, the received signal is split into two orthogonal subspaces known as the signal subspace and the noise subspace using spectral (or Eigen) decomposition, which is based on the Singular Value Decomposition (SVD) algorithm. These approaches show improvement in estimating the propagation delay over the LS approach [1]. However, the orthonormal Eigen vector bases formed by the SVD algorithm assume that the received rays are independent. If some of the rays are partially correlated, which is the case in closely spaced MP rays, the Eigen value matrix is no longer diagonal (i.e. becomes defective), and I therefore cannot reconstruct the received signal due to the shortage of Eigen vectors [6]. Signal decorrelation by smoothing was found in [1] to be helpful but not efficient in the use of the observation data. MUltiple Signal Identification and Classification (MUSIC), one of the super-resolution algorithms, is based on the sub-space methods. Appendix A discusses MUSIC and its corresponding signal decorrelation by smoothing [1].

In this chapter, I am going one-step further to consider the correlation between closely spaced rays. I am not only projecting the received signal into two orthogonal sub-spaces: signal and noise, but additionally, in the signal subspace, I propose to conduct a multi-dimensional orthogonal search to guarantee projecting a number of the correlated rays into different orthogonal bases. In order to ensure the sufficiency of the proposed multi-resolution orthogonal search, at each step, the Mean Square Error (MSE) is minimized to evaluate the contribution of the resolved ray(s). This process is performed using an orthogonal search technique based on the Orthogonal Least Square Regression (OLSR) algorithm. A Fast Orthogonal Search (FOS) technique, which is based on the OLSR algorithm, is discussed in Appendix B.

2.2 Problem Formulation

In this section, I consider signals that are transmitted through a radio channel and which are corrupted only by Additive White Gaussian Noise (AWGN) and by MP. The MP channel is generally modeled as a linear filter. If $s(t)$ is the transmitted lowpass equivalent signal, then over a MP channel, the received lowpass equivalent signal, $r(t)$, can be modeled as

$$r(t) = \sum_{k=1}^{M} a_k s(t - \tau_k) e^{j\theta_k} + n(t) \tag{1}$$

where

M	is the number of MP arrivals,
a_k	is the amplitude of the k^{th} arrival,
τ_k	is the time delay of the k^{th} arrival,
θ_k .	is the phase of the k^{th} arrival,
$n(t)$	is the AWGN.

Of interest here is that the received signal is the sum of a number of scaled, phase shifted, and time delayed replicas of the transmitted signal. Without loss of generality, I will assume throughout the thesis that $\tau_1 < \tau_2 < \cdots < \tau_M$, and that the time delay τ_1, of the first replica, $\boldsymbol{s}_1$, is the desired value to be estimated.

I can rearrange the sampled version of (1) into a matrix form

$$\underbrace{\begin{bmatrix} r(t_1) \\ r(t_2) \\ \vdots \\ r(t_N) \end{bmatrix}}_{\substack{N\times 1 \\ \boldsymbol{R}}} = a_1 e^{j\theta_1} \underbrace{\begin{bmatrix} s(t_1-\tau_1) \\ s(t_2-\tau_1) \\ \vdots \\ s(t_N-\tau_1) \end{bmatrix}}_{\substack{N\times 1 \\ \boldsymbol{s}_1}} + a_2 e^{j\theta_2} \underbrace{\begin{bmatrix} s(t_1-\tau_2) \\ s(t_2-\tau_2) \\ \vdots \\ s(t_N-\tau_2) \end{bmatrix}}_{\substack{N\times 1 \\ \boldsymbol{s}_2}} + \cdots$$

$$+ a_M e^{j\theta_M} \underbrace{\begin{bmatrix} s(t_1-\tau_M) \\ s(t_2-\tau_M) \\ \vdots \\ s(t_N-\tau_M) \end{bmatrix}}_{\substack{N\times 1 \\ \boldsymbol{s}_M}} + \underbrace{\begin{bmatrix} n(t_1) \\ n(t_2) \\ \vdots \\ n(t_N) \end{bmatrix}}_{N\times 1} \qquad (2)$$

where $t_1, t_2, \dots, t_N$ are the sampling times.

Equivalently,

$$\underbrace{\boldsymbol{R}}_{N\times 1} = \underbrace{\boldsymbol{S}}_{N\times M} \underbrace{\boldsymbol{A}}_{M\times 1} + \underbrace{\boldsymbol{N}}_{N\times 1} \qquad (3)$$

where

$\boldsymbol{R} = [r(t_1) \quad \cdots \quad r(t_N)]^T$ is a vector form of the sampled received signal,

$\boldsymbol{S}$ is an $N \times M$ matrix, which represents the M delayed replicas of the transmitted signal,

$\boldsymbol{A} = [a_1 e^{j\theta_1} \quad a_2 e^{j\theta_2} \quad \cdots \quad a_M e^{j\theta_M}]^T$, is a vector, which represents the amplitude and the phase of the M arrival rays, and

$N = [n(t_1) \quad \cdots \quad n(t_N)]^T$, is a vector form of the sampled noise.

$\boldsymbol{S}$ can be rearranged, so that $\boldsymbol{S} = [\boldsymbol{s}_1 \quad \cdots \quad \boldsymbol{s}_M]$, where $\boldsymbol{s}_k = [s(t_1 - \tau_k) \quad s(t_2 - \tau_k) \quad \cdots \quad s(t_N - \tau_k)]^T, 1 \leq k \leq M,$

2.3 The Proposed Multi-Resolution Estimation (MRE) Technique

In this section, the proposed MRE technique is explored. The OLSR algorithm, which is the core algorithm of the orthogonal search in the proposed technique, is customized for the problem at hand.

2.3.1 Orthogonal Search: the OLSR algorithm

The OLSR algorithm is a forward regression procedure used to select a suitable set of regressors or bases, from a large set of candidates. It involves the transformation of the set of bases vectors, $\boldsymbol{s}_k$, into a set of orthogonal basis vectors 1D at a time, and thus makes it possible to calculate the individual contribution of each basis vector to the problem at hand. At each step, the newly added basis vector is examined in order to maximize its contribution toward our desired goal of estimating the time delay τ_1. Therefore, the problem of oversized and ill-conditioned matrices associated with the LS method, can be automatically avoided [7].

In OLSR, the basis matrix $\boldsymbol{S}$ is decomposed into

$$\underbrace{\boldsymbol{S}}_{N\times M} = \underbrace{\boldsymbol{W}}_{N\times M}\ \underbrace{\boldsymbol{T}}_{M\times M} \tag{4}$$

where

$\boldsymbol{T}$ is an upper triangle matrix with 1's on the diagonal, and zeros below the diagonal, and

$\boldsymbol{W}$ is an $N \times M$ matrix with its k^{th} column $\boldsymbol{w}_k = [w_1 \quad w_2 \quad \cdots \quad w_N]^T$ chosen to be orthogonal to the other columns of $\boldsymbol{W}$ for $k = 1, \dots, M$.

Any orthogonal decomposition method such as Gram-Schmidt (GS), modified GS, QR factorization, or Householder transformation can be used to decompose $\boldsymbol{S}$ in (4). Using (4) in (3), I obtain:

$$\underbrace{\boldsymbol{R}}_{N\times 1} = \underbrace{\boldsymbol{W}}_{N\times M}\ \underbrace{\boldsymbol{T}}_{M\times M}\ \underbrace{\boldsymbol{A}}_{M\times 1} + \underbrace{\boldsymbol{N}}_{N\times 1} \tag{5}$$

$$\underbrace{\boldsymbol{R}}_{N\times 1} = \underbrace{\boldsymbol{W}}_{N\times M}\ \underbrace{\boldsymbol{G}}_{M\times 1} + \underbrace{\boldsymbol{N}}_{N\times 1} \tag{6}$$

where $\boldsymbol{G} = \boldsymbol{T}\boldsymbol{A}$ is an $M \times 1$ vector.

The LS solution $\widehat{\boldsymbol{G}}$ for $\boldsymbol{G}$ in (6) is given by

$$\underbrace{\widehat{\boldsymbol{G}}}_{M\times 1} = (\underbrace{\boldsymbol{W}^T}_{M\times N}\ \underbrace{\boldsymbol{W}}_{N\times M})^{-1}\ \underbrace{\boldsymbol{W}^T}_{M\times N}\ \underbrace{\boldsymbol{R}}_{N\times 1} \tag{7}$$

or equivalently, the k^{th} element $\hat{g}_k$ of $\widehat{\boldsymbol{G}}$ is given by

$$\hat{g}_k = \frac{\boldsymbol{w}_k^T \boldsymbol{R}}{(\boldsymbol{w}_k^T \boldsymbol{w}_k)} \tag{8}$$

The geometrical interpretation of (8) can be described as the projection of the matrix $\boldsymbol{R}$ into its new basis vectors $\boldsymbol{w}_k$.

The number M of basis vectors, $\boldsymbol{w}_k$, selected on $\boldsymbol{W}$ is determined based on a stopping criterion. In general, there are three possible stopping criteria in the OLSR:

1) An acceptable MSE is reached:

$$\text{MSE} = \boldsymbol{R}^T \boldsymbol{R} - \sum_{k=1}^{M} g_k^2\, \boldsymbol{w}_k^T \boldsymbol{w}_k \tag{9}$$

2) A specific number, M, of terms is selected, or

3) When none of the remaining candidate basis vectors yields a sufficient MSE reduction.

At the k^{th} step, the size of the space spanned by the selected vector, $\boldsymbol{w}_k$, is increased from $k-1$ to k by introducing a new basis vector. The newly added basis vector further reduces the MSE. Let us define a function, $\mathrm{O}_{1\mathrm{D}}$, that measures the contribution of the newly added basis vector. The reduction of the MSE, which is given by (9), indicates the contribution of the newly added basis vector $\boldsymbol{w}_k$:

$$\mathrm{O}_{1\mathrm{D}} = g_k^2 \boldsymbol{w}_k^T \boldsymbol{w}_k \tag{10}$$

The value of $\mathrm{O}_{1\mathrm{D}}$ has to be evaluated for a candidate to be selected in the system model [7].

2.3.2 The Multi-Resolution Estimation (MRE) Procedure

In the previous section, I explored how to project the received signal into orthogonal vectors, and hence decompose the received signal into independent rays. In this section, I explore the 1D level and the 2D level of the MRE technique.

The 1D level of the Multi-Resolution Estimation (MRE) Technique

The aim of the 1D level is 1) to increase the sensitivity of the ML estimator and 2) to resolve MP rays that are separated in their arrival times by more than the duration of the Rayleigh resolution of the system relative to the first arrival ray. The procedure is as follows:

Step 1: Form the set $\mathcal{S} = \{\boldsymbol{s}_1, \boldsymbol{s}_2, \dots, \boldsymbol{s}_{\mathrm{M}}\}$ of all candidates $\boldsymbol{s}_1, \boldsymbol{s}_2, \dots, \boldsymbol{s}_{\mathrm{M}}$, which correspond to the time delays $\tau_1, \tau_2, \dots, \tau_{\mathrm{M}}$, respectively.

Step 2: Determine their corresponding weights $\hat{g}_1, \hat{g}_2, \dots, \hat{g}_{\mathrm{M}}$ as follows:

$$\hat{g}_1 = \frac{\boldsymbol{s}_1 \boldsymbol{R}}{\boldsymbol{s}_1^T \boldsymbol{s}_1}, \qquad \hat{g}_2 = \frac{\boldsymbol{s}_2 \boldsymbol{R}}{\boldsymbol{s}_2^T \boldsymbol{s}_2}, \qquad \cdots, \qquad \hat{g}_{\mathrm{M}} = \frac{\boldsymbol{s}_{\mathrm{M}} \boldsymbol{R}}{\boldsymbol{s}_{\mathrm{M}}^T \boldsymbol{s}_{\mathrm{M}}}$$

Step 3: Choose the candidate in $\mathcal{S} = \{\boldsymbol{s}_1, \boldsymbol{s}_2, \dots, \boldsymbol{s}_{\mathrm{M}}\}$ that maximizes the function $(\hat{g}_i)^2 \boldsymbol{s}_i^T \boldsymbol{s}_i$. I will refer to such candidate as $\boldsymbol{w}_1 \in \mathcal{S}$.

Step 4: Orthogonalize the remaining candidates in $\mathcal{S}$ with respect to $\boldsymbol{w}_1$ to obtain the set $\mathcal{W}$ of orthogonal bases vectors, where $\mathcal{W} = \{\boldsymbol{w}_1, \boldsymbol{w}_2, \dots, \boldsymbol{w}_{\mathrm{M}}\}$.

Step 5: Determine the weights $\hat{g}_1', \hat{g}_2', \dots, \hat{g}_M'$, corresponding to $\boldsymbol{w}_1, \boldsymbol{w}_2, \dots, \boldsymbol{w}_{\mathrm{M}}$ respectively, where

$$\hat{g}_1' = \hat{g}_1, \qquad \hat{g}_2' = \frac{\boldsymbol{w}_2 \boldsymbol{R}}{\boldsymbol{w}_2^T \boldsymbol{w}_2}, \qquad \cdots, \qquad \hat{g}_M' = \frac{\boldsymbol{w}_{\mathrm{M}} \boldsymbol{R}}{\boldsymbol{w}_{\mathrm{M}}^T \boldsymbol{w}_{\mathrm{M}}}$$

Step 6: Arrange the set $\mathcal{W}$ in a descending order according to its $\mathrm{O}_{1\mathrm{D}}$ value, i.e. according to: $(g_1')^2 \boldsymbol{w}_1^T \boldsymbol{w}_1$, $(g_2')^2 \boldsymbol{w}_2^T \boldsymbol{w}_2$, $\cdots$, $(g_{\mathrm{M}}')^2 \boldsymbol{w}_{\mathrm{M}}^T \boldsymbol{w}_{\mathrm{M}}$

Step 7: Use the chosen stopping criterion to estimate M.

Step 8: Choose the time delay that corresponds to the earliest time delay among the M selected candidates as $\hat{\tau}_1^{1D}$, i.e. as the estimated time delay of the DP using a 1D search.

In the case when closely spaced MP rays are present, a multi-dimensional search has to be conducted since the 1D orthogonal search often fails to distinguish between such rays.

The 2D level of the Multi-Resolution Estimation (MRE) Technique

The aim of the proposed 2D level of the MRE technique (i.e. of the 2D orthogonal search) is to resolve closely spaced MP rays. The procedure of the proposed multi-resolution algorithm is as follows:

Step 1: Obtain the time delay estimate $\hat{\tau}_1^{1D}$ of the DP ray using the 1D level of the MRE technique as discussed above.

Step 2: Form a search domain, which consists of two independent search windows: A backward search window to the left of $\hat{\tau}_1^{1\mathrm{D}}$ and a forward search window to the right of $\hat{\tau}_1^{1\mathrm{D}}$. Each search window spans a time duration equal to the Rayleigh resolution, t_R, of the system, i.e. it spans $[\hat{\tau}_1^{1D} - t_R, \hat{\tau}_1^{1D} + t_R]$ as shown in Figure 7. The two search windows correspond to the 2D orthogonal search of the proposed algorithm.

Step 3: Form the set $\mathcal{S}_b = \{\boldsymbol{s}_{1b}, \dots, \boldsymbol{s}_{\mathrm{M}b}\}$ of 1D vectors $\boldsymbol{s}_{1b}, \dots, \boldsymbol{s}_{\mathrm{M}b}$ which correspond to the backward time delays $\tau_{1b}, \tau_{2b}, \dots, \tau_{\mathrm{M}b}$, respectively. Also, form the set $\mathcal{S}_f = \{\boldsymbol{s}_{1f}, \dots, \boldsymbol{s}_{\mathrm{M}f}\}$ of 1D vectors $\boldsymbol{s}_{1f}, \dots, \boldsymbol{s}_{\mathrm{M}f}$ which correspond to the forward time delays $\tau_{1f}, \tau_{2f}, \dots, \tau_{\mathrm{M}f}$, respectively.

Step 4: Form the set $\mathcal{S}^{2D} = \{\cdots, (\boldsymbol{s}_{ib}, \boldsymbol{s}_{jf}), \cdots\}$ of 2D vectors, which consists of all possible combinations of 1D vectors in $\mathcal{S}_b$ and in $\mathcal{S}_f$.

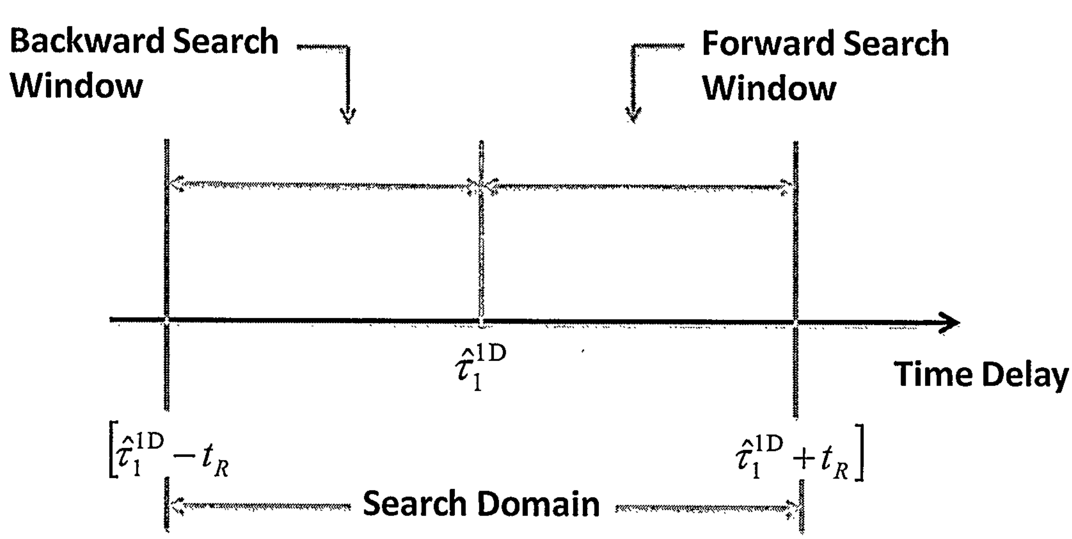

Figure 7 The two search windows for the 2D level of the MRE technique.

Step 5: Orthogonalize each 2D vector in $\mathcal{S}^{2D}$ to obtain a set $\mathcal{W}^{2D} = \{\cdots, (\boldsymbol{w}_{ib}, \boldsymbol{w}_{jf}), \cdots\}$ of orthogonal 2D vectors.

Step 6: Determine the corresponding weights $\hat{g}_{ib}^{2D}$ and $\hat{g}_{jf}^{2D}$ for each 2D vector $(\boldsymbol{w}_{ib}, \boldsymbol{w}_{jf})$, where

$$\hat{g}_{ib}^{2D} = \frac{\boldsymbol{w}_{ib}\boldsymbol{R}}{\boldsymbol{w}_{ib}^{T}\boldsymbol{w}_{ib}}, \qquad \hat{g}_{jf}^{2D} = \frac{\boldsymbol{w}_{if}\boldsymbol{R}}{\boldsymbol{w}_{jf}^{T}\boldsymbol{w}_{jf}}, \qquad \forall\ i,j$$

Step 7: Arrange the set $\mathcal{W}^{2D}$ in a descending order according to its $\mathrm{O}_{2\mathrm{D}}$ value: i.e. according to $(\hat{g}_{ib}^{2D})^2\boldsymbol{w}_{ib}^{T}\boldsymbol{w}_{ib} + \left(\hat{g}_{if}^{2D}\right)^2\boldsymbol{w}_{jf}^{T}\boldsymbol{w}_{jf} \qquad \forall\ i,j.$

Step 8: Choose the set that corresponds to the maximum $\mathrm{O}_{2\mathrm{D}}$ as the set which corresponds to the DP. I will refer to such set as $(\boldsymbol{w}_{ib}, \boldsymbol{w}_{jf})_{opt}$. The time delay $\hat{\tau}_1^{2D}$ that corresponds to the estimated DP is obtained as the backward time delay in $(\boldsymbol{w}_{ib}, \boldsymbol{w}_{jf})_{opt}$.

In the case when no set has sufficiently contributed to the MSE threshold, an upgrade of the search can be conducted. A 3D orthogonal search can be used where two independent backward search windows and one forward search window are selected.

2.4 Simulation Results

In this chapter, I examine the capability of the proposed MRE technique in resolving correlated MP rays through simulation. The simulation parameters are found in Table I.

2.4.1 The 1D level of the Multi-Resolution Estimation (MRE) Technique:

A comparison for the MSE of the time delay estimates between the 1D level of the proposed MRE technique and the conventional peak detector is shown in Figure 8 for different values of Signal-to-Noise Ratio (SNR). When the SNR reaches a certain threshold, the noise generates false peaks that can be larger than the true correlation peak, hence confusing the peak detector and causing outliers. This is referred to as the "threshold effect". Figure 8 shows that the threshold effect for the proposed multi-resolution orthogonal search occurs at 15 dB, while for the conventional peak detector it occurs at 12 dB. This implies that the sensitivity of the proposed 1D orthogonal search outperforms the sensitivity of the peak detector by 3 dB.

A comparison for the Probability of Detection (P_D) between the 1D level of the proposed MRE technique and the peak detector is shown in Figure 9 for different SNR levels. In this simulation, I assume that if the error in the time delay estimate is less than 1.25 μs, then a correct decision (i.e. a correct detection) has been made. Figure 9 shows that the proposed MRE technique has a 3 dB performance improvement over the peak detector.

2.4.2 The 2D level of the Multi-Resolution Estimation (MRE) Technique:

In this chapter, I consider the 2D level of the proposed MRE technique. In the examined scenarios, I consider the case of one MP ray that is correlated to the DP ray and many MP rays that are separated in their arrival time by durations larger than the Rayleigh resolution of the system. In these simulations, I use high SNR levels to compare the performance of the 2D level of the proposed MRE technique with the performance of the peak detector to guarantee that the bias in the time delay estimate of the DP ray is due to correlated MP rays and not caused by the threshold effect. Table II to IV compare the error in the time delay estimates for the 2D level of the proposed MRE technique with that of the MLE for various delays and phase shifts between the DP and the MP. These results corresponds to a multipath channel with two rays: the DP ray and the MP component. The P_D is defined in Table II to IV as the probability of detecting the two rays (i.e. the DP ray and the MP component). Table II to IV show that the peak detector has a TOA eror with a mean that is directly proportional to the delay of the MP component.

Table I Simulation Parameters for the Positioning Layer

Parameter	Value
Rayleigh resolution of the system	1 μs
system bandwidth	1 MHz
oversample	8
no. of iterations	10000

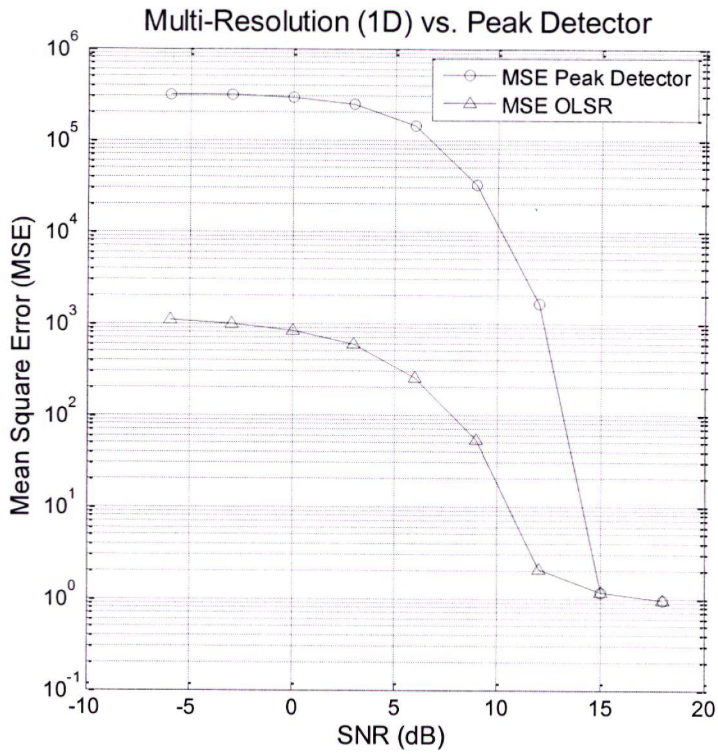

Figure 8 The MSE of the time delay estimation of the 1D of the proposed MRE technique and of the MLE technique.

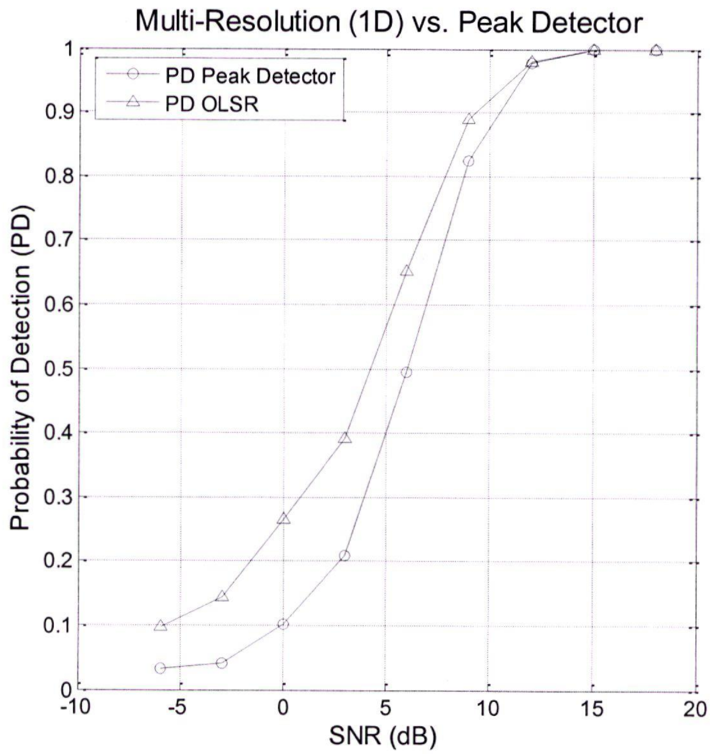

Figure 9 The P_D of the 1D of the proposed MRE technique and for the MLE technique.

Table II MRE vs. MLE, SNR=22 dB, Ration between the DP and the MP component = 6 dB, Phase Difference between the DP and the MP component is 0°

Delay of MP component relative to the DR ray is (ns)	Peak Detector TOA Error Mean in ns	2D MRE TOA Error Mean in ns	Peak Detector TOA P_D	2D MRE TOA P_D
No Mp	-4	-192	0%	0%
250	164	-6	0%	7%
500	336	117	0%	33%
750	512	137	0%	70%
1000	700	12	0%	97%
1250	911	-84	0%	100%
2000	1850	184	100%	100%
3000	3141	-25	100%	100%

Table III MRE vs. MLE, SNR=22 dB, Ration between the DP and the MP component = = 6 dB, Phase Difference between the DP and the MP component is 90°

Delay of MP component relative to the DR ray is (ns)	Peak Detector TOA Error Mean in ns	2D MRE TOA Error Mean in ns	Peak Detector TOA P_D	2D MRE TOA P_D
250	238	-4	0%	20%
500	486	48	0%	80%
750	754	-71	43%	97%
1000	1034	-99	90%	100%
1250	1305	-94	100%	100%
2000	2022	-30	100%	100%
3000	2960	8	100%	100%

Table IV MRE vs. MLE, SNR=22 dB, Ration between the DP and the MP component = = 6 dB, Phase Difference between the DP and the MP component is 180°

Delay of MP component relative to the DR ray is (ns)	Peak Detector TOA Error Mean in ns	2D MRE TOA Error Mean in ns	Peak Detector TOA P_D	2D MRE TOA P_D
250	266	76	0%	7%
500	549	210	17%	57%
750	840	4	67%	97%
1000	1120	-102	100%	97%
1250	1374	-134	100%	100%
2000	2036	-41	100%	100%
3000	2927	7	100%	100%

Table V MRE vs. MLE, SNR=15 dB, Ration between the DP and the MP component = = 6 dB, Phase Difference between the DP and the MP component is 0°

Delay of MP component relative to the DR ray is (ns)	Peak Detector TOA Error Mean in ns	2D MRE TOA Error Mean in ns	Peak Detector TOA P_D	2D MRE TOA P_D
No Mp	5	-157	0%	0%
250	164	-69	0%	3%
500	337	31	0%	20%
750	514	10	0%	40%
1000	704	-104	0%	40%
1250	916	-159	0%	53%
2000	1890	151	17%	57%
3000	2973	-47	80%	50%

Table VI MRE vs. MLE, SNR=15 dB, Ration between the DP and the MP component = = 6 dB, Phase Difference between the DP and the MP component is 90°

Delay of MP component relative to the DR ray is (ns)	Peak Detector TOA Error Mean in ns	2D MRE TOA Error Mean in ns	Peak Detector TOA P_D	2D MRE TOA P_D
250	246	-171	0%	7%
500	500	-140	0%	47%
750	765	-57	7%	70%
1000	1019	-22	27%	80%
1250	1284	12	37%	80%
2000	2018	-7	37%	83%
3000	2971	8	43%	77%

Table VII MRE vs. MLE, SNR=15 dB, Ration between the DP and the MP component = = 6 dB, Phase Difference between the DP and the MP component is 180°

Delay of MP component relative to the DR ray is (ns)	Peak Detector TOA Error Mean in ns	2D MRE TOA Error Mean in ns	Peak Detector TOA P_D	2D MRE TOA P_D
250	273	58	0%	13%
500	577	222	0%	20%
750	859	-1	7%	30%
1000	1139	81	20%	37%
1250	1383	86	30%	47%
2000	2026	-43	43%	50%
3000	2929	-76	43%	67%

2.5 Conclusion

In this chapter, a novel Multi-Resolution Estimation (MRE) technique based on orthogonal search is introduced to enhance the performance of the MLE. More specifically, the proposed technique attempts to resolve the problem of closely spaced rays (i.e. of correlated MP rays), and to estimate their time delays without bias. Simulation results have shown that when the 1D MRE algorithm is used, the sensitivity of the MLE is improved by 3 dB. A comparison between the conventional MLE and the

2D MRE algorithm showed a significant improvement in resolving correlated MP rays in addition to the 3 dB improvement in sensitivity.

Chapter Three: SELECTION LAYER
A NOVEL SKEW-NORMAL OUTLIER DETECTION TECHNIQUE

This chapter deals with the problem of estimating the 2D position of a radio device based on the collection of a number of ranging estimates obtained between the radio device and a number of RSs of known positions.

3.1 Introduction

Different positioning estimation techniques are available, see for example [1][18]. The overall objective of these techniques is to minimize the effect of ranging measurements error on the positioning error. In the previous chapter, I have improved the sensitivity of the Maximum Likelihood range estimator by 3 dB and reduced the effect of multipath on the biasing of the range estimate. In this chapter, I limit once again the sources of error in the ranging estimates to two: 1) AWGN and 2) bias. In other words, I have two scenarios per received delay estimate: A scenario where the propagation delay estimate is unbiased Additive White Gaussian (AWG), and a scenario where the propagation delay estimate is biased AWG. I will refer to the unbiased scenario as the DP scenario, and to the biased scenario as the MP scenario (also known as the NLOS scenario).

Many studies offer a solution for the biased scenario based on estimating an extra parameter, which is the bias in the ranging estimate. Meanwhile, different analytical studies for CRLB show that by detecting and then rejecting biased estimates, position estimates improve considerably [20][21][22]. Hence, different techniques have been developed to detect biased estimates. Generally, the problem of detecting biased estimates is modeled as a binary hypothesis detection problem. The probability density function (pdf) of the ranging measurements under the unbiased hypothesis is usually known except for its mean, which is determined by the true range. If the distribution under the biased hypothesis is also known, then the detection problem can be solved using conventional hypothesis testing. However, the pdf of ranging measurements under the biased hypothesis is usually unknown. Therefore, a detection technique, which does not assume the knowledge of the biased pdf should be developed [23].

In this chapter, a novel selection technique based on the SNOD technique is introduced. The SNOD technique is based on the $\mathcal{S}\mathrm{kew} - \mathcal{N}\mathrm{ormal}$ ($\mathcal{SN}$) distribution, which is a new class of distributions that have not been considered before either in wireless communication nor in wireless location. The $\mathcal{SN}$ class of pdf's extends the Gaussian distribution model by allowing a shape parameter to account for its skewness [29][31][32][33], hence, encompassing a large number of popular distributions as shown below.

3.2 Background

Currently, there are two techniques are used to select RSs to be used to fix the position of a radio device. These techniques are 1) Received Signal Strength (RSS) and 2) Geometrical Dilution of Precision (GDOP). RSS is used by allowing RSs that their RSS at the radio device are exceeding certain threshold.

3.2.1 Geometrical Dilution of Precision

GDOP is a factor that links between the ranging error to the positioning error, as follows

$$P_E = R_E \cdot GDOP \tag{11}$$

where

P_E is the positioning error, and

R_E is the ranging error

Equation (11) implies that I can have different values for the positioning error, P_E, for the same ranging error, R_E, due to GDOP. Figure 10 shows fixed ranging errors for different positioning errors of a receiver with an unknown position using two RSs: RS1 and RS2, with known positions.

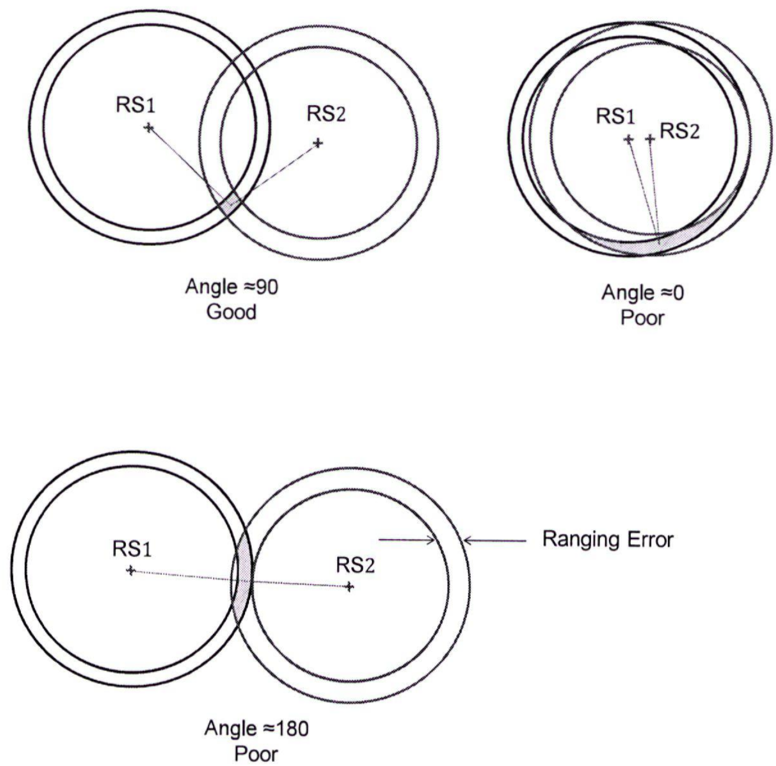

Figure 10 The effect of GDOP is illustrated as a function of the ranging error. The shaded areas are the different positioning errors.

3.2.2 Preliminaries

Consider a simple case of propagation delay estimation, where a radio device (e.g. a mobile device or a GPS receiver) with an unknown location receives a radio signal from a number of RSs with known locations (e.g. Cellular Base-Stations or GPS satellites). Without loss of generality, I will assume in this chapter that the position of the radio device is estimated using hand-set based wireless location. In other words, in this chapter, wireless location is performed based on the delay estimates obtained from all

RSs. Let $\boldsymbol{R} = \{1,2,\cdots,R\}$ be the set of indices of the RSs, whose positions $\{p_r = (x_r, y_r)^T, r \in \boldsymbol{R}\}$ are known. Let $\boldsymbol{NL} = \{k_1, k_2, \cdots, k_N\}$ be a set of biased estimates, which can be relabelled as $\{1,2,\cdots,N\}$. Let the complement of $\boldsymbol{NL}$, be denoted as $\boldsymbol{L} = \boldsymbol{R} - \boldsymbol{NL}$ (i.e.the set of unbiased estimates). The parameters to be estimated are the position $\hat{p} = (x, y)^T$of the radio device and the N propagation induced path length biases, $\boldsymbol{l} = (l_1, l_2, \cdots, l_N)^T$, with $l_i > 0,\ \forall i,\quad i = 1, \cdots, N$. For convenience, I define an $(N+2)$-dimensional vector θ by concatenating the unknown p and $\boldsymbol{l}$ parameters.

$$\boldsymbol{\theta} \equiv (x, y, l_1, l_2, \cdots, l_N)^T \tag{12}$$

A delay estimate can be approximated as

$$\hat{\tau}_r = \tau_r + n_r, \quad \text{for} \quad r \in \boldsymbol{R} \tag{13}$$

where the delay τ_r is

$$\tau_r = \frac{1}{c}\left(\sqrt{(x_r - x)^2 + (y_r - y)^2} + l_r\right), \quad \text{for} \quad r \in \boldsymbol{R} \tag{14}$$

with $l_r = 0$ for $r \in \boldsymbol{L}$, and the estimation error n_r in (12) conforms to a Gaussian distribution $\mathcal{N}(0, \sigma_r^2)$ with zero mean and variance σ_r^2.

This leads the r^{th} unbiased estimates to have a Gaussian pdf $\mathcal{N}(\mu_{DP}, \sigma_{DP}^2)$ with mean μ_{DP} and variance σ_{DP}^2 where μ_{DP} is the true range $\sqrt{(x_r - x)^2 + (y_r - y)^2}$, assumed in this chapter to be a deterministic unknown quantity. On the other hand, the i^{th} biased estimate must have a Gaussian pdf $\mathcal{N}(\mu_{MP,i}, \sigma_{MP,i}^2)$, where the mean $\mu_{MP,i} = \mu_{MP,i} + l_i$, for $i = 1, \cdots, N$. In the following analysis, I assume that no a priori statistic of $\boldsymbol{l} = (l_1, l_2, \cdots, l_N)^T$ is available.

A literature review is carried out in the following subsections. Previously proposed statistical models for the NLOS environment are reviewed in subsection 3.3 followed by their corresponding detection techniques in subsection 3.4.

3.3 Distributions Models for the biased estimates

Knowing the distribution model for the biased estimates can give insight about the best detection technique to use and its corresponding threshold value. There are two sources of bias in the range estimate as discussed in chapter two. The first source is due to MP and the second is due to the threshold effect. In this chapter, I will deal uniquely with MP. Therefore, in this section, I review previous studies in modeling the pdf distributions of MP. The Rician model and by extension the Rayleigh model have been suggested to model the pdf of MP signals [34]. Rician and Rayleigh distributions are based on some key assumptions. For both models, a large number of independent components are presumed to be received, with unknown amplitudes and random phases. Another key assumption behind the Rician model is that the DP signal is present. In most cases, DP signals are visible, but generally shadowed due to propagation through building materials. Therefore, the lognormal distribution is used to model shadowing. A statistical distribution called a Loo distribution combines the MP characteristic of Rayleigh fading with a lognormal distribution for the shadowed DP signal [34]. Considering the application of Loo`s pdf distribution for MP, some improvement over the Rician model is possible because the Loo distribution accounts for a shadowed signal. A Karasawa Three State Fade Model (KTSFM) consisting of a weighted distribution of Rayleigh, Rician, and Loo functions is proposed in [34]. A modified version of KTSFM called Urban Three State Fade Model (UTSFM) is proposed in [34]. An evaluation of the KTSFM and of the UTSFM can be found in [34].

Numerical analysis has also been conducted to further examine the CRLB in the presence of MP signals. CRLB is the inverse of the Fisher Information Matrix (FIM). It is found that the FIM becomes generally singular in the presence of MP signals, making its inverse non-existent, i.e. there can be no guarantee of a finite error variance [20]. Based on the singularity of the FIM, [20] suggests to model the MP distribution as a "half-Gaussian" distribution because the distribution must have a local maximum. Another analytical study suggests modeling the MP distribution as a Gamma distribution due to the nonnegative nature of the additive MP bias [21][35][36].

3.4 Detection of Multipath (MP) signals

3.4.1 Theoretical Decision Approach

[37] proposes a theoretical decision framework for the detection of MP signals. The analysis assumes a complete lack of characterization of the MP signal, hence, the approach in [37] relies on the fact that the variance of the MP signals is greater than that of the DP signals. Therefore, the hypothesis testing can be based on

$$\begin{aligned} H_0&:\ \sigma^2 = \sigma_{DP}^2 \\ H_1&:\ \sigma^2 = \sigma_{MP}^2 \end{aligned} \tag{15}$$

The unbiased estimator using sample variance estimates is given by:

$$\hat{\sigma}^2 \underset{H_0}{\overset{H_1}{\gtrless}} \gamma \tag{16}$$

where

γ is an unknown threshold value to be found. If I consider H_1 such that $\hat{\sigma}^2 > \sigma_{DP}^2$, then $\gamma = \sigma_{DP}^2$.

3.4.2 Non-Parametric Approach

This approach has been proposed by [23]. In this case, the hypothesis testing is based on:

$$\begin{aligned} H_0: &\quad g(r) = g_{DP}(r) = r + n_r \\ H_1: &\quad g(r) = g_{MP}(r) = r + n_r + e_i \end{aligned} \tag{17}$$

where

e_i corresponds to the bias.

The pdf of the noise, n_r, is given by $f_n(x)$, which is completely known. Thus, the pdf of the measurements in the DP hypothesis case is given by $f_n(x - r)$. Note that this distribution is completely known except for one parameter,r, which affects only the mean of the distribution. The main idea in the non-parametric MP detection technique is to compare the closeness of this pdf to the pdf of the range measurements. Thus, [23] first approximates the pdf of the range measurements non-parametrically, then it compares the closeness of this pdf to the DP pdf by defining a distance metric, and finally it decides on a DP hypothesis versus a MP one after a threshold test.

3.4.3 Statistical Approach

Since MP signals add a large positive bias to the true range, it can be expected that the measured range has a skew distribution [38][39]. To test if MP signals are present, certain outlier tests can be employed as shown below.

<u>Skewness and Kurtosis Test:</u>

When a normal sample with an unknown mean contains some observations, which have a shift in the mean (also unknown) in the same direction, the locally best invariant single-sided test for detecting MP signals is the Skewness test. The third moment of skewness test is based on the *skewness*, which is defined as:

$$Skewness = \frac{1}{T_s}\sum_{i=1}^{T_s}\left(\frac{x_i-\bar{x}}{\sigma}\right)^3 \qquad (18)$$

where

T_s is the number of x_i samples

$\bar{x}$ is the average of the samples

σ is the standard deviation

When the *Skewness* is greater than zero, the data is skewed to the right of the mean and vice versa. When less than 21% of the observations are normal with a shift in the mean, regardless of direction, then the Kurtosis test, which is based on the fourth moment, is the locally best invariant test for detecting outliers. In other words, the Kurtosis test is based on the value of the *Kurtosis*, which is defined as:

$$Kurtosis = \frac{E(x_i-\mu)^4}{\sigma^4} \tag{19}$$

where μ is the mean value of x_i

The Skewness and Kurtosis tests lead to acceptance or rejection of one of the hypotheses at some significant level. However, while using moment based tests, problems might arise when a skewed distribution has odd moments of zero or when a non-normal density has a kurtosis of three, similar to a Gaussian distribution [39].

Reliability Analysis (A posterior Outlier Detection):

From normal probability theory, residuals are expected to be small and randomly distributed. Although residual sizes can suggest observational errors, they do not necessarily identify the observations that contain outliers. This is due to the fact that Least Squares (LS), which is a common estimation method used in wireless location, generally spreads a large observational error or outliers out radially from its source.

However, this condition is not unique to LS since any closed form estimation method will also spread a single observational error throughout the entire observational set [73].

3.5 Problem Formulation Based on the Skew-Normal Distribution

A detection problem is considered in this section. The radio device to be located receives a radio signal transmitted from a number of RSs. The best location estimate of the radio device is obtained by processing the delay estimates obtained only from DP signals.

In this section, I propose to use a new type of distribution called the $\mathcal{SN}$ distribution [40]. $\mathcal{SN}$ refers to a parametric class of probability distributions which includes the Gaussian distribution among others. The $\mathcal{SN}$ class of densities extends the normal distribution model by allowing a shape parameter to account for its skewness [40][43][44]. In this chapter, the pdf of the $\mathcal{SN}$ distribution is given by

$$f(x;\sigma,\mu,\lambda) = \frac{2}{\sigma}\varphi\left(\frac{x-\mu}{\sigma}\right)\Phi\left(\lambda\frac{x-\mu}{\sigma}\right) \tag{20}$$

where φ and Φ represent the pdf and the cumulative density function (cdf) of the Gaussian distribution, respectively, and λ is a real number which indicates the skewness of the distribution. If λ is a positive number, the $\mathcal{SN}$ distribution is positively skewed, while a negative λ indicates that the $\mathcal{SN}$ distribution is negatively skewed.

The $\mathcal{SN}$ distribution, due to its mathematical tractability and inclusion of the standard normal distribution, has attracted a lot of attention in the statistical literature. [32][33] discuss basic mathematical and probabilistic properties of the $\mathcal{SN}$ distribution. [41][45] focus on the theoretical developments of varies extensions and multivariate generalizations of the $\mathcal{SN}$ distribution. [47] tabulates the cdf of the $\mathcal{SN}$ distribution and illustrates the use of their table in a goodness-of-fit testing. [48] analyzes the $\mathcal{SN}$ distribution based on the Bayes approach. The $\mathcal{SN}$ distribution was found to be quite useful in modeling real data in [41]. There is a growing statistical literature focused on the use of sampling models that are able to capture the non-Gaussian behaviour of real data [31].

Some basic properties of the $\mathcal{SN}$ distribution are as follows [29][42] :

1) When $\lambda = 0$, the $\mathcal{SN}(\mu, \sigma, \lambda)$ distribution becomes a Gaussian distribution $\mathcal{N}(\mu, \sigma)$.

2) When $\lambda \longrightarrow \pm\infty$, the $\mathcal{SN}(\mu, \sigma, \lambda)$ distribution tends to the half-normal distribution.

3) For any positive value of λ, the $\mathcal{SN}(\mu, \sigma, \lambda)$ can be modeled as a positively skewed distribution. Therefore, the $\mathcal{SN}$ distribution matches the analytical derivations and the experimental studies, in which:

i. When only DP signals are present, its distribution is Gaussian, which is the case when $\lambda = 0$,

ii. When MP signals are present, the FIM is singular [20], which is the case when $\lambda \longrightarrow \pm\infty$, since in this case, the corresponding distributions are half-normal.

iii. One of the analytical studies [35] assumed that the distribution in the case of MP signals belong to a Gamma distribution, while many experiments modeled the MP distribution as other distributions as discussed above. All such distributions can be grouped under the class of the $\mathcal{SN}$ distribution.

This chapter presents a novel SNOD technique based on the $\mathcal{SN}(\mu, \sigma, \lambda)$ distribution to be used to detect MP signals.

3.6 The Skew-Normal Outlier Detection (SNOD) Technique

3.6.1 Binary Hypothesis

As mentioned before, I have two scenarios per received delay estimate: A DP scenario where the propagation delay estimate is unbiased AWG, and a MP scenario where the propagation delay estimate is biased AWG. First, I propose to find the six possible location estimates, also referred to as crossings, formed from the intersection of three circles as shown in Figure 11. Three is a minimum number of RSs required to obtain a unique solution for the DS position $p = (x, y)^T$. Each circle in Figure 11 is centered around a RS and its radius corresponds to the time delay estimate of the signal traveling from the RS to the DS. In this chapter, I shall define two types of crossings: clustered crossings and non-clustered crossings. In Figure 11, there are three clustered crossings, shown in a dark color, and three non-clustered crossings, shown in a light color. The two types of crossings originate from the fact that every two intersecting circles cross in a maximum of two points. Over a noiseless DP channel, one of the two intersection points correspond to the position of the radio device while the second correspond to an ambiguity solution. In order to remove the ambiguity, a third circle is required. Over an AWGN DP signal channel, the three clustered crossings are unbiased estimates of the position of the radio device while the three non-clustered crossings are biased estimates of the position of the radio device.

The type of crossings in Figure 11 is not unique. Figure 12 shows a second type of crossings, where there are two sets of clustered crossings. Over an AWGN DP channel, only one set of the clustered crossings correspond to unbiased AWG estimates of the position of the radio device. I will refer to the second set of clustered crossings, which correspond to biased estimates of the position of the radio device, as the set of bifurcating crossings.

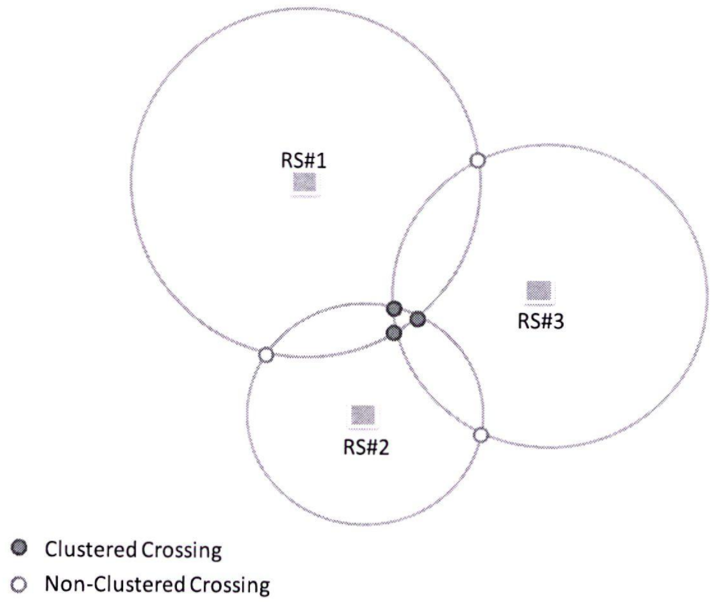

Figure 11 The six possible location estimates, crossings, are formed from the intersection of three circles each formed around one RS with the radius of each circle corresponding to its respective time delay estimate.

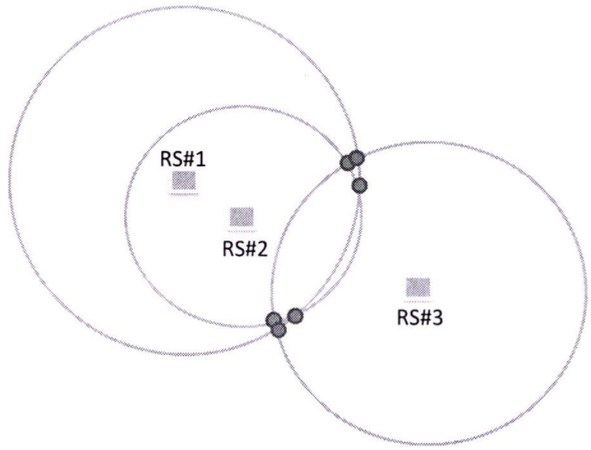

Figure 12 Two cluster sets are formed each consisting of three crossings. This scenario occurs due to poor RSs geometry.

Generally speaking, one can have the situation where one or more circles do not intersect. In this chapter, I only consider the case of intersecting circles. Hence, for each set of three RSs, I have a set of six crossings. Each crossing is associated with a position estimate $\hat{p}$ which has two elements: $\hat{x}_p$ and $\hat{y}_p$. I can model $(\hat{x}_p, \hat{y}_p)$ as having a bivariant $\mathcal{SN}$ distribution. For the sake of simplicity, I will talk about $\hat{x}_p$or $\hat{y}_p$ individually as having a univariant $\mathcal{SN}$ distribution defined as $\mathcal{SN}(\mu_p, \sigma_p, \lambda_p)$. If the received signals, which are used to estimate the DS position are DP signals, the pdf of the estimated position, $\hat{p}_{DP}$, belongs to $\mathcal{SN}(\mu_p, \sigma_p, \lambda_p = 0)$. On the other hand, when at least one of the RSs, which is used to locate the radio device, encounters a MP condition, the pdf of the estimated position, $\hat{p}_{MP}$, belongs to $\mathcal{SN}(\mu_p, \sigma_p, \lambda_p)$, where $\lambda_p \neq 0$. Therefore, (16) can be tuned to model the detection problem as follows:

$$
\begin{aligned}
H_0&:\ \lambda_p = 0 \quad ,\hat{p}_{DP} \\
H_1&:\ \lambda_p \neq 0 \quad ,\hat{p}_{MP}
\end{aligned}
\tag{21}
$$

In the next subsection, I investigate the proposed method to distinguish the $\mathcal{SN}$ distributions according to (21).

3.6.2 Test of Skewness

In this section, I discuss the common statistics that are used to define the middle or the center of a distribution. The mean is certainly the best-known center of a distribution, while the median is known to be the middle of the distribution. For a Gaussian distribution, the mean and the median are asymptotically equal i.e. for an infinite number of samples [46]. However, for a finite number of samples, the mean and median are very close but not necessarily equal. In this chapter, I use the difference between the mean and the median to examine the skewness of the distribution of a random variable. In other words, I detect if λ_p is equal to zero or not based on:

$$
|mean - median| \underset{H_0}{\overset{H_1}{\gtrless}} \delta \tag{22}
$$

where

δ is a threshold to be estimated and H_0 and H_1 are defined in (21).

3.7 The Proposed Receiver for Wireless Location

In this section, the four steps of the proposed wireless location receiver as shown in Figure 13 are investigated. The proposed technique is based on the assumption that redundancy exists in the number of RSs that are visible to the radio device to be located. In other words, I assume in this chapter that more than three RSs form intersecting circles.

- Step 1: Generally speaking, the receiver of the radio device is responsible to estimate the time delay corresponding to the DP signal received from each visible RS. I propose in this chapter to use the MRE technique that was proposed in chapter two to estimate the time delay for the signal received from each visible RS.. In this chapter, I shall consider that the MRE provides up to two estimates for the time delay of each received signal: $\hat{\tau}_{i1}$ and $\hat{\tau}_{i2}$. The first estimate $\hat{\tau}_{i1}$ is the value generated from the 1D level of the proposed MRE technique, while the second estimate $\hat{\tau}_{i2}$ is the value generated from the 2D level of the proposed MRE technique. This can be generalized to include any number of estimates generated from any time delay estimator.

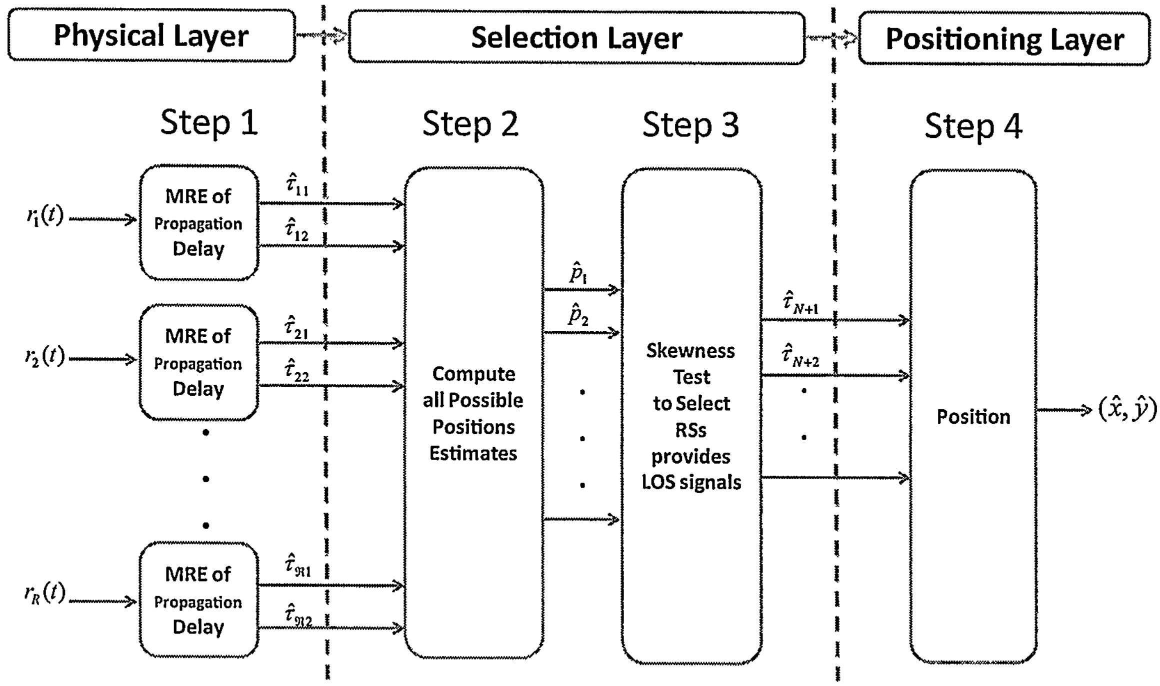

Figure 13 The proposed wireless location receiver.

- Step 2: Using all delay estimates, $\hat{\tau}_{i1}$ and $\hat{\tau}_{i2}$, for $i = 1, \dots, R$ from step 1, a circle centered at each corresponding RS is formed per estimate. Hence, I obtain six crossings for each set of three intersecting circles. Equation (22) gives the number of combinations of three RSs by taking three circles out of a total of n:

$$\frac{n!}{(n-3)!3!} \tag{23}$$

where n is the total number of delay estimates, which is equal to two R according to Figure 13.

- Step 3: For each set of three intersecting circles, detect the three non-clustered crossings using the skewness test. This is accomplished as follows. Given the fact that I have six crossings per three intersecting circles, form all twenty combinations of three crossings out of the six crossings. Perform the skewness test for each one of the twenty combinations of three crossings. If all three circles correspond to DP signals, with no bifurcation crossings, only the three clustered crossings pass the test. If any one of the three circles corresponds to a biased time delay estimate, there will be no combinations of crossings that will pass the skewness test. If all three circles correspond to DP signals with bifurcation crossings, both sets of clustered crossings will pass the skewness test. Hence, the occurrence of bifurcation can be detected. In order to decide which set of clustered crossings is non-bifurcating, two possible treatments are available: 1) ignore such a set of crossings due to its poor geometry, or 2) find the median of the other sets of crossing combinations that do not bifurcate and choose from the set of crossings which are encountering bifurcation the set of crossings that are close to such a median value.

Sometime, I encounter the special case where two of the circles with outliers, are approximately equal in magnitude but of opposite directions. In this case, different sets of crossings will pass the skewness test. If this happens, the RS selection process encounters a conflict in selecting the RSs, hence, a second stage test, which tests the standard deviation of the selected sets has to be conducted.

The standard deviation examines the dispersion of the data. Hence, the set, which has two outliers with approximately equal magnitude but opposite directions, is expected to have a smaller standard deviation.

- Step 4: In this step, the selected RSs from step three are used to find a final location estimate. When the number of selected RSs is three, a unique solution is available. When the number of selected RSs is less than three, an infinite number of solutions is available. When the number of selected RSs is more than three, no solution is available. In the last case, a Least Square Estimator (LSE) can be used to find a solution after linearizing (13). This is discussed further in chapter five.

The four steps in the SNOD technique are illustrated through the following three examples.

***Example 1*:**

Step 1: Consider the case of four intersecting circles $\{C_1, C_2, C_3, \text{and } C_4\}$.

Step 2: Compute all sets of six crossings, using three circles per set.

Set 123:	C_1	C_2	C_3
Set 124:	C_1	C_1	C_4
Set 134:	C_1	C_3	C_4
Set 234:	C_2	C_3	C_4

Step 3: Perform a skewness test for each of the twenty combinations of three crossings for Set 123. If a combination passes the skewness test, hence this combination can be used to estimate the true position of the radio device. By repeating the skewness test for Set 124, Set 134, and Set 234, I obtain all combinations that pass the skewness test.

Step 4: All combinations identified from the last step are used to find the final position estimate for the radio device using LSE.

Example 2:

Step 1: Consider the case of five intersecting circles $\{C_1, C_2, C_3, C_4 \text{and } C_5\}$, where $\{C_4 \text{and } C_5\}$ corresponds to the same RS, say RS4 (i.e. the circle C_4 has a radius $\hat{\tau}_{41}$ and the circle C_5 has a radius $\hat{\tau}_{42}$).

Step 2: Compute all sets of six crossings, using three intersecting circles per set.

Set 123:	C_1	C_2	C_3
Set 124:	C_1	C_2	C_4
Set 125:	C_1	C_2	C_5
Set 134:	C_1	C_3	C_4
Set 135:	C_1	C_3	C_5
Set 145:	$\times$	$\times$	$\times$
Set 234:	C_2	C_3	C_4
Set 235:	C_2	C_3	C_5
Set 245:	$\times$	$\times$	$\times$
Set 345:	$\times$	$\times$	$\times$

Notice that $\{C_4 \text{and } C_5\}$ are not used simultaneously in one set. Step 3 and Step 4 are the same as in the previous example.

Example 3:

Consider the case of five circles used to estimate the position of a radio device. In this example, I would like to consider two methods for Step 2: Method A: choose sets of three circles to fix the position of the radio device, and Method B: choose sets of four circles to fix the position of the radio device. The robustness of the two cases is investigated here:

Case I: Only one biased time delay estimate is present,

Case II: Two biased time delay estimates are present.

Step 2: Method A: choosing all sets of three circles, I have eight sets: Set 123, Set 124, Set 125, Set134, Set 135, Set 234, Set 235, and Set 345.

Method B: choosing all sets of four circles, I have five sets: Set 1234, Set 1235, Set 1245, Set 1345, and Set2345

- Case I: One biased time delay estimate exists corresponding to C_1
  - In Method A: Set 234, Set235, and Set 345 will pass the skewness test performed in Step 3, and three circles will be selected in Step 4.
  - In Method B: Only Set2345 will pass the skewness test performed in Step 3, and Step 4 will not add anything in this case.

- Case II: Two biased time delay estimate exist corresponding to C_1 and C_2
  - In Method A: Only Set 345 will pass the skewness test performed at Step 3, and Step 4 will not add anything in this case.
  - In Method B: no sets will pass the skewness test performed in Step 3.

Example 3, shows that by choosing the minimum number of RSs (i.e. three) provides for better RS selectivity and therefore, provides for better robustness against biased time delay estimates.

This can be explained from the following simple rule

$$n_b \leq n - n_i \tag{24}$$

where

n_b is the number of biased circles to be detected

n_i is the number of intersecting circles in Step 2.

n is the total number of circles, RSs.

In order to maximize n_b, n_i must be minimized which in this case, corresponds to three.

3.8 Simulations

In this section, I examine the performance of the proposed SNOD technique through simulations. The parameters of the simulation environment are summarized in Table VIII.

Throughout the simulations, the four steps described in the last section are followed, using $n_i = 3$, hence generating six crossings in Step 2.

Table VIII Simulation Environment for Selection Layer

Parameter	Value
BW	50 MHz
Tx Power	0 dBm
large time delay error (outlier)	$2 - 8$ μs
position of RS1	(0,0) m
position of RS2	(10,150) m
position of RS3	(120,900) m
position of RS4	(500,700) m
position of DS	(30,300) m

In this section, I investigate the performance of the SNOD technique with respect to the Probability of Detection (P_D) and the Probability of False Alarm (P_{FA}). In this chapter, I use two different types of probability of detection: 1) the Probability of total Detection (P_{D_t}) which is defined as the probability of detecting all DP RSs and rejecting all RSs that are encountering MP signals, and 2) the Probability of partial Detection (P_{D_p}) which is defined as the probability of detecting some DP RSs.

3.8.1 Only One Circle per RS

Figure 14 to Figure 18 examine the SNOD technique for four RSs when there is zero, one, two, three, or four outliers, respectively. The threshold value is chosen to keep the P_{FA} below 10%. I can see from Figure 14 that the P_{D_t} for the RSs that are not encountering an outlier is over 95%, while the P_{D_p} is 100% in this case. Figure 15 shows that the P_{D_p} is almost 93% while the P_{D_t} reaches 40% when a MP signal follows the LOS signal by 3 μs. The P_{D_t} reaches 65% when the MP signal follows the LOS signal by 8 μs. Figure 16 shows that for two outliers, the P_{D_p} after 0.06 μs is 100%, while the P_{D_t} reaches 80% and 90% when the MP signal follows the LOS signal by 4 and 8 μs, respectively. Figure 17 and Figure 18 show that as the number of outliers increases the P_{D_t} also increases. As I can see in Figure 17 that at 1 μs with three outliers, the P_{D_t} reaches 65%, while for four outliers, the P_{D_t} reaches 75% as shown in Figure 18. The P_{D_p} for two, three, or four outliers are all almost the same.

3.8.2 Multiple Circles per RS

Figure 19 to Figure 21 examine the performance of the SNOD technique in the presence of multiple propagation delay estimates for a RS. In these three simulations, I consider three RSs, in which multiple delay estimates are available. Figure 19 shows the performance of the SNOD technique when I have three RSs, one of them with two delay estimates. Figure 19 shows that the P_{FA} is less than 5%, while the P_{D_p} is almost 98%. The P_{D_t} increases as the MP signal is delayed from the actual LOS signal. One can see that the P_{D_t} reaches 68%, when the MP signal is delayed around 1.2 μs. Figure 20 shows the performance of SNOD technique when two RSs have two propagation delay estimates. The P_{FA} is less than 10%, while the P_{D_p} is almost 92%. The P_{D_t} reaches 52%, when the MP signal is delayed by 3 μs. Figure 21 shows the performance of SNOD technique when three RSs have two propagation delay estimates. The P_{FA} is less than 10%, while the P_{D_p} is almost 94%. The P_{D_t} reaches 55%, when the MP signal is delayed by 5 μs relative to the actual DP signal.

3.8.3 Up to Two Circles per RS

Figure 22 shows the performance of the SNOD technique for four RSs. One of these RSs has an outlier, while another RS has two propagation delay estimates. The P_{FA} is less than 10%, while the P_{D_p} is almost 94%. The P_{D_t} reaches 55%, when the MP signal is delayed by 2 μs relative to the actual DS signal.

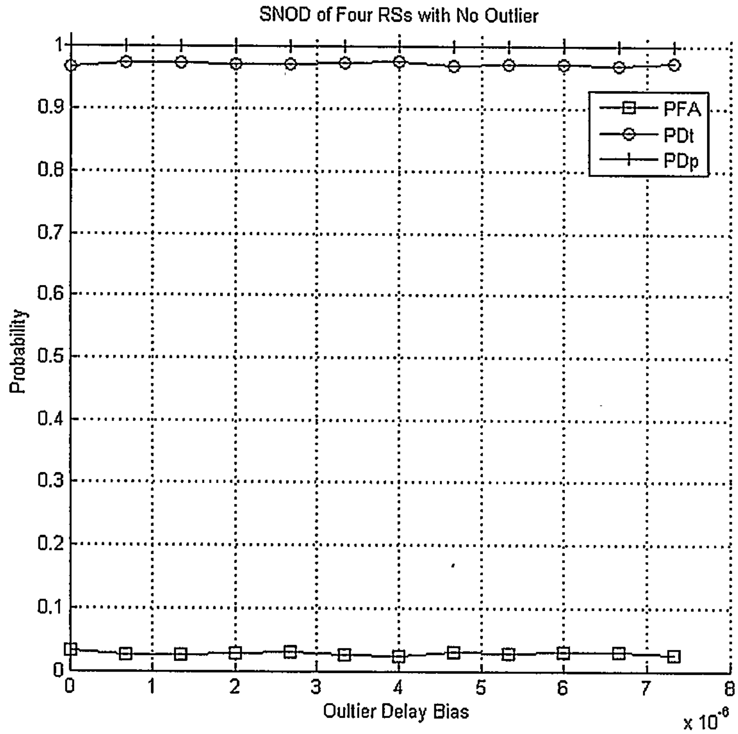

Figure 14 The P_{FA}, P_{D_t} and P_{D_p} for four RSs with no outlier.

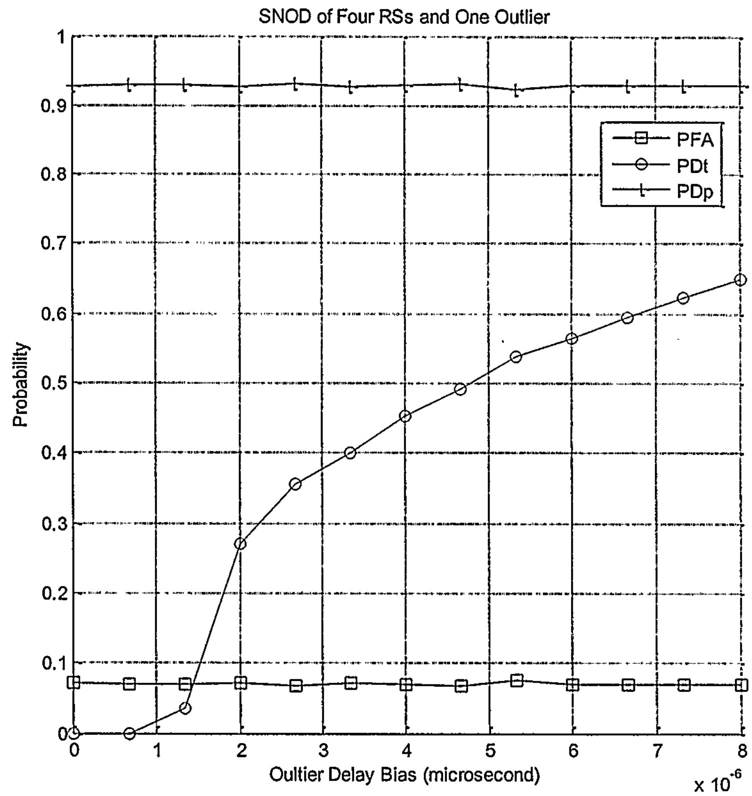

Figure 15 The P_{FA}, P_{D_t}, and P_{D_p} for four RSs with one outlier.

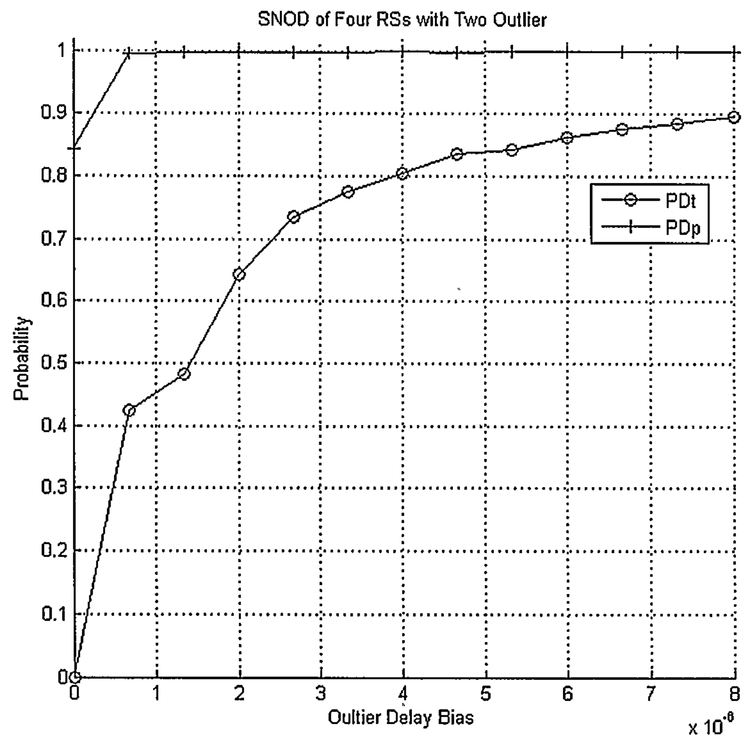

Figure 16 The P_{D_t} and P_{D_p} for four RSs with two outlier.

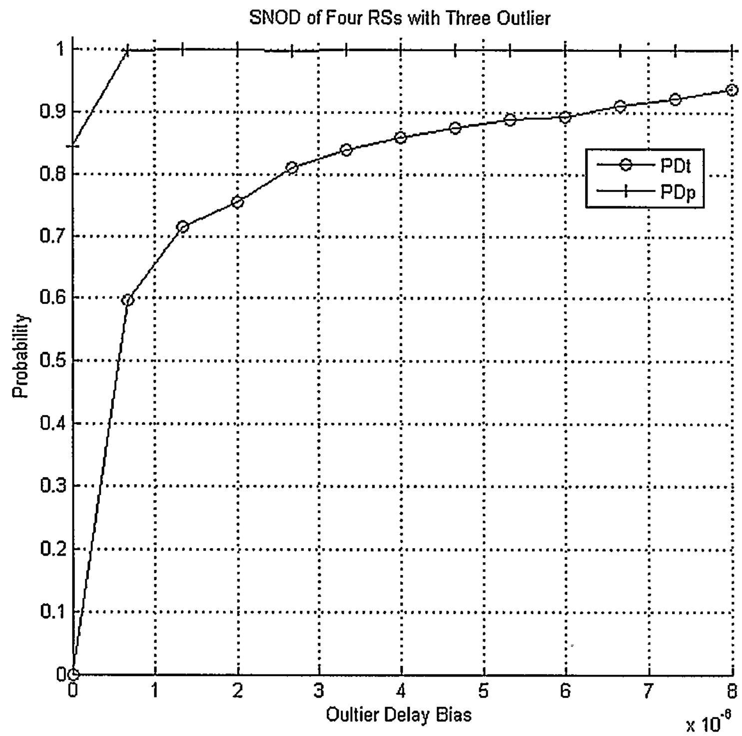

Figure 17 The P_{D_t} and P_{D_p} for four RSs with three outlier.

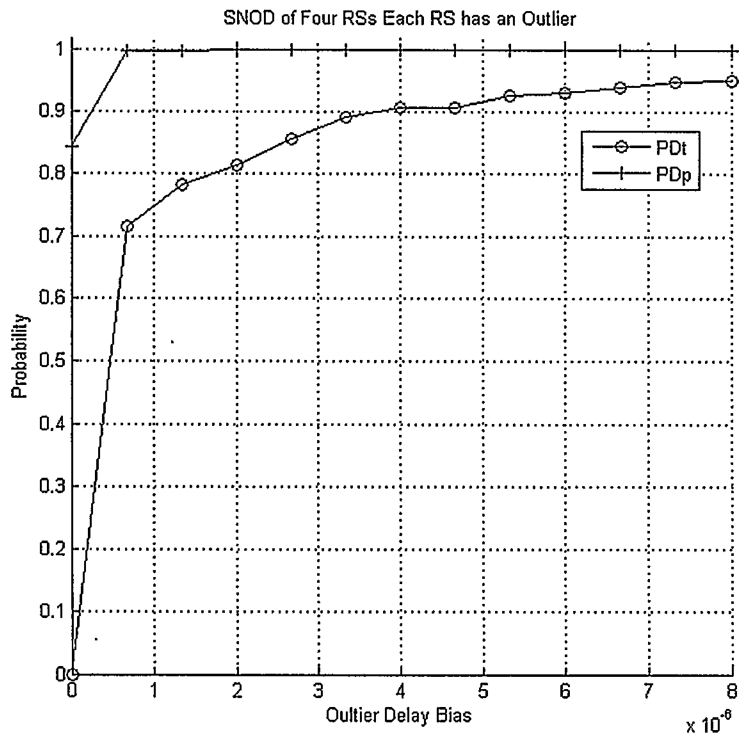

Figure 18 The P_{D_t} and P_{D_p} for four RSs with four outlier.

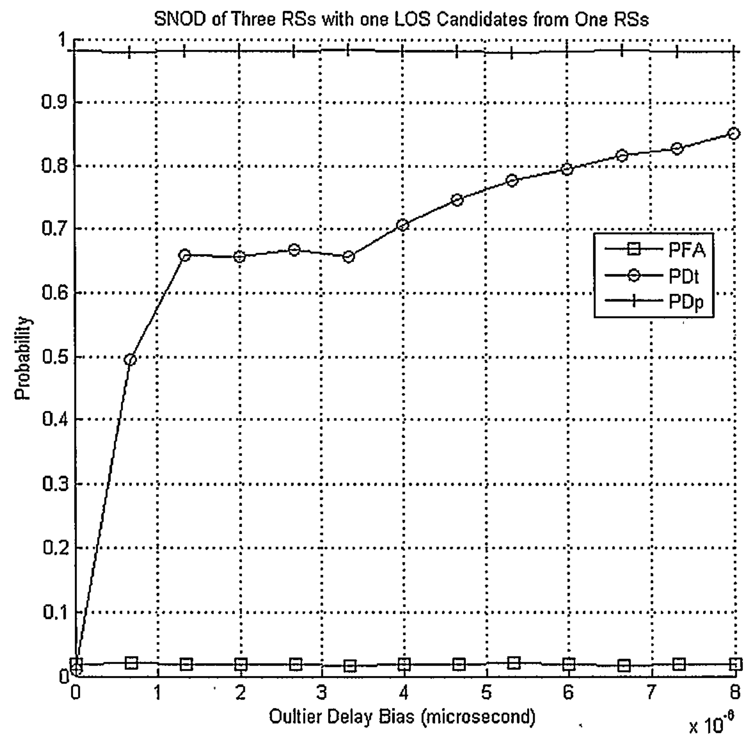

Figure 19 The P_{FA}, P_{D_t}, and P_{D_p} for three RSs, with one of the RSs having two propagation delay estimates.

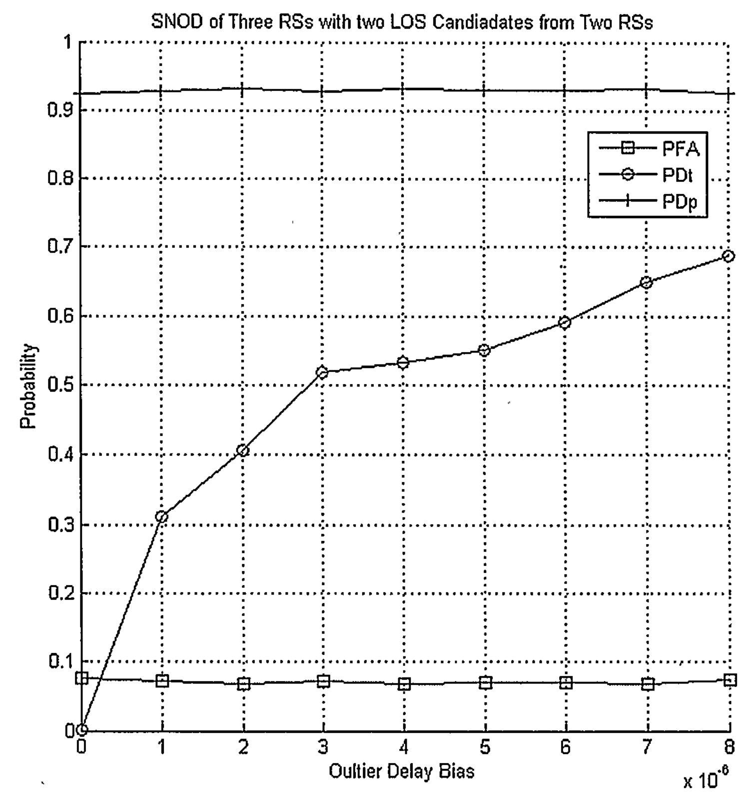

Figure 20 The P_{FA}, P_{D_t}, and P_{D_p} for three RSs, with two of the RSs having tow propagation delay estimates.

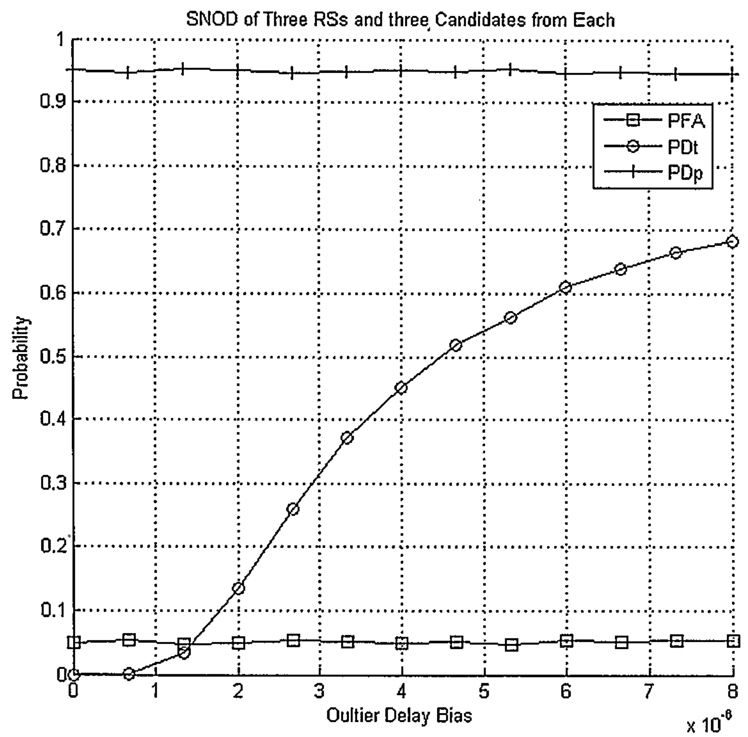

Figure 21 The P_{FA}, P_{D_t}, and P_{D_p} for three RSs, each of the three RSs having two propagation delay estimates.

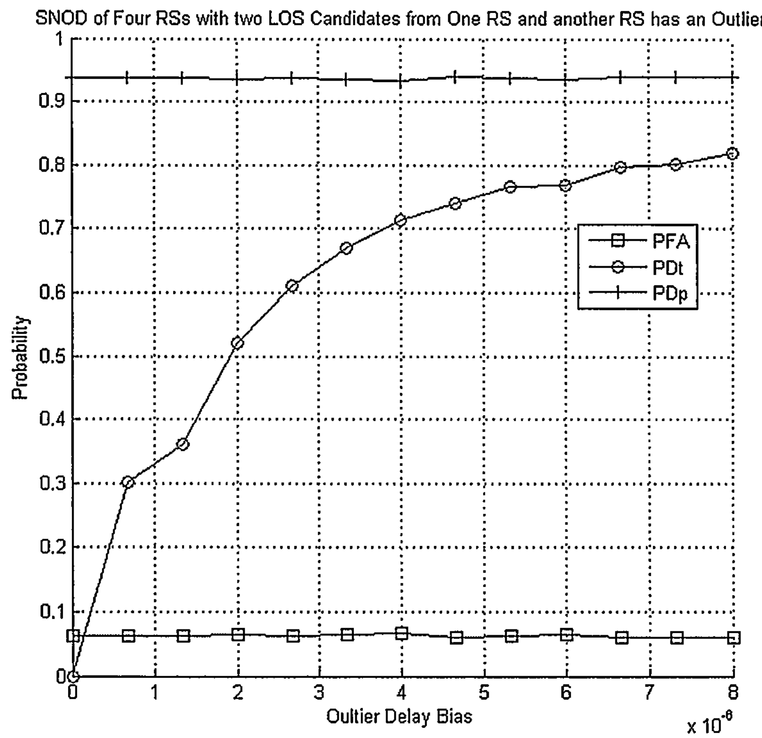

Figure 22 The P_{FA}, P_{D_t}, and P_{D_p} for four RSs, with one RS having an outlier and another RS having two propagation delay estimates.

3.9 Conclusion

In this chapter, I have introduced a novel wireless location receiver based on the SNOD technique. I have proposed the $\mathcal{SN}$ distribution as a general distribution model for multipath (MP) signals. When the RS has two propagation delay estimates, I proposed to use two time delay estimates per RSs. Simulation results demonstrate the capacity of the SNOD technique in detecting outliers.

Chapter Four: **POSITIONING LAYER**
FIXING POSITIONS USING ROBUST ESTIMATION TECHNIQUES

4.1 Introduction

This chapter deals with the problem of fixing the position of a radio device using a number of RSs. In network-based and in handset-based systems, the RSs have known location, while in distributed networks (e.g. WSN), there are neither infrastructure nor RSs to rely on. In this chapter, I propose several estimation techniques to fix the position in infrastructure (e.g. network based and handset based) and in distributed (e.g. WSN) systems.

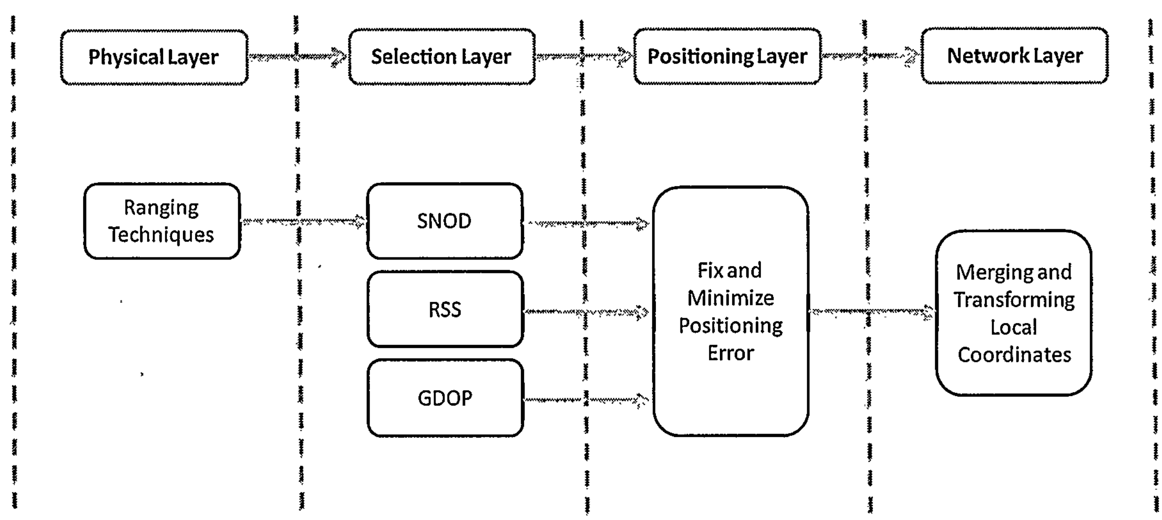

Figure 23 A Cross-Layer representation in wireless location.

4.2 Problem Formulation

The main geometrical approach to solve for the location of a radio device using either Received Signal Strength (RSS), Time Of Arrival (TOA), or Round Trip Delay (RTD) is through circular trilateration. The ranging measurement equation can be written generally as:

$$d_{ij} = \sqrt{(x_j - x_i)^2 + (y_j - y_i)^2} + e_{ij} \qquad (25)$$

where

d_{ij}	is the estimated range between radio device j and RS i;
(x_j, y_j)	are the estimated coordinates for radio device j;
(x_i, y_i)	are the known coordinates for RS i;
e_{ij}	is the error in the ranging measurement which follows a Gaussian distribution $\mathcal{N}(\mu, \sigma^2)$, with a mean μ and a variance σ^2. When d_{ij} is biased, μ is non zero.

4.3 Fixing Positions Using the Iterative Reweighted Least Square (IRLS) Estimation

In this section, a popular technique used in robust estimation, is presented. Let e_{ij} be the error of the ranging measurement between a RS i and a radio device j. The standard Least Square (LS) estimation tries to minimize $\sum_{ij} e_{ij}^2$, i.e. the summation of ranging errors, which can be sensitive if there are outliers (i.e. large ranging error) present in the ranging measurements [76]. M-estimators have been proposed to reduce the effect of outliers by replacing the squared error e_{ij}^2, by another function of the error, $\rho(e_{ij})$, yielding

$$\min \sum_{ij} \rho(e_{ij}) \tag{26}$$

where ρ is a symmetric, positive function with a unique minimum at zero, and is chosen to be less increasing than the square function in e_{ij}^2.

Instead of solving this problem directly, I can implement it using the IRLS estimation [76], which is given by

$$\min \sum_{ij} w(e_{ij}[n-1])e_{ij}^2 \tag{27}$$

where $[n]$ indicates the iteration number, and $w(\cdot)$ is a robust weighting function.

In general, the procedure of Iterative Reweighted Least Square (IRLS) estimation can be summarized as follows:

- Step 1: Find an initial solution based on standard LS estimation.

- Step 2: Use errors obtained from the first step of the IRLS procedure to obtain new weights, which are rescaled based on a robust weighting function.

- Step 3: Use the new weights to obtain a new solution based on LS estimation.

- Step 4: Iterate by repeating the second and the third steps of IRLS procedure until termination. The are several possible criteria for termination [77]: 1) based on the maximum number of iterations, 2) based on the maximum amount of corrections, and 3) based on the monitoring of the reference variance [71]. In this chapter, a combination of the first and second termination criteria is used.

4.3.1 The First step of the IRLS Procedure to fix positions of radio devices

Solving for the two unknowns (x_j, y_j), in (25) using linear LS estimation has been proposed in several literature. LS estimation problems fall into two categories, linear and nonlinear. The linear LS problem has a closed form solution, while the non-linear LS problem has to be solved by iterative refinement, as it does not have a closed form solution, unless it can be replaced by a linear LS problem through: 1) a transformation of parameters or 2) a separability of parameters. The transformation of parameters method is used in the next chapter.

For non-linear problems, initial values must be found for the parameters. Parameters are refined iteratively, in which values are obtained by successive approximations. In this section, I have elected to solve (25) using LS estimation for nonlinear problems. In this case, a first-order Taylor series approximation is used to linearize (25). Hence, the linearized form is given by:

$$d_{ij} \approx d_{i_0 j_0} + \left(\frac{dd_{ij}}{dx_i}\right)_0 dx_i + \left(\frac{dd_{ij}}{dy_i}\right)_0 dy_i \left(\frac{dd_{ij}}{dx_j}\right)_0 dx_j + \left(\frac{dd_{ij}}{dy_j}\right)_0 dy_j + H.O.T + e_{ij} \tag{28}$$

where $H.O.T$ are the higher order terms of Taylor series expansion; $\left(\frac{dd_{ij}}{dx_i}\right)_0$ and $\left(\frac{dd_{ij}}{dy_i}\right)_0$ are the partial derivatives of the ranging measurement function d_{ij} with respect to x_i and y_i, which are evaluated with coordinate value approximates (x_{j0}, y_{j0}); (x_j, y_j) are unknown parameters, and dx_j and dy_j are unknown corrections to the coordinate value approximates such that

$$\begin{aligned} x_j &= x_{j_0} + dx_j \\ y_j &= y_{j_0} + dy_j \end{aligned} \tag{29}$$

By dropping the $H.O.T$ from the Taylor series, (28) becomes only a linear approximation of (25). (28) shows that there are four unknowns per radio device that are required to be estimated. These unknowns are 1) two initials coordinate values and 2) two coordinate corrections.

To estimate the two initial coordinate values, a minimum number of RSs can be used using the RSS and the GDOP found at the selection layer. After I have estimated the initial coordinate values, the weighted LS estimation for the second set of unknowns (i.e. the coordinate corrections) can be obtained as:

$$\widehat{\Theta} = (J^T W J)^{-1} J^T W K = N^{-1} J^T W K \tag{30}$$

where

$$\Theta = \underbrace{\begin{bmatrix} dx_i \\ dy_i \\ \hline dx_j \\ dy_j \\ \hline \vdots \\ \hline dx_n \\ dy_n \end{bmatrix}}_{2z\times 1}$$

is the coordinate correction for the unknown radio devices, and z is the number of radio devices within the network. In case of a handset-based system, $z = 1$,

$$J = \underbrace{\begin{bmatrix} \overbrace{\frac{\partial F_1}{\partial x_i} \quad \frac{\partial F_1}{\partial y_i}}^{z_i} & \cdots & \overbrace{\frac{\partial F_1}{\partial x_n} \quad \frac{\partial F_1}{\partial y_n}}^{z_n} \\ \vdots & \ddots & \vdots \\ \frac{\partial F_m}{\partial x_i} \quad \frac{\partial F_m}{\partial y_i} & \cdots & \frac{\partial F_m}{\partial x_n} \quad \frac{\partial F_m}{\partial y_n} \end{bmatrix}}_{m\times 2z}$$

is the Jacobean matrix for the unknowns,

and m is the number of observations,

$$W = Q^{-1} = \underbrace{diag\left[\sigma_{ij}^2 \quad \cdots \quad \sigma_{mm}^2\right]}_{m\times m}$$

is the weighting matrix, which is equal to the inverse of the variance-covariance matrix Q of the ranges,

$$K = \underbrace{\begin{bmatrix} \hat{l}_{ij} - F_{ij} \\ \vdots \\ \hat{l}_{lh} - F_{lh} \end{bmatrix}}_{m\times 1}$$

is the misclosure vector, which is the difference between the observed ranges and the Euclidean distances $\hat{l}_{ij}$ evaluated from the estimated coordinates, and

$N = (J^T WT)$ is the normal matrix.

4.3.2 The second step of the IRLS procedure

There are many robust weighting functions $w(\cdot)$, which can be used in the IRLS procedure [76][81]. In this chapter, I am proposing both the Huber weighting function and the $L_1 - L_2$ weighting function. The Huber weighting function is defined as

$$w_{Huber}(e) = \begin{cases} 1 & , \quad |e| \leq k \\ \frac{k}{|e|} & , \quad |e| > k \end{cases} \tag{31}$$

Equation (31) shows that the Huber's weighting function behaves like a parabola in the vicinity of zero, and increases linearly at a given level where $|e| > k$. The 95% asymptotic efficiency on the Gaussian distribution is obtained with a tuning constant $k = 1.345$ [76].

The $L_1 - L_2$ weighting function combines the advantage of the $L_1 - norm$ estimation, which reduces the influence of outliers with that of the $L_2 - norm$ estimation, which forces the objective function to be convex [76]. The $L_1 - L_2$ weighting function behaves like an $L_2 - norm$ estimation for small errors and like an $L_1 - norm$ estimation for large errors. The $L_1 - L_2$weighting function is defined as

$$w_{L_1 - L_2}(e) = \frac{1}{\sqrt{1 + \frac{e^2}{2}}} \tag{32}$$

The LS error vector E is given by

$$E = J\Theta - K \tag{33}$$

Elements of the error vector E are rescaled using one of the weighting functions found in equations (31) or (32).

4.3.3 The third Step of the IRLS procedure

The solution vector of the IRLS estimation is obtained as

$$\widehat{\Theta}[n] = (J^T W[n-1]J)^{-1} W[n-1]K \tag{34}$$

4.4 Fixing Positions Using the $L_1 - norm$ Estimation

A novel minimizing position technique based on $L_1 - norm$ estimation is developed. $L_1 - norm$ estimation is very robust against outliers. The robustness breakdown point for $L_1 - norm$ estimation is 50% due to the median used in parameter estimation [81].

There is no closed form solution for $L_1 - norm$ estimation. Combinations of three RSs with known locations are required to estimate the position of a radio device using circular trilaterations. A radio device can have several position estimates from different RSs combinations. The median (med) is used to estimate the final location of the radio device. Hence, the location of a radio device is estimated as

$$\begin{aligned} \hat{x}_i &= med([p_{1x} \quad \cdots \quad p_{\Gamma_{\mathrm{RS}}x}]) \\ \hat{y}_i &= med([p_{1y} \quad \cdots \quad p_{\Gamma_{\mathrm{RS}}y}]) \end{aligned} \tag{35}$$

where

p_{ix} and p_{iy}	are the x and the y coordinates, estimated from the i^{th} combination of RSs, respectively.
Γ_{RS}	is the number of RSs.

4.5 Fixing Positions Using Combined Estimation

A solution based on a combination of IRLS and $L_1 - norm$ estimation is proposed in this section. The IRLS estimation procedure starts with estimated errors based on LS estimation. Hence, in the presence of outliers, the LS estimation will be perturbed due to its sensitivity to outliers. Therefore, errors estimated from LS estimation will be affected as well. Hence, an initial error estimated from the $L_1 - norm$ procedure is used instead of the LS estimation errors used in the first step of the IRLS procedure. The second and the third steps of the IRLS estimation procedure are the same as discussed above.

4.6 Distributed Systems: Wireless Sensor Networks

In WSNs, sensor nodes must cooperate to define their reference sensor nodes, build their own Cluster Local Coordinate systems (CLCs), and then merge these local coordinates to a unique coordinate system for the WSN. Hence, this type of wireless localization is referred to in this thesis as Collaborative Localization (CL). In this chapter, I present the part of the process that belongs to the positioning layer, which is the building of CLCs. In the next chapter, I will learn about merging CLCs to form a unique set of coordinates for the entire distributed network.

In the considerable literature, such systems have alternatively been described as "cooperative," "relative," "distributed," "GPS-free," "multihop," "self-localization;" "adhoc" or "sensor" positioning. CL radios, typically used to convey the sensed data, are also used to determine pair-wise distances between adjacent sensor nodes. Hence, CL does not contribute generally to the sensor node cost, size, or transmission power consumption. Furthermore, the proposed solution offers the following features:

- *Self-configurability*: the proposed CL technique is decentralized. Each cluster has a cluster head which is responsible for scheduling communication, routing data, and acting as a gateway for other sensor nodes within each cluster [56], [57]. Figure 24 shows a WSN consisting of three clusters, each having its own CLC system.

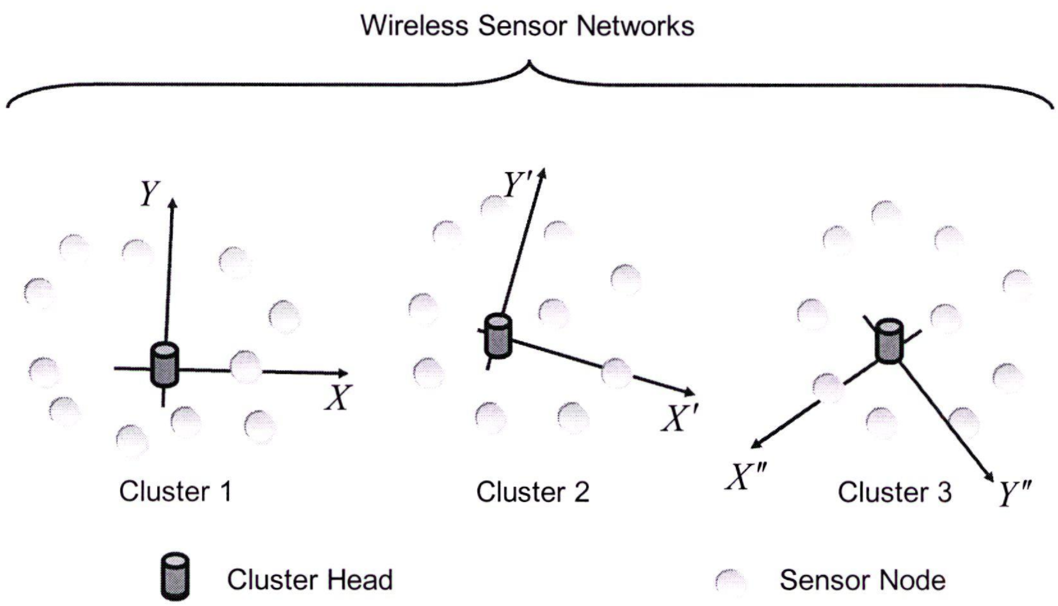

Figure 24 Example of a WSN which consists of three clusters. Each cluster has its local coordinates.

- *Scalability*: the proposed CL solution can be scaled by adding WSN clusters or adding new sensor nodes within a cluster or both. Adding a new cluster does not require remerging the entire set of CLC systems. The new cluster will be integrated with minimum computational effort by estimating its merging parameters with respect to the WSN global coordinate system as I will see at the network layer in the next chapter. Adding new sensor nodes within a cluster means extra ranging measurements that can improve the overall sensor node positioning accuracy.

- *Independence*: the proposed CL solution is a stand-alone solution, which does not depend on any existing network. However, the global WSN coordinate system can be tuned to the global GPS coordinate system, if there are at least two sensor nodes equipped with a Global Navigation Satellite System (GNSS) receiver or with known global GPS coordinates (in 2D positioning). Further discussion can be found at the network layer contained in chapter six.

- *Robustness*: the proposed CL solution can tolerate large ranging measurement errors. Ranging measurement errors are divided into: 1) WGN ranging errors with zero mean and σ^2 variance, and 2) large ranging errors (outliers) commonly found in the wireless channel due to MP arrival, threshold effect and bifurcation. In this chapter, I treat ranging outliers as an additive ranging bias [58]-[61].

In this subsection, the proposed CL is divided into a two-step process. Step (A) is responsible for building local coordinates, and Step (B) is responsible for minimizing positioning error in the CLC systems. Figure 25 shows the CL algorithm within the wireless location stack provided in this thesis.

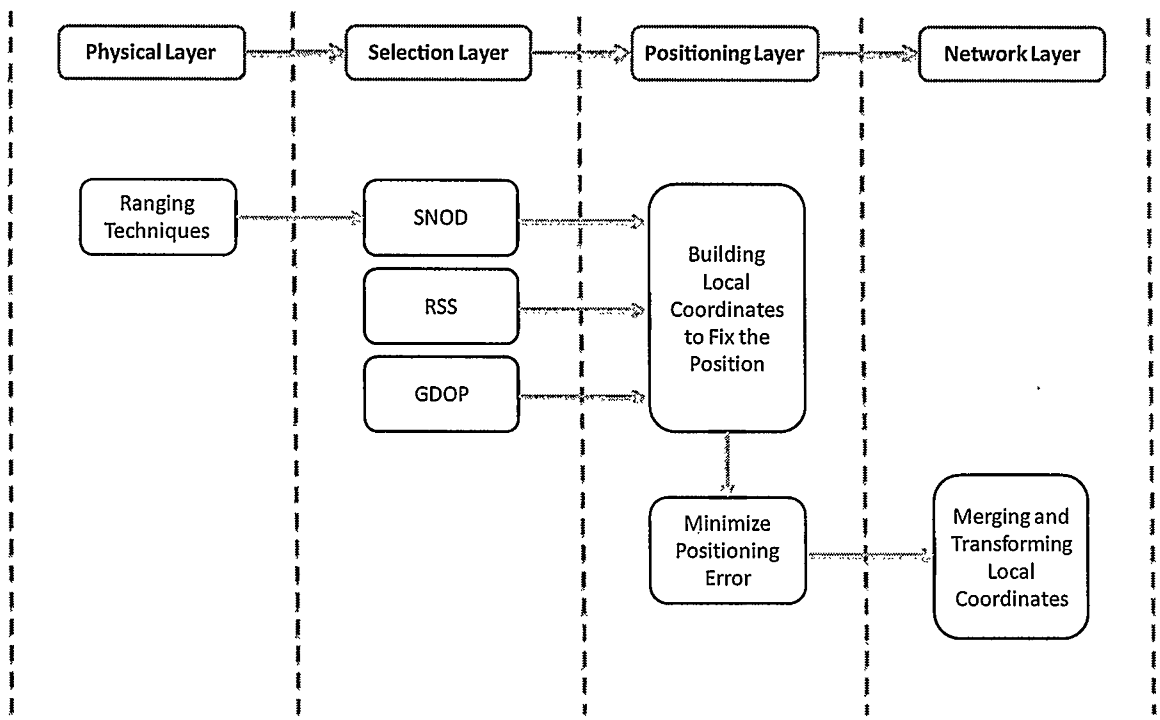

Figure 25 A Cross-Layer representation in CL.

4.6.1 Step (A): Building Cluster Local Coordinates

[62] introduces a method to build WSN local coordinates, which is the only work found in the literature as far as building local coordinates within a WSN is concerned. The algorithm builds a local coordinate system for each sensor node. Each sensor node

becomes the center of its own local coordinate system with the position (0,0) and the positions of its neighbors are computed accordingly. This algorithm has the following drawbacks: 1) the method requires that each sensor node builds its local coordinate system. Hence, the number of local coordinate systems grows linearly with the size of the WSN. 2) The algorithm does not consider the effect of measurement imperfections such as noise and large ranging errors (outliers). 3) The algorithm does not consider the effect of GDOP [63][64] on the location accuracy. For all these reasons,

- I introduce a modified algorithm to build each CLC system using the RSS and the GDOP found at the selection layer.

- I propose to use a Free Network Adjustment (FNA) technique [73][74], which is an approach commonly used in the field of Surveying Engineering, to minimize positioning error. FNA is based on LS optimization.

- I propose to use a subspace method to resolve the singularity found in the normal matrix of the LS required in the FNA technique.

- I propose to use several robust FNA techniques that provide robustness against large ranging errors. These techniques are based on the IRLS estimation and on the $L_1 - norm$ estimation, as introduced in sections 4.3 and 4.4, respectively.

In distributed systems, equation (28) shows that there are eight unknowns per pair-wise sensor nodes that are required to be estimated. These unknowns are 1) four initials CLC coordinates and 2) four coordinate corrections. First, I start by finding the initial CLCs for the sensor nodes by building a CLC system. A cluster head communicates in a peer-to-peer manner with adjacent sensor nodes to determine its 1-hop sensor nodes. Adjacent sensor nodes communicate with each other to determine their pair-wise distances.

Let us choose two sensor nodes, p and q, within the 1-hop to the cluster head i, such that: 1) the inter-distance between sensor nodes p and q, is known and 2) they are not lying on the same line as the cluster head i (i.e. $d_{pq} < d_{ip} + d_{iq}$, where d_{lh} represent the Euclidean distances between sensor node l and sensor node h). Without loss of generality, assume that p and q are two sensor nodes having positive x-values and positive y-values as shown in Figure 26. I can uniquely define the CLC system of the cluster head i, by two sensor nodes, p and q, such that: CLCs of i, p and q are $(0,0)$, $(d_{ip}, 0)$, and $(d_{iq} cos\theta, d_{iq} sin\theta)$, respectively, where γ is the angle $\angle(p, i, q)$ as shown in Figure 26 and can be estimated as:

$$\gamma = \cos^{-1}\left(\frac{d_{iq}^2 + d_{ip}^2 - d_{pq}^2}{2d_{iq}}\right) \tag{36}$$

To locate another sensor node j, where j is located within the 1-hop to cluster head i, distances d_{ij}, d_{qj}, and d_{pj} must be estimated. Therefore, CLCs of the sensor node j can be estimated as:

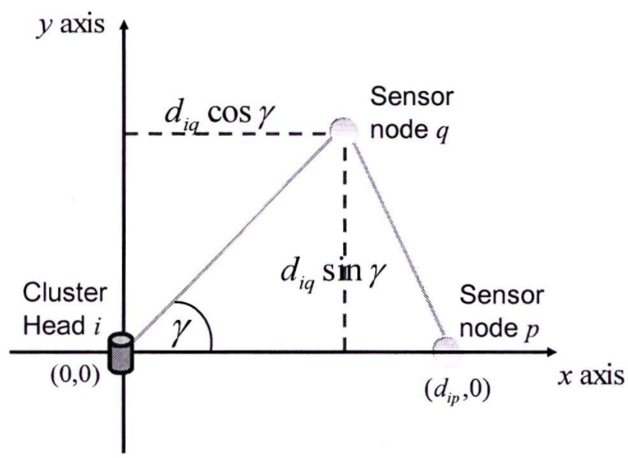

Figure 26 Illustration of the local coordinates within a WSN cluster.

$$\begin{aligned} \hat{j}_x &= d_{ij} \cdot \cos \alpha_j \\ \hat{j}_y &= \begin{cases} d_{ij} \cdot \sin \alpha_j & , \quad [\beta_j - |\alpha_j - \gamma|] \ll [\beta_j - |\alpha_j + \gamma|] \\ -d_{ij} \cdot \sin \alpha_j & , \quad [\beta_j - |\alpha_j - \gamma|] \geq [\beta_j - |\alpha_j + \gamma|] \\ \Diamond & , \quad otherwise \end{cases} \end{aligned} \tag{37}$$

where

α_j is the angle $\angle(p, i, j)$ as shown in Figure 27.

β_j is the angle $\angle(j, i, q)$ as shown in Figure 27.

◊ indicates that I have to choose a different sensor node with a better GDOP to locate the j sensor node.

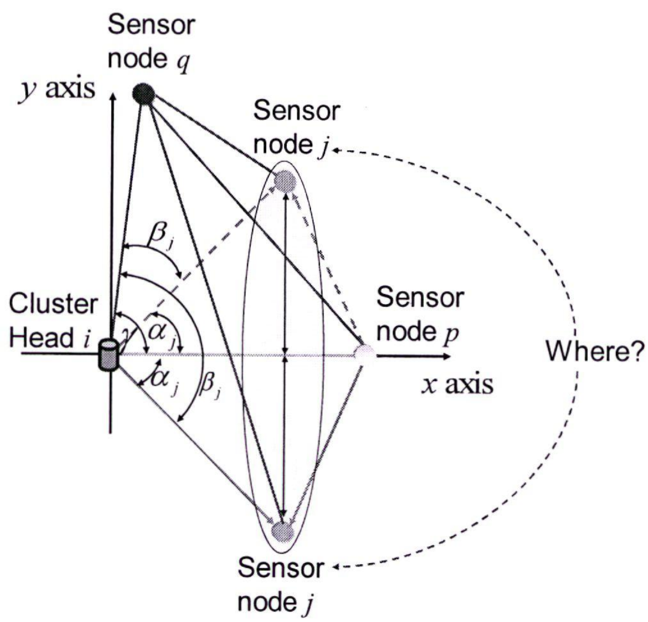

Figure 27 An example illustrating how to locate sensor node j within a WSN cluster.

The same notations in [62] are used here in order to show that the proposed solution is able to tolerate expected imperfections in the estimated angles due to the introduction of GDOP as a factor in building CLC systems. More specifically, (37) can be considered as a comparison between 1) the two Euclidean distances formed by the positive and negative $y-axes$ and 2) the observed ranges between sensor nodes j and q.

RSS and GDOP discussed earlier at the selection layer are used in this chapter: 1) in order to improve the position estimate of sensor node j by selecting sensor nodes that have relatively higher RSS and good geometry with respect to sensor node j to cooperate in determining its location; 2) in order to reduce the effect of outliers by rejecting small angles. Sensor nodes encountering outliers generally have a position far from other sensor nodes due to the large ranging error caused by the outlier. Figure 28 shows the relationship between a position affected by an outlier and the angle formed using other sensor nodes. Hence, if I restrict angles formed between sensor nodes which cooperate in determining the position of a sensor node to be within $(0^o - 150^o)$, I will diminish the chances of any sensor node which is encountering an outlier to cooperate [74].

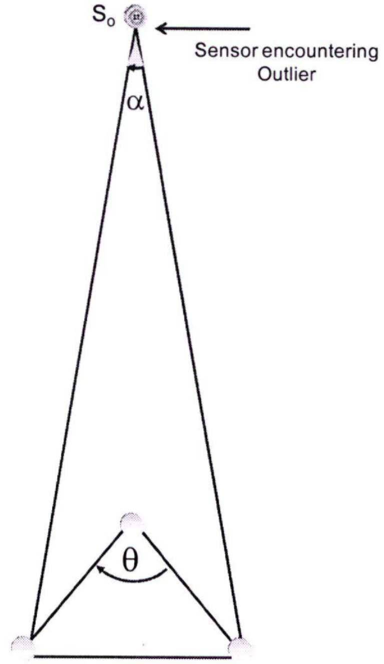

Figure 28 The angle α formed between S_0, which is encountering an outlier and two other sensor nodes is small compared to a typical angle, θ, in a WSN cluster.

4.6.2 Step (B): Minimize Positioning Error

The main geometrical approach to solving for the location of a sensor node using either RSS or RTD is through circular trilateration. In this case, the RTD between a sensor node and three other sensor nodes is measured. In order to minimize positioning error, several CL techniques have been developed. Most of these approaches are based on convex optimization, gradient, and conjugate gradient algorithms [65]-[68]. [55] shows a comparison between these techniques with respect to 1) the WSN deployment type, 2) the WSN size, 3) the real time vs. post mission time, and 4) 2D positioning vs. 3D positioning. After I have estimated the initial CLCs of a sensor node, the weighted LS estimation is used to estimate the second set of unknowns (i.e. the CLC corrections) found in (30).

It is common for the normal matrix N of this type of ranging problems to have a singularity (i.e. be defective) [73][74]. The rank defect occurs due to the large number of unknowns (i.e. the CLCs of sensor nodes) compared to the number of known parameters (i.e. observations). The rank defect indicates that the geometry of the network must remain fixed, which means that the corrections of the estimated coordinates cannot change the network geometry [78].

In Geomatics Engineering, the singularity of the normal matrix is overcome by fixing two points (four coordinates), i.e. the coordinates of two points are considered to be known [71][74]. Therefore, estimating their coordinate corrections is not required. The two points chosen to be fixed are called control coordinates. Precise surveying must be conducted to diminish any position error found in the control coordinates, which may propagate to the network. This solution is inadequate for WSN. Hence, in order to avoid the arbitrariness of fixing sensor node coordinates, a subspace method is used instead to resolve the rank defect of the normal matrix [79] as follows: 1) compute the SVD for the Jacobean matrix. 2) Arrange the eigenvalues diagonal matrix $\Lambda = diag[\lambda_1 \quad \cdots \quad \lambda_{2n}]$, in a descending order, where λ_i are the corresponding eigenvalues. 3) Remove the eigenvalues which are too small or equal to zero. 4) Recompute the inverse of the normal matrix [79], [80].

4.7 Simulation Results

Table IX summarizes the simulation environment parameters assumed in this chapter. The system bandwidth is assumed to be 50 MHz, whereas the SNR varies from $16-31$ dB. A Free space wireless channel model is assumed. Outliers are modeled as an additive bias of 900 meter, which is equivalent to a 3 μs time delay.

Table IX Simulation Environment for the Positioning Layer

Parameter	Value
no. of Mont-Carlo runs	10,000
no. of sensor nodes per cluster	6
no. of clusters	2
SNR	$16-31$ dB
bandwidth	50 MHz
outliers	3 μs
path loss exponent	2
total CL algorithm execution time	~162 sec.

4.7.1 Evaluating Robust Positioning Estimation Techniques

Comparisons between the various proposed robust estimation techniques are investigated. Figure 29 and Figure 30 compare the average radial error of one cluster using LS, $L_1 - L_2$, Huber, $L_1 - norm$, and Huber(L_1) estimation techniques. The radian error is defined as the Mean Square Errors (MSE) found in the $x - axis$ and $y - axis$ for a radio device. The LS estimation outperforms other estimation techniques for AWGN, while the proposed $L_1 - norm$ estimation shows a better performance in the presence of outliers.

For distributed systems, I examine two WSN clusters each one consisting of six sensor nodes. Within each cluster, sensor nodes must communicate in a peer-to-peer manner with at least three other sensor nodes in order to be localized. The location of these sensor nodes is randomly selected. Four of the twelve sensor nodes are randomly chosen to be tie senor nodes.

In order to further investigate the difference between the proposed closed-form and open-form estimation techniques, two sensor nodes, S_3 and S_4, are examined. Figure 31 and Figure 32 compare the estimation performance for the various proposed estimation techniques in the presence of outliers affecting one of the ranging measurements of sensor node S_4. Figure 31 and Figure 32, show that the radial error estimated by the $L_1 - norm$ estimation for sensor nodes S_3 and S_4 behaves differently due to the outlier that is affecting S_4. Hence, $L_1 - norm$ estimation shows superior resilience against outliers by isolating the effect of outliers that affect some sensor nodes, from affecting the entire cluster due to its open form solution.

4.7.2 Evaluating Building Local Coordinates Algorithm

The examined clusters consist of six sensor nodes. I assume that sensor nodes CLCs are randomly selected. The range estimate between any two sensor nodes is subjected to two types of ranging measurement errors as discussed before: AWGN and bias. Figure 33 shows that GDOP can reduce the coordinate mirroring error rate, which is the probability of error for the $y - axis$ direction of a sensor node to be chosen in the positive side while the negative side of the $y - axis$ is the correct side, and vice versa. Figure 34 shows that the GDOP factor can also enhance the receiver resilience against outliers by rejecting small angles.

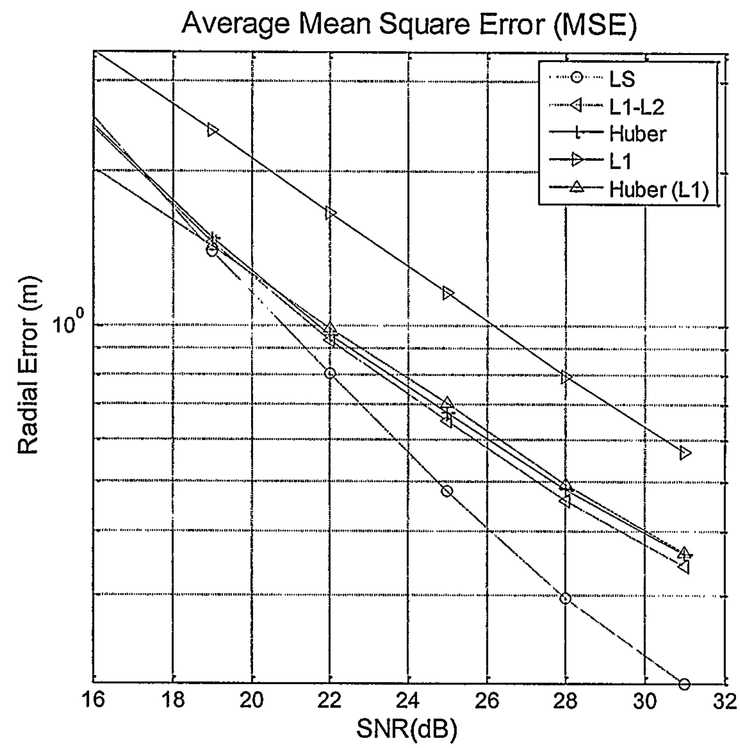

Figure 29 The average MSE for the position of a radio device for different SNR in AWGN in the absence of outliers.

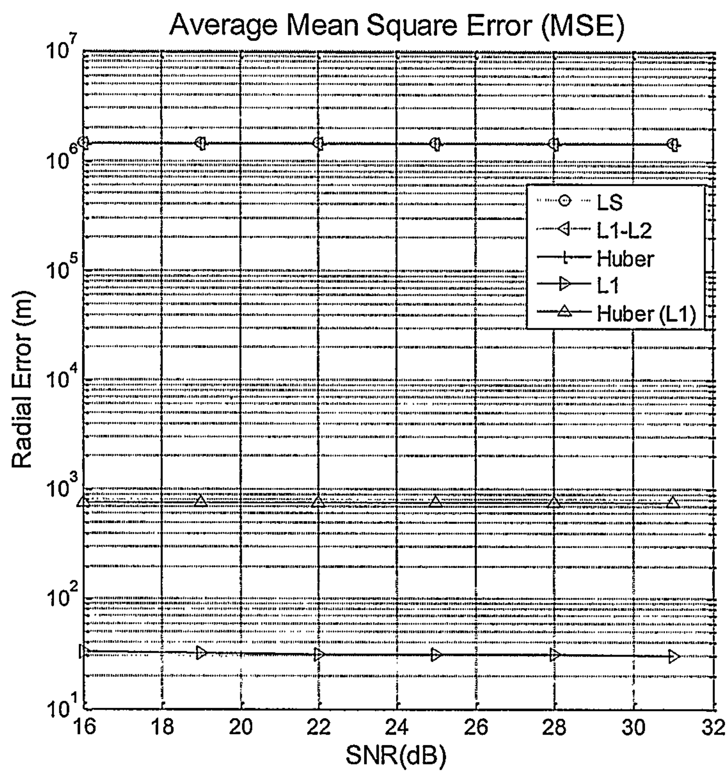

Figure 30 The average MSE for the position of a radio device for different SNR in non-Gaussian noise in the presence of outliers.

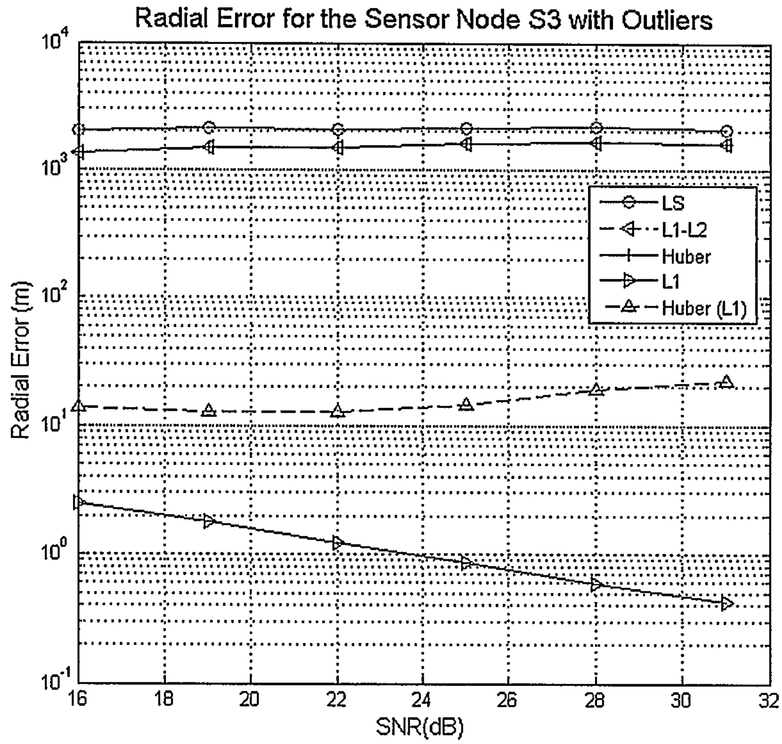

Figure 31 The radial error of the sensor node S_3 for different SNR in non-Gaussian noise in the presence of outliers.

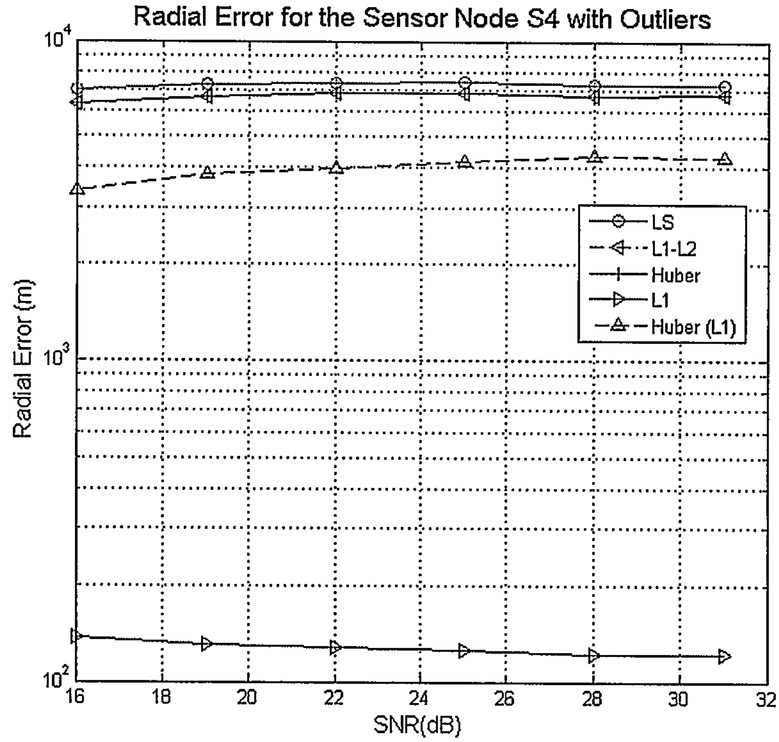

Figure 32 The radial error of the sensor node S_4 for different SNR in AWGN, in the presence of outliers.

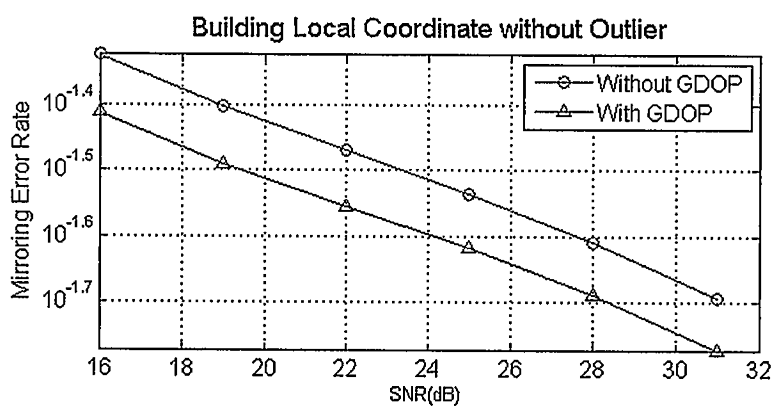

Figure 33 The effect of GDOP in the mirroring error without outliers.

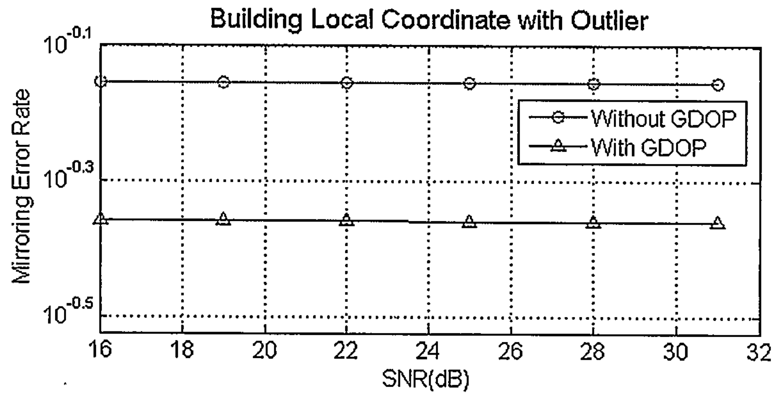

Figure 34 The effect of GDOP in the mirroring error in the presence of outliers.

4.8 Conclusion

The proposed robust estimation techniques to fix the positions of radio devices outperform the LS in the non-Gaussian environment due to the presence of outliers. The proposed CL solution is self-configurable, scalable and independent of any positioning system. Extensive simulations have been carried out to evaluate its performance in terms of accuracy, and robustness under different wireless channel environments using several estimation techniques. I introduced the GDOP as a factor for building CLCs. I proposed the subspace method to be used within FNA to resolve the singularity found within the normal matrix. I introduced novel FNA techniques, which are robust against outliers.

Chapter Five: NETWORK LAYER
MERGING LOCAL COORDINATES USING ROBUST ESTIMATION TECHNIQUES

This chapter deals with the problem of merging local coordinates in distributed systems. In this chapter, I complete the CL solution, which has been introduced at the positioning layer to build WSN Cluster Local Coordinates (CLCs), by merging these coordinates in order to create a set of global WSN.

5.1 Introduction

Merging CLCs is mandatory to have a unique global coordinate system for the entire distributed network. [62] introduces a method, referred to as the directional method, which is used to merge local coordinates built by sensor nodes. The drawbacks of this method are as follows. 1) The local coordinates are merged without attention to positioning errors implicit to the sensor nodes position estimates. This can lead to substantial positioning error within the entire WSN due to the propagation of ranging errors. 2) The directional method requires more than twice the number of computations compared to a technique I propose to use in this chapter: Two-Dimensional Coordinate Transformation Model (2D-CTM) [73]. The 2D-CTM method is commonly used in surveying Engineering to merge network coordinates. 3) The directional method does not consider the scaling factor between the various local coordinates systems as a merging parameter to be estimated. Another paper [69], proposes a robust geodetic coordinate merging model based on $L_1 - norm$ estimation. However, it does not consider all the parameters required for 2D-CTM.

At the network layer, as presented in this chapter:

- I introduce a novel 2D-CTM based on General LS (GLS) estimation in order to take into account the positioning errors found in the CLC systems.

- I demonstrate the need for estimating a scale factor to merge the CLC systems.

- I propose several novel 2D-CTMs that provide robustness against outliers, based on the Iterative Reweighted Least Square (IRLS) technique and the $L_1 - norm$ technique.

5.2 Problem Formulation

I assume that some sensor nodes can be located within another cluster. These sensor nodes are referred to as tie sensor nodes. At least, two tie sensor nodes are required to merge 2D local coordinates [65]. The 2D-CTM is a model that involves 1) translation: to create a common origin for the two coordinate systems; 2) rotation: to make the reference axes of the two systems parallel and 3) scaling: to create equal dimensions between the two CLC systems [71][74].

Consider two 2D CLC systems, xy and XY, corresponding to two clusters. The basic equations to merge the CLC system xy to the CLC system XY is given by

$$\begin{aligned} X &= (S \cdot cos\theta) \cdot x - (S \cdot sin\theta) \cdot y + T_X \\ Y &= (S \cdot sin\theta) \cdot x - (S \cdot cos\theta) \cdot y + T_Y \end{aligned} \tag{38}$$

where

θ	is the rotation angle between the two CLC systems, and
T_X and T_Y	are the translations in the $X - axis$ and in the $Y - axis$ directions, respectively.

To overcome the nonlinearity found in equation (38) the following transformations are assumed $S \cdot cos\theta = a$, $S \cdot sin\theta = b$, $T_X = c$, and $T_Y = d$. Therefore, the linear version of equation (28) is given by

$$\begin{aligned} X &= a \cdot x - b \cdot y + c \\ Y &= b \cdot x + a \cdot y + d \end{aligned} \tag{39}$$

where a, b, c and d are the unknown 2D-CTM parameters, which I would like to estimate.

5.3 Merging Coordinates Using the Iterative Reweighted Least Square (IRLS) Estimation

In this section, robust 2D-CTMs are considered. 2D-CTMs based on IRLS estimation are introduced. I propose an improvement in the first step of the IRLS estimation procedure which is to find a solution based on General LS (GLS) estimation. The linear LS estimation discussed before is not suitable for merging WSN CLC systems due to the positioning errors found in CLC systems at each cluster. GLS is investigated in [71] to propagate the variance-covariance of the sensor nodes CLCs found after minimizing position error within two clusters.

GLS estimation not only considers $a, b, c,$ and d as unknowns, but it also considers $x, y, X,$ and Y found in equation (39) as parameters to be adjusted. Hence, a nonlinear observation model is developed and is given by:

$$\begin{aligned} F_i(x, y, X, Y) &= a(x + e_x) - b(y + e_y) + c - (X + e_X) \\ G_i(x, y, X, Y) &= b(x + e_x) + a(y + e_y) + d - (Y + e_Y) \end{aligned} \tag{40}$$

where $e_x, e_y, e_X, and\ e_Y$ are the ranging errors of the tie sensor nodes at the two CLCs systems.

Equation (40) is a nonlinear function and Taylor series is used once again for linearization. Hence, initial approximates for the eight unknowns $a, b, c, d, x, y, X,$ and Y have to be obtained. The approximate values of $x, y, X,$ and Y are chosen to be the CLCs of the tie sensor nodes in both clusters, while the initial approximations for $a, b, c,$ and d are chosen either by using standard LS estimation of all tie sensor nodes, or by solving equation (39) for two tie sensor nodes [71].

In solving the GLS, an equivalent solution is obtained by evaluating the following equivalent weight matrix:

$$W_e = (B Q_{\text{MC}} B^T)^{-1} \tag{41}$$

where

$$B = \underbrace{\left[\begin{array}{c|c|c|c|c} \overbrace{\begin{matrix} \frac{\partial F_1}{\partial x} & \frac{\partial F_1}{\partial y} & \frac{\partial F_1}{\partial X} & \frac{\partial F_1}{\partial Y} \\ \frac{\partial G_1}{\partial x} & \frac{\partial G_1}{\partial y} & \frac{\partial G_1}{\partial X} & \frac{\partial G_1}{\partial Y} \\ \hline & & 0 & \\ & & \vdots & \\ & & 0 & \end{matrix}}^{S_1} & \cdots & \overbrace{\begin{matrix} 0 & \cdots & 0 \\ 0 & \cdots & 0 \\ \cdots & \ddots & \cdots \\ 0 & \ddots & 0 \\ 0 & \cdots & 0 \end{matrix}}^{S_i} & \cdots & \overbrace{\begin{matrix} & & 0 & \\ & & \vdots & \\ & & 0 & \\ \hline \frac{\partial F_\Gamma}{\partial x} & \frac{\partial F_\Gamma}{\partial y} & \frac{\partial F_\Gamma}{\partial X} & \frac{\partial F_\Gamma}{\partial Y} \\ \frac{\partial G_\Gamma}{\partial x} & \frac{\partial G_\Gamma}{\partial y} & \frac{\partial G_\Gamma}{\partial X} & \frac{\partial G_\Gamma}{\partial Y} \end{matrix}}^{S_\Gamma} \end{array}\right]}_{2\Gamma\times4\Gamma}$$ is the

Jacobean matrix for CLCs of the tie sensor nodes, and

Γ is the number of tie sensor nodes, F_i and G_i represent (40) for tie sensor nodes $i \in \{1, \dots, \Gamma\}$;

$$Q_{MC} = \underbrace{\left[\begin{array}{c|c|c|c|c} \overbrace{\begin{matrix} \sigma_x^2 & \sigma_{xy} & 0 & 0 \\ \sigma_{xy} & \sigma_y^2 & 0 & 0 \\ 0 & 0 & \sigma_X^2 & \sigma_{XY} \\ 0 & 0 & \sigma_{XY} & \sigma_Y^2 \\ \hline & & 0 & \\ & & \vdots & \\ & & 0 & \end{matrix}}^{S_1} & \cdots & \overbrace{\begin{matrix} 0 & \cdots & 0 \\ 0 & \cdots & 0 \\ \cdots & \ddots & \cdots \\ 0 & \ddots & 0 \\ 0 & \cdots & 0 \end{matrix}}^{S_i} & \cdots & \overbrace{\begin{matrix} & & 0 & \\ & & \vdots & \\ & & 0 & \\ \hline \sigma_x^2 & \sigma_{xy} & 0 & 0 \\ \sigma_{xy} & \sigma_y^2 & 0 & 0 \\ 0 & 0 & \sigma_X^2 & \sigma_{XY} \\ 0 & 0 & \sigma_{XY} & \sigma_Y^2 \end{matrix}}^{S_\Gamma} \end{array}\right]}_{4\Gamma\times4\Gamma},$$ is

the coordinate variance-covariance matrix for the tie sensor nodes propagated from the first step of the CL process, The variance-covariance matrix of the tie sensor nodes at both coordinates are propagated from the FNA formed at each cluster and is given by:

$$\Psi_{\mathrm{i}} = \left(\frac{E_i^T W_i E_i}{r_i}\right) \cdot N_i^{-1} \tag{42}$$

where

i is the cluster number,

r_i is the number of degrees of freedom for the i^{th} cluster.

The GLS solution vector is obtained as:

$$\widehat{\Theta}_{\mathrm{MC}} = (J_{MC}^T W_e J_{MC})^{-1} J_{MC}^T W_e K_{MC} \tag{43}$$

where

$\Theta_{\mathrm{MC}} = [a \quad b \quad c \quad d]^T$

$$J_{MC} = \underbrace{\begin{bmatrix} \frac{\partial F_1}{\partial a} & \frac{\partial F_1}{\partial b} & \frac{\partial F_1}{\partial c} & \frac{\partial F_1}{\partial d} \\ \frac{\partial G_1}{\partial a} & \frac{\partial G_1}{\partial b} & \frac{\partial G_1}{\partial c} & \frac{\partial G_1}{\partial d} \\ \hline & \vdots & & \\ \hline \frac{\partial F_\Gamma}{\partial a} & \frac{\partial F_\Gamma}{\partial b} & \frac{\partial F_\Gamma}{\partial b} & \frac{\partial F_\Gamma}{\partial d} \\ \frac{\partial G_\Gamma}{\partial a} & \frac{\partial G_\Gamma}{\partial b} & \frac{\partial G_\Gamma}{\partial b} & \frac{\partial G_\Gamma}{\partial d} \end{bmatrix}}_{2\Gamma \times 4}$$

is the Jacobean matrix of the unknown 2D-CTM parameters,

$$K_{MC} = \underbrace{\begin{bmatrix} X_1 - (ax_1 - by_1 + c) \\ Y_1 - (bx_1 + ay_1 + d) \\ \hline \vdots \\ \hline X_\Gamma - (ax_\Gamma - by_\Gamma + c) \\ Y_\Gamma - (bx_\Gamma + ay_\Gamma + d) \end{bmatrix}}_{2\Gamma \times 1}$$

is the misclosure vector of the difference between the CLCs of the tie sensor nodes within the *XY* CLC system and the estimated coordinates using $a, b, c,$ and d estimated within the merged solution.

X_i and Y_i are the tie sensor nodes CLCs at *XY* coordinate system, whereas x_i and y_i are the tie sensor nodes CLCs at *xy* coordinate system, for tie sensor nodes $i \in \{1, \cdots, \Gamma\}$.

The four 2D-CTM parameters required for merging coordinates are estimated as:

$$\hat{T}_X = c, \quad \hat{T}_Y = d, \quad \hat{\theta} = \tan^{-1}\left(\frac{b}{a}\right), \quad \hat{S} = \frac{a}{\cos\theta} \tag{44}$$

The error vector of the merging coordinates is given by:

$$E_{\text{GLS}} = Q_{\text{MC}} B^T W_e (J_{\text{MC}} \widehat{\Theta}_{\text{MC}} - K_{\text{MC}}) \tag{45}$$

The second and the third steps for IRLS estimation are the same as described in the previous chapter.

5.4 Merging Coordinates Using the $L_1 - norm$ Estimation

In this section, I propose a complete 2D-CTM based on $L_1 - norm$ estimation. [69] proposes a technique to estimate the two translation parameters, while assuming that the other two parameters, i.e. the rotation angle and the scale factor, vary slightly and are independent of the translation parameters. The CLCs built within the WSN can freely have any direction. Therefore, a precise estimate for the rotation angle parameter has to be considered. A mathematical derivation showing the dependency between the four 2D-

CTM transformation parameters based on $L_1 - norm$ estimation is shown in Appendix C.

The median of the differences between the CLCs of the two tie sensor nodes is used to estimate the two translation parameters, as follows:

$$\begin{aligned} \hat{T}_x &= c = med[(x_i - X) \quad , i = 1, \cdots, \Gamma] \\ \hat{T}_y &= d = med[(y_i - Y) \quad , i = 1, \cdots, \Gamma] \end{aligned} \tag{46}$$

The scale a and b merging parameter, a_{med} and b_{med}, respectively, can be estimated by :

$$\begin{aligned} \hat{a} &= med\left[\frac{1}{x_i} \cdot \left(X_i - c \cdot \left(1 - \frac{y_i}{(x_i)^2 + (y_i)^2}\right)\right) + \frac{1}{(x_i)^2 + (y_i)^2} \cdot (Y_i - y_i - d)\right] \\ \hat{b} &= med\left[\frac{x_i(Y_i - d) - y_i(X_i - c)}{(x_i)^2 + (y_i)^2}\right] \end{aligned} \tag{47}$$

(47) shows a dependency between the four 2D-CTM parameters based on $L_1 - norm$ estimation. A mathematical proof is shown in appendix D. The scaling factor, S_{med}, and the rotation angle, θ_{med}, can be estimated using (43).

5.5 Simulation Results

Table X summarizes the simulation environment parameters assumed in this chapter. In these simulations, I examine two WSN clusters each one consisting of six sensor nodes. Within each cluster, sensor nodes must communicate in a peer-to-peer manner with at least three other sensor nodes in order to be localized. The location of these sensor nodes is randomly selected. Four of the twelve sensor nodes are randomly chosen to be tie senor nodes. The system bandwidth is assumed to be 50 MHz, whereas the SNR varies from $16 - 31$ dB. A Free space wireless channel model is assumed. Outliers are modeled as an additive bias of 900 meters which is equivalent to a 3 μs time delay.

Table X Simulation Environment for the Network Layer

Parameter	Value
no. of Mont-Carlo runs	10,000
no. of sensor nodes per cluster	6
no. of tie sensor nodes	4
no. of clusters	2
SNR	$16 - 31$ dB
bandwidth	50 MHz
outliers	3 μs
path loss exponent	2
total CL algorithm execution time	~162 sec.

5.5.1 Evaluating Merging CLC algorithm

Figure 35 – Figure 43 compare the estimation of the four 2D-CTM parameters based on the GLS, Huber, $L_1 - L_2$, and $L_1 - norm$ estimation techniques in AWGN where the GLS estimation shows a superior estimation performance. Figure 38 – Figure 40 examine the four 2D-CTM parameters in the presence of an outlier. The $L_1 - norm$ estimation outperforms GLS and the other examined robust estimators. The two translations parameters, T_X and T_Y, estimated using the $L_1 - norm$ estimator are shown in Figure 35 – Figure 40 match the conclusions found in [69]. In this chapter, I further investigate the complete $L_1 - norm$ estimation performance for 2D-CTM. I investigate two CLC systems, which are inclined with respect to each other by large inclination angles. The attached simulation corresponds to one of these cases, which has a $\frac{\pi}{6}$ inclination angle. Figure 41– Figure 43 show significant performance degradation for $L_1 - norm$ estimation occurring due to the large inclination angle found between the two CLC systems. The 2D-CTM based on $L_1 - norm$ estimation has a bias due to the independence between the translation parameters and the rotation angle. Simulation results show that when the rotation angle is $0^o, 90^o, 180^o \ or \ 270^o$, the 2D-CTM based on the $L_1 - norm$ estimation behave properly. A mathematical proof for this conclusion can be found in Appendix D.

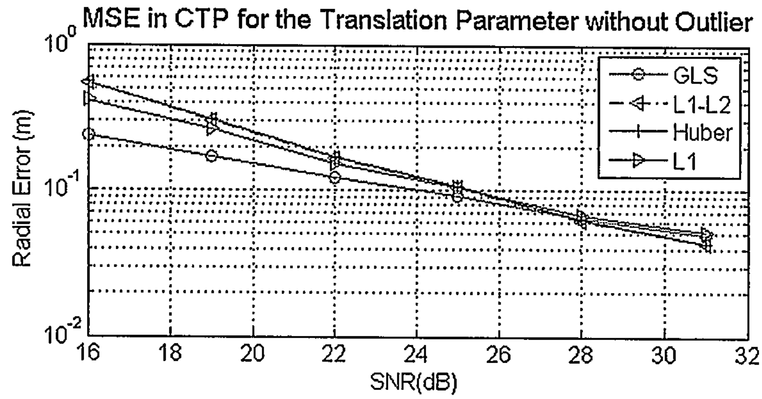

Figure 35 The MSE of the two transformation parameters T_x and T_y for different SNR in AWGN in the absence of outliers.

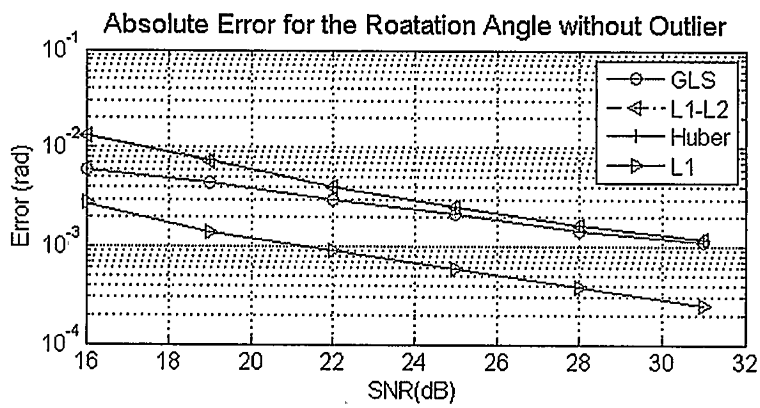

Figure 36 The absolute error of the rotation angle transformation parameter for different SNR in AWGN, in the absence of outliers.

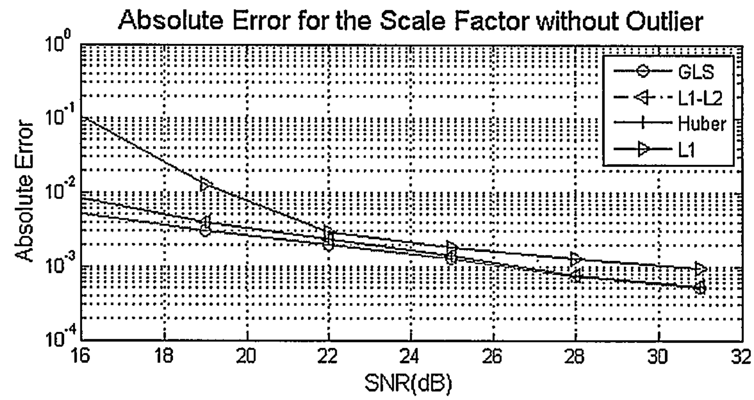

Figure 37 The absolute error of the scale factor transformation parameter for different SNR in AWGN, in the absence of outliers.

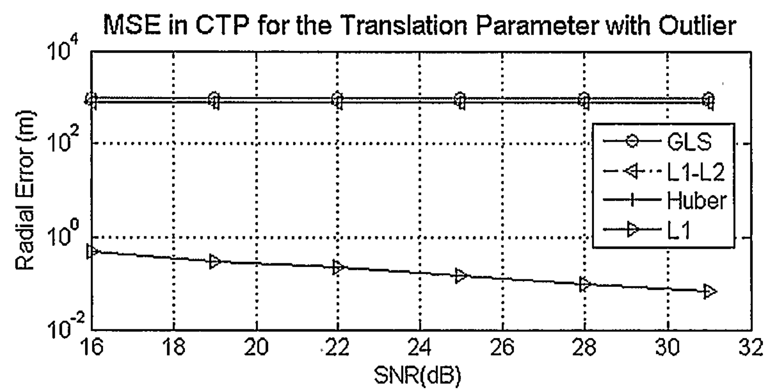

Figure 38 The MSE of the two transformation parameters T_x and T_y for different SNR in non-Gaussian noise, in the presence of outliers.

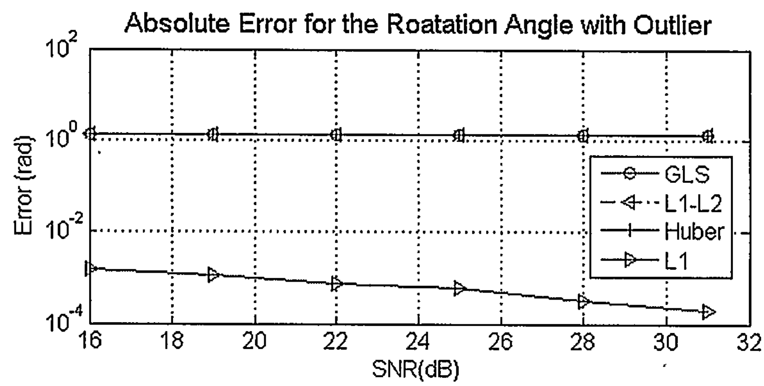

Figure 39 The absolute error of the rotation angle transformation parameter for different SNR in non-Gaussian noise, in the presence of outliers.

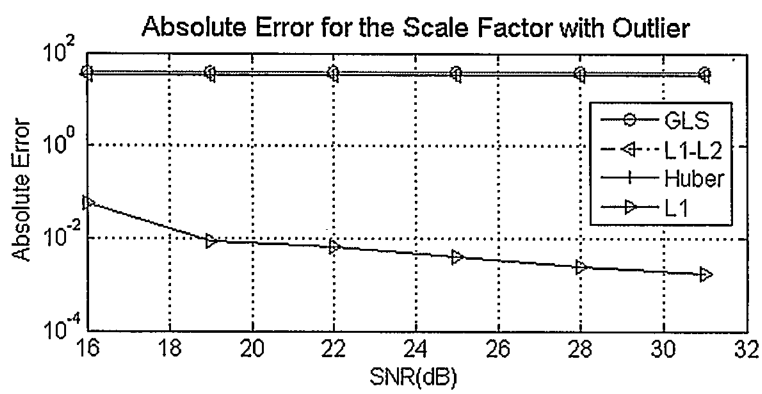

Figure 40 The absolute error of the Scale Factor transformation parameter for different SNR in non-Gaussian noise, in the presence of outliers.

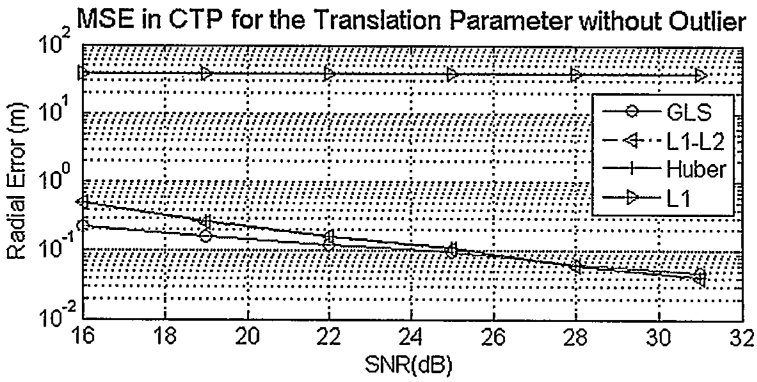

Figure 41 The MSE of the two transformation parameters T_x and T_y for different SNR in AWGN, in the absence of outliers. The two coordinate systems have $\frac{\pi}{6}$ rotation angle between them.

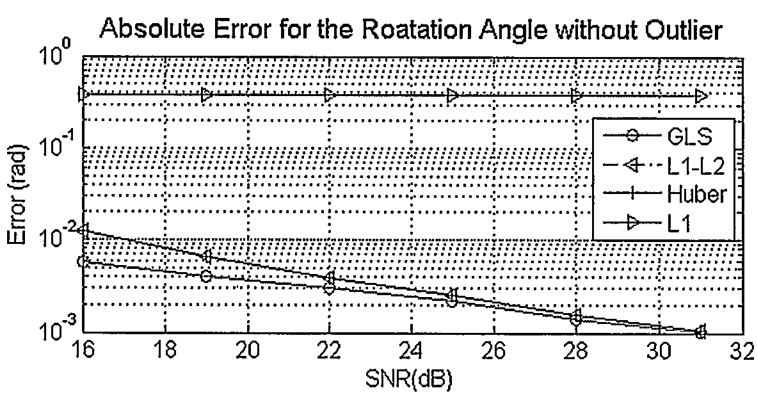

Figure 42 The absolute error of the rotation angle transformation parameter for different SNR in AWGN, in the absence of outliers. The two coordinate systems have $\frac{\pi}{6}$ rotation angle between them.

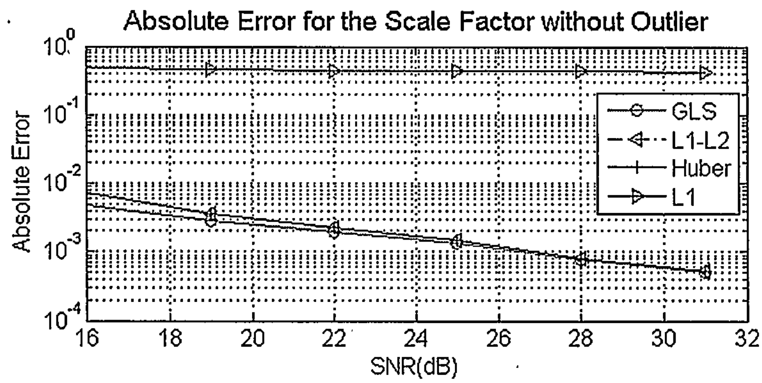

Figure 43 The absolute error of the Scale Factor transformation parameter for different SNR in AWGN, in the absence of outliers. The two coordinate systems have $\frac{\pi}{6}$ rotation angle between them.

5.6 Conclusion

I introduced a 2D-CTM based on General LS (GLS) estimation to take into account the positioning errors found in the CLC systems. I introduced augmented 2D-CTMs, which are robust against large ranging errors. The scale factor was suggested as a merging parameter to be estimated due to the different ranging errors found between clusters. A complete 2D-CTM based on $L_1 - norm$ estimation was introduced. New conclusion about the suitability of the 2D-CTM based on $L_1 - norm$ estimation was achieved by derivation and simulations.

Chapter Six: **CONCLUSION AND FUTURE WORK**

The objective of thesis is to use a cross-layer approach to investigate three major problems in wireless location. These problems are 1) weak received signal (i.e. low received SNR), 2) multipath reception (i.e. correlated and non-correlated), and 3) the unavailability of RSs in distributed systems (e.g. Wireless Sensor Networks (WSNs)). The objective of the thesis has been achieved by introducing fundamental contributions to wireless location. Figure 44 summarizes such contributions within the wireless location layer stack and section 6.1 reviews them. Potential research directions for future work are addressed in section 6.3.

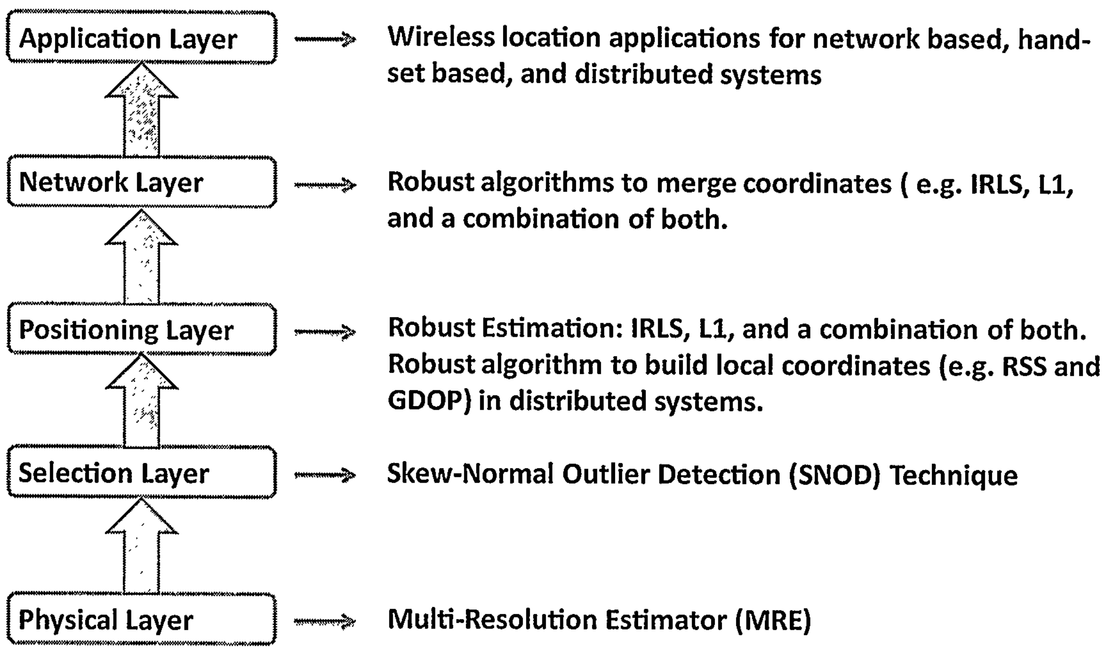

Figure 44 Contributions of the thesis within the wireless location stack

6.1 Thesis Conclusions

6.1.1 Contributions to the Physical Layer

The contribution to this layer is contained in chapter two of the thesis. A novel MRE technique, based on an orthogonal search, is introduced to enhance the performance of the MLE. More specifically, the proposed technique attempts to resolve the problem of closely spaced rays (i.e. of correlated MP rays), and to estimate their time delays without bias. Simulation results show that when a 1D orthogonal search is used, the sensitivity of the MLE is improved by 3 dB. A comparison between the conventional peak detector and a 2D orthogonal search shows a significant improvement in resolving correlated MP rays in addition to the 3 dB improvement in sensitivity.

6.1.2 Contributions to the Selection Layer

The contribution to this layer is contained in chapter three of the thesis. Several CRLB studies recommend the detection and rejection of RS observations, which are encountering large ranging errors rather than estimating and removing their respective biases. In this context, a novel wireless location receiver is proposed in order to detect and reject such large ranging errors where a $\mathcal{SN}$ distribution is used as a statistical model for MP signals and a SNOD technique is introduced. Simulation results of the proposed SNOD technique show that the average P_{D_p} of the SNOD is up to 95%, while the average P_{D_t} is up to 79%, which varies based on the delay amount of the MP signal and the type of outlier.

6.1.3 Contributions to the Positioning Layer

The contribution to this layer is contained in chapter four of the thesis. Novel robust estimation techniques based on Iterative Reweighted Least Squares (IRLS) estimation, $L_1 - norm$ estimation, and a combination of both are proposed to fix the positions of radio devices in a robust fashion. For distributed systems, WSN consisting of several clusters is considered for localization. Sensor nodes within each cluster are responsible in building their own CLC systems. In this layer, GDOP is used to minimize initial positioning errors and to mitigate large ranging errors (outliers). FNA technique is augmented for CL to match the WSN theory of operation and to offer robustness against outliers. Simulation results are presented to prove the GDOP effect in building robust CLC systems. LS, IRLS, and $L_1 - norm$ estimations are compared with respect to FNA. For FNA, LS estimation demonstrates a superior performance in Gaussian noise compared to IRLS estimation and compared to $L_1 - norm$ estimation. While, in the presence of outliers, the proposed $L_1 - norm$ estimation outperforms LS estimation and IRLS estimation.

6.1.4 Network Layer

The contribution to this layer is contained in chapter five of the thesis. Novel robust 2D-CTMs based on IRLS estimation and $L_1 - norm$ estimation are introduced to merge CLCs built at the positioning layer. The 2D-CTM IRLS estimation outperforms other examined estimation techniques.

6.2 Thesis Outcomes

6.2.1 Patents

1. Mohamed Youssef, Naser El-Sheimy, and Michel Fattouche, "Method and Apparatus for Collaborative Localization", in preparation

2. Mohamed Youssef, Michel Fattouche, and Naser El-Sheimy, "Outlier Detection Technique", in preparation

3. Mohamed Youssef, Michel Fattouche, and Naser El-Sheimy, "Multi-Resolution Propagation Delay Estimation Technique", in preparation

6.2.2 Journal Papers

1. Mohamed Youssef, Naser El-Sheimy, and Michel Fattouche, "Robust Collaborative Localization Techniques for Wireless Sensor Networks," IEEE Journal of Selected Topics in Signal Processing. Submitted

2. Mohamed Youssef, Michel Fattouche, and Naser El-Sheimy, "A Novel Skew-Normal Outlier Detection Technique," IEEE Transaction in Communication. To be submitted upon patent submission.

3. Mohamed Youssef, Michel Fattouche, and Naser El-Sheimy, “A Novel Multi-Resolution Technique Based on Orthogonal Search,” IEEE Transaction in Wireless Communication. To be submitted upon patent submission.

6.2.3 Conference Papers

1. Mohamed Youssef, Naser El-Sheimy, “Wireless Sensor Networks: Research vs. Reality”, the Fifth Annual IEEE/ACM Conference on Communication Networks and Services (CNSR 2007) New Brunswick, Canada.

2. Mohamed Youssef, Aboelmagd Noureldin, Abdel Fattah Yousif, and Naser El Sheimy, “Self Localization Techniques for Wireless Sensor Networks,” IEEE/ION Position Location and Navigation Symposium, PLANS 2006, CA, USA.

6.3 Potential Research Directions for Future Work

The focus of my future research is to investigate jointly reliable communication and location techniques for infrastructure and distributed systems with a particular emphasis on statistical and digital signal processing. Some of the potential projects are described below.

1. Build over my PhD research work by going one-step further by investigating wireless location tracking, especially for GPS systems. The novel methods developed during my PhD requires new techniques to be investigated in order to be able to track people and merchandise (i.e. indoor applications).

2. Knowing the location of the radio device can help in several research areas such as: synchronization, channel estimation, interference cancellation and cooperate communication. These have not yet been deeply investigated, except in WiMAX where ranges have been used to help in synchronization.

3. Develop a technique that can reduce the positioning error propagation in distributed systems though the use of virtual nodes.

References

[1] A. H. Sayed, A. Tarighat and N. Khajehnouri, "Network-Based Wireless Location [Challenges faced in developing techniques for accurate wireless location information]," IEEE Signal Processing Magazine, 2005.

[2] J. H. Reed, "An overview of the challenges and progress in meeting the E-911 requirement for location service," Communications Magazine, IEEE, vol. 36, pp. 30-37, 1998.

[3] J. Li, J. Jannotti, D. De Couto, D. Karger, R. Morris, "A Scalable Location Service for Geographic Ad Hoc Routing," Proc. IEEE/ACM Mobicom 2000, pp. 120-30.

[4] F. Ahao, L.Guibas, Wireless Sensor Networks [An Information Processing Approach]. 2004

[5] Klukas R. ", A Superresolution Based Cellular Positioning System Using GPS Time Synchronization", [Ph.D. dissertation]. University of Calgary, 1997.

[6] Linear Algebra and Its Applications, by Gilbert Strang. Third Edition

[7] Chen, S.; Cowan,C.F.N. ", Orthogonal least squares learning algorithm for radial basis function networks", IEEE Trans. on Neural Networks, Vol. 2, Issue 2, 1991.

[8] Korenberg Michael J. , Paarmann Larry D. ", Applications of Fast Orthogonal Search: Time-Series", Journal of Annals of Biomedical Engineering, Volume 17, Number 3, May, 1989.

[9] Korenberg M. J. ", A Robust Orthogonal Algorithm for System Identification And Time-Series Analysis", Journal of Biological Cybernetics, Volume 60, Number 4, February, 1989.

[10] Johnston, Craig G. ", High Resolution Wavelet De-Noising For MEMS-Based Navigation Systems", [M.Sc. dissertation]. Canada: Royal Military College of Canada (Canada); 2007.

[11] Armstrong, Justin L. K. ", Application Of Fast Orthogonal Search To Accuracy Enhancement Of Inertial Sensors For Land Vehicle Navigation" [M.Sc. dissertation]. Canada: Royal Military College of Canada (Canada); 2006.

[12] Collins, Jeff J.", Torpedo Detection Using Multi-Path Signals And Fast Orthogonal Search Techniques" [M.Sc. dissertation]. Canada: Royal Military College of Canada (Canada); 2005.

[13] Farouk E. ",Application Of The Fast Orthogonal Search In Automatic Target Detection" [Ph.D. dissertation]. Canada: Royal Military College of Canada, Canada, 2003.

[14] Mikael Eklund J., Nonlinear system identification and control using fast orthogonal search [Ph.D. dissertation]. Canada: Queen's University at Kingston (Canada); 2003.

[15] Mcgaughey Donald R., Korenberg Michael J., Adeney Kathryn M., Collins Susan D., Aitken G. J. M., "Using the Fast Orthogonal Search with First Term Reselection to Find Subharmonic Terms in Spectral Analysis", Annals of Biomedical Engineering, Vol. 31, pp. 741–751, 2003.

[16] Korenberg Michael, Paarmann L. D. ", Orthogonal approaches to time-series analysis and system identification", IEEE Signal Processing Magazine, Volume: 8, Issue: 3, Jul 1991

[17] Adeney K.M., Korenberg M.J.", Fast Orthogonal Search for Array Processing and Spectrum Estimation", IEE Proc. Vision, Image and Signal Processing, Volume 141, Issue 1, Feb 1994.

[18] G. Sun, J. Chen, W. Guo and K. J. R. Liu, "Signal processing techniques in network-aided positioning: a survey of state-of-the-art positioning designs," IEEE Signal Processing Magazine, vol. 22, pp. 12- 23, 2005.

[19] C. Botteron, "A Statistical Analysis of the Performance of Radio Location Techniques," 2003.

[20] L. Mailaender, "On the Geolocation Bounds for Round-Trip Time-of-Arrival and All Non-Line-of-Sight Channels," EURASIP Journal on Advances in Signal Processing, 2008.

[21] Y. Qi, "Wireless Geolocation in a Non-Line-Of-Sight Environment," 2003.

[22] Y. Qi, "On Time-of-arrival Positioning in a Multipath Environment," Vehicular Technology, IEEE Transactions on, vol. 55, pp. 1516-1526, 2006.

[23] S. Gezici, H. Kobayashi, H. V. Poor, "Non-parametric Non-Line-of-Sight identification," IEEE 58th Vehicular Technology Conference Volume 4, , 2003

[24] S. Gezici, "Nonparametric nonline-of-sight identification," Vehicular Technology Conference, 2003. VTC 2003-Fall. 2003 IEEE 58th, vol. 4, pp. 2544-2548 Vol.4, 2003.

[25] Daniele Coin, "Testing normality in the presence of outliers," Journal of Statistical Methods and Applications, vol. 17, 2008.

[26] M. O. Sunay, "Mobile location tracking in DS CDMA networks using forward link time difference of arrival and its application to zone-based billing," Global Telecommunications Conference, 1999. GLOBECOM '99, vol. 1A, pp. 143-147 vol.1a, 1999.

[27] Li Cong, "Nonline-of-sight error mitigation in mobile location," Wireless Communications, IEEE Transactions on, vol. 4, pp. 560-573, 2005.

[28] L. S. Shapiro and M. Brady, "Rejecting Outliers and Estimating Errors in an Orthogonal-Regression Framework," Philosophical Transactions: Physical Sciences and Engineering, vol. 350, pp. 407-439, Mar. 15. 1995.

[29] J. J. Lehtomaki, "CFAR Outlier Detection With Forward Methods," Signal Processing, IEEE Transactions on [See also Acoustics, Speech, and Signal Processing, IEEE Transactions on], vol. 55, pp. 4702-4706, 2007.

[30] A. K. Gupta, T. T. Nguyen and Sanqui, Jose Almer T., "Characterization of the skew-normal distribution," vol. 56, pp. 351-360, 2004.

[31] F. Bartolucci, G. De Luca, N. Loperfido,"A generalization for skewness in the basic stochastic volatility model," Proc. Of the 15th International Workshop on Statistical Modelling, 2000

[32] A. Azzalinin, "A class of distributions which includes the normal ones," Scandinavian Journal of Statistics, 1985.

[33] M. Chiong, " Some results on the scale skew-normal distribution," Journal of the Italian Statistical Society, 1998.

[34] J. R. Watson, "High-Sensitivity GPS L_1 Signal Analysis," M.Sc. University of Calgary, 2005.

[35] Yihong Qi, "Analysis of wireless geolocation in a non-line-of-sight environment," Wireless Communications, IEEE Transactions on, vol. 5, pp. 672-681, 2006.

[36] Yihong Qi, "On time-of-arrival positioning in a multipath environment," Vehicular Technology Conference, 2004. VTC2004-Fall. 2004 IEEE 60th, vol. 5, pp. 3540-3544 Vol. 5, 2004.

[37] J. Borras, "Decision theoretic framework for NLOS identification," Vehicular Technology Conference, 1998. VTC 98. 48th IEEE, vol. 2, pp. 1583-1587 vol.2, 1998.

[38] S. Venkatraman, "Wireless Location in Non-Line-Of-Sight Environment," 2004.

[39] S. Venkatraman, "statistical approach to non-line-of-sight BS identification," Wireless Personal Multimedia Communications, 2002. the 5th International Symposium on, vol. 1, pp. 296-300 vol.1, 2002.

[40] A. Azzalini, "The Skew-normal Distribution and Related Multivariate Families," Scandinavian Journal of Statistics, vol. 32, pp. 159-188, 2005.

[41] A. Azzalini, A. Capitanio, "Statistical applications of the multivarient skew-normal distribution," Journal of the Royal Statistical Society, 1999.

[42] A. D. Valle and A. Azzalini, "The multivariate skew-normal distribution," Oxford Journal, Biometrika, vol. 83, pp. 715-726, 1996.

[43] R. B. Arellano-valle and A. Azzalini, "On the Unification of Families of Skew-normal Distributions," Scandinavian Journal of Statistics, vol. 33, pp. 561-574, 2006.

[44] B. C. Arnold, R. J. Beaver, A. Azzalini, N. Balakrishnan, A. Bhaumik, D. K. Dey, C. M. Cuadras, J. M. Sarabia, and R. J. Beaver, "Skewed multivariate models related to hidden truncation and/or selective reporting," TEST: An Official Journal of the Spanish Society of Statistics and Operations Research, vol. 11, pp. 7-54, 2002.

[45] A. Azzalini, A. Capitanio, "Distributions generated by perturbation of symmetry with emphasis on a multivariate skew t distribution," Journal of the Royal Statistical Society, 2003.

[46] K. Lehmann, "Mean versus median," Princeton University, 1997.

[47] A. K. Gupta, T. Chen, "Goodness-of-fit tests for the skew-normal distribution," Journal of Communications in Statistics: Simulation and Computation, 2001.

[48] B. Liseo, N. Loperfido, "Defult Bayesian Analysis of the Skew-Normal Distribution," University of Roma, 2002

[49] A. Azzalini, A. Capitanio, "Statistical applications of multivariate skew-normal distributions," Journal of the Royal Statistical Society, Vol. 61, No. 3, 1999.

[50] R. W. Klukas, "A Superresolution Based Cellular Positioning System Using GPS Time Synchronization," 1997.

[51] J. L. Awange and E. W. Grafarend, "Algebraic Solution of GPS Pseudo-Ranging Equations," vol. 5, pp. 20-32, 2002.

[52] E. W. Grafarend and J. Shan, "GPS Solutions: Closed Forms, Critical and Special Configurations of P4P," Journal of GPS Solutions, vol. 5, pp. 29-41, 2002.

[53] R. Paradiso, G. Loriga and N. Taccini, “A wearable health care system based on knitted integrated sensors,” IEEE Trans. on Information Technology in Biomedicine, vol. 9, pp. 337 - 344, 2005.

[54] N. Patwari, J.N. Ash, S. Kyperountas, A.O. Hero, , R.L. Moses, N.S. Correal, , “Locating the nodes: cooperative localization in wireless sensor networks,” IEEE Signal Processing Magazine, vol. 22, pp. 54-69, 2005.

[55] M. Youssef, A. Noureldin, A. Yousif and N. El-Sheimy, “Self-localization techniques for wireless sensor networks,” Proc. IEEE/ION PLANS Conf., pp. 179 – 186, 2006.

[56] L. Jinyang, J. John, Douglas, S. J. De Couto, R. K. David and M. Robert, “A scalable location service for geographic ad hoc routing,” in Proc.of the 6th annu. Inter. Conf. on Mobile Computing and Networking, Boston, 2002, pp. 120-130.

[57] Crossbow Technology Inc., “wireless sensor networks training manual,” 2006.

[58] Y. Qi, “On Time-of-arrival Positioning in a Multipath Environment,” IEEE Trans. on Vehicular Technology, vol. 55, pp. 1516-1526, 2006.

[59] Yihong Qi, “Analysis of wireless geolocation in a non-line-of-sight environment,” IEEE Trans. on Wireless Communications, vol. 5, pp. 672-681, 2006.

[60] Hongyi Wu, “Novel self-configurable positioning technique for multihop wireless networks,” IEEE/ACM Transactions on Networking, vol. 13, pp. 609-621, 2005.

[61] S. Venkatraman, "Wireless Location in Non-Line-of-Sight Environemnts," Ph.D. dissertation, Dept. Elect. and Comp. Eng., Univ. of Cincinnati, OH, 2004.

[62] S. Capkun, M. Hamdi and J. -. Hubaux, "GPS-free positioning in mobile ad hoc networks," Proc. of the 34th Annual Hawaii Inter. Conf. on System Sciences, vol. 9, pp. 9008, 2001.

[63] M. S. Grewal,L. R. Weill,A. P. Andrews, Global Positioning Systems, Inertial Navigation, and Integration. 2007.

[64] N. Levanon, "Lowest GDOP in 2-D scenarios," IEE Proc. Radar, Sonar and Navigation, vol. 147, pp. 149 – 155, 2000.

[65] N. Patwari, A. Hero, M. Perkins, N. S. Correal and R. J. O'Dea, "Relative Location Estimation in Wireless Sensor Networks," IEEE Trans. on Signal Processing, vol. 51, pp. 2137 – 2148, 2003.

[66] H. Jin, "Scalable Sensor Localization Algorithms for Wireless Sensor Networks," Ph.D. dissertation, Dept. Elect. Eng., Univ. of Toronto, ON, 2005.

[67] R. Nagpal, "Organizing a Global Coordinate System from Local Information on an Amorphous Computer," MIT Artificial Intelligence Lab. A.I. Memo 1666, Aug. 1999.

[68] R. Nagpal, H. Shrobe and J. Bachrach, "Organizing a Global Coordinate System from Local Information on an Ad Hoc Sensor Network," 2nd Intern. Workshop on Information Processing in Sensor Networks, Palo Alto, vol. 5, 2003.

[69] Y. Yang, "Robust estimation of geodetic datum transformation," J. of Geodesy, vol. 73, pp. 268-74, 06. 1999.

[70] X. Peiliang, "On robust estimation with correlated observations," J. of Geodesy, vol. 63, pp. 237-252, 1989

[71] X. Chang and Y. Guo, "Huber's M-estimation in relative GPS positioning: computational aspects," J. of Geodesy, vol. 79, pp. 351-362, 2005.

[72] G. Sun, W. Guo, "Bootstrapping M-estimators for reducing errors due to non-line-of-sight (NLOS) propagation," Communications Letters, IEEE, vol. 8, pp. 509-510, 2004.

[73] C. D. Ghilani and P. R. Wolf, Adjustment Computations - Spatial Data Analysis. 2006.

[74] S. Kuang, Geodetic Network Analysis and Optimal Design-Concepts and Applications. 1996.

[75] N. Patwari, "Locating the nodes: cooperative localization in wireless sensor networks," Signal Proc. Magazine, IEEE, vol. 22, pp. 54-69, 2005.

[76] Z. Zhang, "Parameter estimation techniques: A tutorial with application to conic fitting," Image and Vision Computing J., vol. 15, pp. 59-76, 1997.

[77] S. Baselga, "Global optimization solution of robust estimation," J. Surv. Eng., vol. 133, pp. 123-128, 2007.

[78] Martin Vermeer, Advanced Adjustment Theory. 2007.

[79] Pei-Jung Chung, "Parameter Estimation: Subspace Methods", lecture notes, Univ. of Edinburgh, UK.

[80] G. Strang, K. Borre, Linear Algebra, Geodesy, and GPS. 1997.

[81] E. Mittermayer, "A generalisation of the least-squares method for the adjustment of free networks," J. of Geodesy, vol. 46, pp. 139-157, 1972.

[82] K. R. Koch, Parameter Estimation and Hypothesis Testing in Linear Models. Springer, 1999.

[83] N. Bulusu, J. Heidemann and D. Estrin, "GPS-less low cost outdoor localization for very small devices," IEEE Communication Magazine, vol. 7, pp. 28-34, 2000.

[84] Q. Shi, S. Kyperountas, N. Correal and F. Niu, "Performance Analysis of Relative Location Estimation for Multihop Wireless Sensor Networks," IEEE J. on Selected Areas in Communications, vol. 23, pp. 830- 838, 2005.

Appendix A: MUSIC and Decorrelation of Signals

MUSIC is widely discussed in the literature. A concise summary is given here for convenience. Consider a signal of L uncorrelated sinusoids in AWGN with zero mean and variance σ^2. Let $\boldsymbol{R}_{MUSIC}$ be the $(M+1)$ by $(M+1)$ ensemble averaged correlation matrix of the signal, which can be expressed as

$$\boldsymbol{R}_{MUSIC} = \boldsymbol{S}_{MUSIC}\boldsymbol{D}\boldsymbol{S}_{MUSIC}{}^{H} + \sigma^2\boldsymbol{I} \tag{48}$$

where H indicates Hermitian transpose and $\boldsymbol{I}$ is the $(M+1)$ by $(M+1)$ identity matrix. $\boldsymbol{S}_{MUSIC}$ is an $(M+1)$ by L matrix of the form

$$\begin{aligned} \boldsymbol{S}_{MUSIC} &= \left[\boldsymbol{s}_{MUSIC\_1}, \boldsymbol{s}_{MUSIC\_2}, \dots \boldsymbol{s}_{MUSIC\_L}\right] \\ &= \begin{bmatrix} 1 & 1 & \cdots & 1 \\ e^{-j\omega_1} & e^{-j\omega_2} & \cdots & e^{-j\omega_L} \\ \vdots & \vdots & \ddots & \vdots \\ e^{-jM\omega_1} & e^{-jM\omega_2} & \dots & e^{-jM\omega_L} \end{bmatrix} \end{aligned} \tag{49}$$

where

$\boldsymbol{D}$ is the correlation matrix of the sinusoid.

Let $\{\boldsymbol{v}_1, \boldsymbol{v}_2, \cdots, \boldsymbol{v}_{M+1}\}$ be the eigenvectors of $\boldsymbol{R}_{MUSIC}$. The MUSIC spectrum is obtained from

$$\hat{S}_{MUSIC}(\omega) = \frac{1}{s_{MUSIC}^H(\omega) V_N V_N^H s_{MUSIC}(\omega)} \tag{50}$$

where

$s_{MUSIC}(\omega) = [1 \quad e^{-j\omega} \quad \ldots \quad e^{-jM\omega}]^T$ is the variable frequency scanning vector,

$V_N = [v_{L+i} \quad \cdots \quad v_{M+1}]$

Decorrelation of Signals: Signal decorrelation by smoothing has been found helpful, but not efficient. Consider the N data points $[x(0) \quad x(1) \quad \cdots \quad x(N-1)]$. A subarray is formed consisting of $M+1$ points where $M+1 < N$. Smoothing is introduced by sliding the subarray across the full array of data points in both the forward and backward directions. This is accomplished by structuring a data matrix $\boldsymbol{A}_{MUSIC}$ in the form

$$A_{MUSIC}^H = \left[\begin{array}{ccc|ccc} x(M) & \cdots & x(N-1) & x^*(0) & \cdots & x^*(N-M+1) \\ x(M-1) & \cdots & x(N-2) & x^*(1) & \cdots & x^*(N-M+2) \\ \vdots & \ddots & \vdots & \vdots & \ddots & \vdots \\ x(0) & \cdots & x(N-M+1) & x^*(M) & \cdots & x^*(N-1) \end{array}\right] \tag{51}$$

The left half of A_{MUSIC}^H contains the subarrays for forward smoothing whereas the right half consists of the subarrays for backwards smoothing. The ensemble averaged correlation matrix $\boldsymbol{R}_{MUSIC}$ is defined as the expected value of the product of the data matrix $\boldsymbol{A}_{MUSIC}$, with Hermitian (i.e. complex conjugate). In practice, it is not known and must be estimated from the a sample average. The estimation of $\boldsymbol{R}_{MUSIC}$ will then be

$$\widehat{\boldsymbol{R}}_{MUSIC} = \frac{1}{2(N-M)} A^{H}_{MUSIC} \boldsymbol{A}_{MUSIC} \tag{52}$$

where

$2(N-M)$ is the number of points average

Appendix B: Fast Orthogonal Search (FOS) Procedure

The Fast Orthogonal Search (FOS) method, was developed by Korenberg as a fast efficient method of building models of time-series and of systems with unknown structure. It is a modified version of the OLSR technique.

FOS has been developed to reduce both the computation power and time. The g_k^{FOS} coefficients found by (7) or (8) can be obtained as

$$g^{FOS}{}_k = \frac{C(k)}{D(k,k)} \tag{53}$$

where

$$\begin{gathered} D(0,0) = 1 \\ D(k,0) = \overline{p_k(n)} \end{gathered} \tag{54}$$

$$D(k,r) = \overline{p_k(n)p_r(n)} - \sum_{i=0}^{r-1} \mathfrak{K}_{ri} D(k,i) \tag{55}$$

where

$r = 0, \dots, k-1$, and

$\mathfrak{K}_{kr} = \frac{D(k,r)}{D(r,r)}$

Let $C(0) = \overline{r(n)} = \boldsymbol{R}$, then

$$C(k) = \overline{r(n)p_k(n)} - \sum_{r=0}^{k-1} \mathfrak{K}_{ri}\, C(r) \tag{56}$$

which represents one form of Cholesky decomposition.

In general, the MSE is given by

$$\mathrm{MSE} = \boldsymbol{R}^T \boldsymbol{R} - \sum_{k=1}^{M} (g_k^{FOS})^2\, D(k,k) \tag{57}$$

Equivalently,

$$\mathrm{MSE} = \overline{y^2(n)} - \sum_{k=1}^{M} (g_k^{FOS})^2\, D(k,k) \tag{58}$$

Therefore, the $\mathrm{O}^{\mathrm{FOS}}$ function is given by

$$\mathrm{O}^{\mathrm{FOS}} = (g_k^{FOS})^2 D(k,k) \tag{59}$$

Appendix C: A proof for the special angles of 2D-CTM based on $\mathbf{L_1} - \mathbf{norm}$ estimation

The Euclidean distance estimated from sensor nodes CLCs are equal to the observed ranges due to the unit circle that govern the relation between x and y coordinates based on $L_2 - norm$, while for $L_1 - norm$ this assumption is not valid due to the unit rhomboid which controls the relationship between x and y coordinates. Figure 45 shows how the $L_2 - norm$ unit circle and the $L_1 - norm$ unit rhomboid meet only when the relation between x and y coordinates is $0^{\circ}, 90^{\circ}, 180^{\circ}, or\ 270^{\circ}$. Therefore, $L_1 - norm$ behaves probably if the inclination angle between the two CLC systems is $0^{\circ}, 90^{\circ}, 180^{\circ}, or\ 270^{\circ}$.

Appendix D: A complete derivation for the 2D-CTM based on L_1 − norm estimator

$$a \cdot x - b \cdot y + c = X$$

$$a \cdot y + b \cdot x + d = Y \;\; \Rightarrow a = \frac{X - c + b \cdot y}{x}$$

$$\frac{X - c}{x} \cdot y + \frac{y^2}{x} \cdot b + b \cdot x + d = Y \Rightarrow b = \frac{x \cdot (Y - d) - (x - c) \cdot y}{y^2 + x^2}$$

Therefore, for all tie sensor nodes

$$a = med\left[\frac{X_i - c + \left(\frac{(x_i \cdot (Y_i - d) - (x_i - c) \cdot y_i)}{x_i^2 + y_i^2}\right)}{x_i}\right]$$

$$= med\left[\frac{1}{x_i} \cdot \left(X_i - c \cdot \left(1 - \frac{y_i}{x_i^2 + y_i^2}\right)\right) + \frac{1}{x_i^2 + y_i^2} \cdot (Y_i - y_i - d)\right]$$

$$b = med\left[\frac{x_i \cdot (Y_i - d) - (X_i - c) \cdot y_i}{x_i^2 + y_i^2}\right]$$

where c and d can be given by

$$\begin{aligned} c &= med[(x_i - X_i)] \\ d &= med[(y_i - Y_i)] \end{aligned} \qquad , i \in 1, \ldots, \Gamma$$

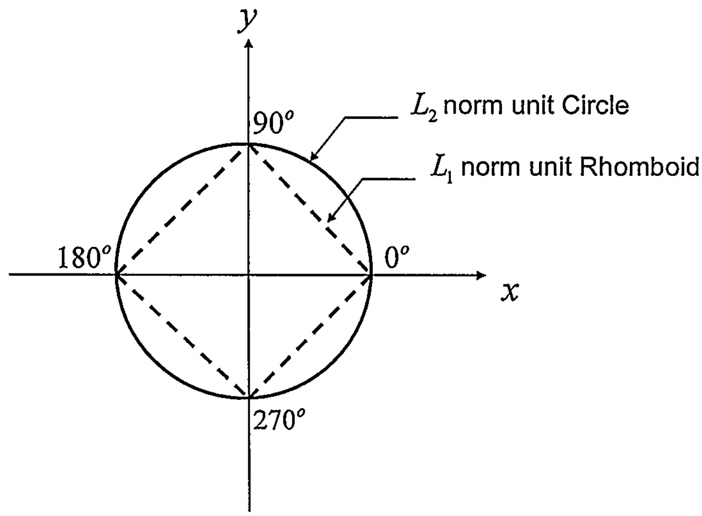

Figure 45 The difference between the unit circle (Euclidean distance) of $L_2 - norm$ and unit the rhomboid of $L_1 - norm$.